Durham University

Durham E-Theses

Some kinetic, equilibrium, and structural studies of the reactions of aromatic nitro-compounds with nucleophiles

Brenda Gibson

How to cite:

Gibson, Brenda (1980) Some kinetic, equilibrium, and structural studies of the reactions of aromatic nitro-compounds with nucleophiles. Doctoral thesis, Durham University.

Use policy

The full-text may be used and/or reproduced, and given to third parties in any format or medium, without prior permission or charge, for personal research or study, educational, or not-for-profit purposes provided that:

- a full bibliographic reference is made to the original source
- a https://etheses.durham.ac.uk/id/eprint/7951/ is made to the metadata record in Durham E-Theses
- the full-text is not changed in any way

The full-text must not be sold in any format or medium without the formal permission of the copyright holders.

Please consult the full Durham E-Theses policy for further details.

Academic Support Office, The Palatine Centre, Durham University, Stockton Road, Durham, DH1 3LE
e-mail: e-theses.admin@durham.ac.uk Tel: +44 0191 334 6107
https://etheses.durham.ac.uk

SOME KINETIC, EQUILIBRIUM, AND STRUCTURAL STUDIES OF THE REACTIONS OF AROMATIC NITRO-COMPOUNDS WITH NUCLEOPHILES

by

Brenda Gibson, B.Sc. (Durham)

(St. Mary's College)

A thesis submitted for the degree of Ph.D.

in the University of Durham, 1980

The copyright of this thesis rests with the author. No quotation from it should be published without his prior written consent and information derived from it should be acknowledged.

ACKNOWLEDGEMENTS

I would like to thank my supervisor, Dr. M.R. Crampton, for his constant help and encouragement, and Dr. R.S. Matthews for guidance with the n.m.r. work.

I acknowledge receipt of a Research Studentship from the Science Research Council.

Thanks are also due to Mrs. Marion Wilson, for typing this thesis.

DECLARATION

The material in this thesis is the result of research carried out in the Department of Chemistry, University of Durham, between October 1977 and June 1980. It has not been submitted for any other degree, and is the author's own work, except where acknowledged by reference.

LIST OF PUBLICATIONS

Some of the results described in this thesis have been published in the following papers:

'Kinetic and Equilibrium Data for Sodium Isopropoxide Addition to Some Aromatic Nitro-compounds in Isopropanol'. The Stabilities of Meisenheimer Complexes. Part 16.

by M.R. Crampton, B. Gibson, and F.W. Gilmore, J.C.S. Perkin 2, 1979, 91.

'The Reactions of 1-X-2,4,6-Trinitrobenzenes with Hydroxide Ions in Water'. The Stabilities of Meisenheimer Complexes. Part 17.

by B. Gibson and M.R. Crampton, J.C.S. Perkin 2, 1979, 648.

'Proton Transfer and σ-Complex Formation in the Reactions of N-Substituted-2,4,6-Trinitroanilines with Sodium Methoxide in Methanol'. The Stabilities of Meisenheimer Complexes. Part 18.

by M.R. Crampton and B. Gibson, J.C.S. Perkin 2, 1980, 752.

'^{1}H N.m.r. Studies of Proton Transfer and σ-Complex Formation in the Reactions of N-Substituted Picramides with Oxygen and Nitrogen Bases'.

by M.R. Crampton, B. Gibson, and R.S. Matthews, Org.Magn.Resonance, in the press.

Some Kinetic, Equilibrium and Structural Studies of the Reactions of Aromatic Nitro-Compounds with Nucleophiles

by Brenda Gibson.

The addition of aqueous sodium hydroxide to 1-X-2,4,6-trinitrobenzenes produces an adduct at C-3, which ionises by loss of the hydroxyl proton. Base addition at C-1, leading to nucleophilic substitution of X, is an order of magnitude slower than that at C-3. Nucleophilic substitution of X occurs in both the substrate and the C-3 adduct.

Stopped-flow and temperature-jump measurements of the reactions of picramide (2,4,6-trinitroaniline) and N-substituted picramides indicate that they undergo both very rapid amino-proton removal and base addition at C-3. The proportion undergoing each reaction varies with the N-substituent.

^{1}H n.m.r. measurements of N-substituted picramides with methoxide ion in methanol-DMSO show that the two major 1:1 interactions are amino-proton abstraction and base addition at C-3. The proportion of substrate reacting in each way depends upon the solvent composition.

The reaction of N-substituted picramides with amide ions (from piperidine and benzylamine) produces σ-adducts at C-3. There is spin-coupling between the amino-proton of benzylamine and the adjacent ring and methylene protons.

Kinetic studies have been made of the reactions of 1,3,5-trinitrobenzene with primary and secondary aliphatic amines, which form σ-adducts *via* zwitterionic intermediates. The observation of base catalysis in some of these reactions indicates that proton transfer from the zwitterionic intermediate may be rate limiting.

CONTENTS

Page No.

Page No.

CHAPTER ONE

MEISENHEIMER COMPLEXES IN NUCLEOPHILIC AROMATIC SUBSTITUTION

Durham University
SCIENCE
30 OCT 1980
SECTION

A SURVEY OF THE REACTIONS OF AROMATIC NITRO-COMPOUNDS WITH BASES

The usual mode of aromatic substitution involves attack by an electrophile, causing displacement of a ring proton. In most of these reactions, a σ-complex is formed by covalent addition of the electrophile at the position of substitution.[1] Substitution can also be effected by free radical attack: this, too, is believed to involve formation of a σ-adduct.[1]

When nucleophilic attack occurs, the leaving group is generally one which can take with it the bonding electron pair, and have a reasonable degree of stability as either an anion or a molecule carrying a lone pair of electrons.[2] For this reason, hydrogen is very rarely displaced in nucleophilic aromatic substitution.

Various mechanisms are possible for nucleophilic substitution in aromatic compounds; the route taken depends upon the conditions. The S_N1 mechanism, common in aliphatic compounds, is rare in aromatic compounds, for various structural and electronic reasons.[3] The benzyne (elimination-addition) mechanism is found for unactivated aryl halides[1], and requires the use of a strong base, e.g. amide ion in liquid ammonia. The substitution occurs in both the position occupied by the displaced group and that of the adjacent proton. Nucleophilic attack by a free radical, the $S_{RN}1$ mechanism[4], competes with the benzyne mechanism in some reactions, but gives rise to non-rearranged products, i.e. the nucleophile replaces only the leaving group, and not the adjacent group.

The aromatic rings in compounds which contain electron-withdrawing substituents are electron-deficient and are therefore more open to nucleophilic attack. The nitro-group is one of the strongest electron-withdrawing groups known,[5,6] and is the one most widely used in studies of nucleophilic aromatic substitution. Several types of interaction are possible for the electron-deficient aromatic species.[7]

Partial electron transfer from a nucleophile to the electron-deficient ring forms a π-complex, 1.1, while total transfer produces a radical anion, 1.2. Proton abstraction from either the ring 1.3 or a side-chain 1.4 are also possible.

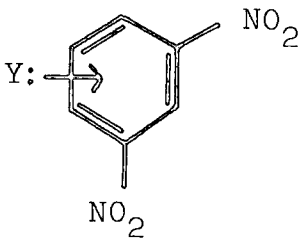

1.1

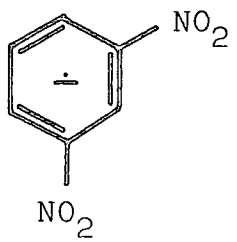

1.2

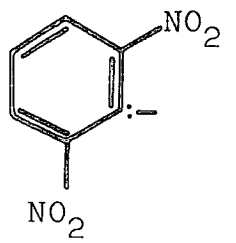

1.3

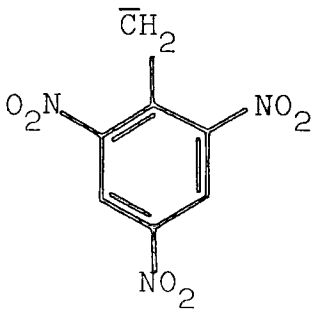

1.4

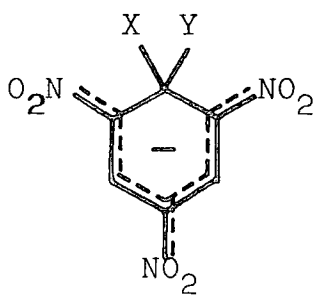

1.5

Covalent bond formation between the lone pair of the base and the aromatic ring produces a σ-complex, 1.5, analogous to those found in electrophilic and free radical reactions (above). If the substrate contains a good leaving

group, formation of the σ-complex can lead to nucleophilic substitution. In the absence of a suitable leaving group, the reaction stops with formation of the adduct, generally known as a Meisenheimer complex.[8] Meisenheimer complexes are widely used as models for the intermediate in nucleophilic aromatic substitution, and can be considered as particularly stable examples of a general type of adduct.

ACTIVATED NUCLEOPHILIC AROMATIC SUBSTITUTION

The S_N2 reaction of aliphatic compounds is a synchronous process involving a 5-coordinate transition state, while S_EAr reactions involve a tetrahedral (4-coordinate) intermediate.[1] Experimental results suggest that activated S_NAr reactions also follow a two-stage mechanism,[7] with the formation of a discrete intermediate.

The conditions[9] for activated S_NAr are the presence in the substrate of electron-withdrawing groups (usually two or three nitro-groups ortho and/or para to the leaving group) and a leaving group which is able to remove the bonding electrons, and to have some measure of stability either as an anion, or as a molecule carrying a lone pair of electrons. A wide variety of nucleophiles and solvents have been used in these reactions.

Brightly coloured solutions are obtained on adding base to the activated substrate. These colours fade as the reaction proceeds, showing that they are not due to the product of substitution. Previously, structural identification of the coloured intermediates could only be tentative, made on the basis of comparisons with isolable complexes. However, recent n.m.r. work in flowing systems[10] has determined the structures of some intermediates, confirming their identity as σ-complexes. For example, in the reaction between 2,4,6-trinitroanisole and n-butylamine in 50% DMSO-methanol,[11] the substitution product is preceded by the C-1 adduct, 1.6, with the C-3 adduct, 1.7, being formed in a rapid side-equilibrium.[12]

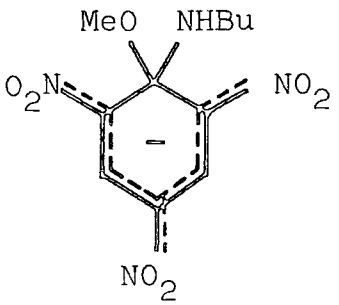

1.6

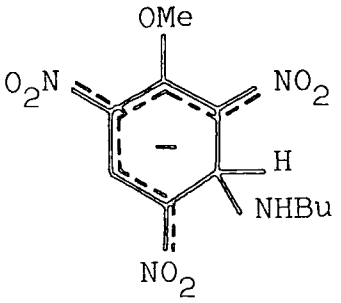

1.7

A considerable body of evidence for the two-stage nature of activated S_NAr has been obtained from studies of base catalysis in reactions where the nucleophile is a primary or secondary amine[13] (see Chapter Seven).

It should be noted that the observation of a transient species during the course of a substitution reaction does not necessarily imply its direct involvement in that reaction. For example,[14] addition of methoxide ion to trinitrobenzene produces an adduct at C-H, but the main substitution product is formed by replacement of a nitro-group by methoxide ion.

KINETIC, EQUILIBRIUM, AND STRUCTURAL STUDIES OF MEISENHEIMER COMPLEXES

The bright colours produced on the addition of a base to solutions of trinitro-aromatic compounds have been known for almost a century.[15] The reactions are reversible, the addition of acid allowing quantitative recovery of the substrate. They are sometimes followed by slow nucleophilic substitution, often of one or more of the nitro-groups. However, in some cases, highly coloured solids can be isolated, and some structural determinations have been carried out. Before crystallographic and spectroscopic techniques were available, several possible structures were proposed for the complexes. Support for the quinoid structure, 1.8[16], was obtained by Meisenheimer[17], who showed that the same complex is produced from 2,4,6-trinitrophenetole and methoxide ion as from 2,4,6-trinitroanisole and ethoxide ion.

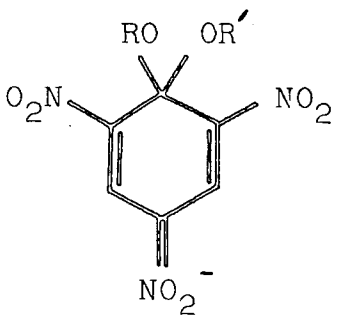

1.8

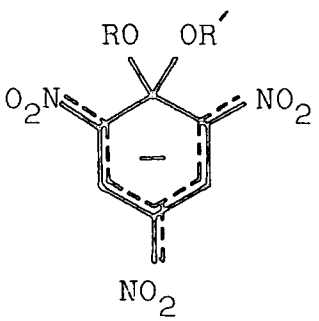

1.9

More recent spectroscopic and crystallographic work has confirmed this structure for the stable adducts formed from picryl ethers and alkoxides. The structure is generally shown as 1.9, with the negative charge delocalised around the ring and the electron-withdrawing substituents, although some M.O. calculations[18] indicate that the para nitro-group

carries more of the negative charge than do either of the ortho substituents. In the case of the diethoxy complex,[19] the C-1 atom is sp^3 hybridised (tetrahedral), the two alkoxy groups lie above and below the plane of the ring, and the three nitro-groups are virtually coplanar with the ring.

The most widely-used technique for studying σ-complexes is uv/visible spectroscopy. Because of its sensitivity, and the high intensity of visible absorption of these complexes, it can be used for kinetic and equilibrium work in dilute solutions. Kinetic measurements can be made either by conventional spectrophotometry, for fairly slow reactions, or by stopped-flow and/or temperature-jump spectrophotometry for faster processes (*vide infra*). Equilibrium constants are obtained from measurements of the variation with base concentration of the optical density at a particular wavelength, generally using the Benesi-Hildebrand method[20], or a modification of it.

Although it is very sensitive, uv/visible spectroscopy is not structurally diagnostic; complexes containing different groups can have very similar visible spectra[21]. However, some distinctions can be made on the basis of visible spectra: 1:1 adducts of 1,3,5-trinitrobenzene generally show two absorption maxima in the visible region, while 1:2 adducts have only one.[8]

Several methods are available for determining the structure of σ-complexes. When the complex is isolable as a solid, X-ray crystallography can be used (see above). Infra-red spectroscopy is also useful in such cases.[22] These techniques have been used to confirm the structure of adducts from picryl ethers and alkoxides.

^{1}H n.m.r. spectroscopy, first applied to the study of σ-complexes in 1964[23,24], has proved very useful in the elucidation of the structures of σ-complexes in solution. While the conventional technique is limited to complexes of moderate stability (with half-lives of the order of minutes), the development of flow and stopped-flow n.m.r.[10] has allowed the detection and characterisation of transient intermediates with half-lives down to circa 50 ms. ^{13}C n.m.r. has been used, together with M.O. calculations, to determine the charge distribution pattern in Meisenheimer complexes.[25] These studies have confirmed the strong electron-withdrawing effect of the nitro-group.

In unsymmetrical substrates, there is more than one position at which a 1:1 adduct may be formed. For example, in the reaction between 2,4,6-trinitroanisole and methoxide ion[8,26], addition at C-3 (C-H) is very much faster than addition at C-1 (C-OMe), but the C-1 adduct has the greater thermodynamic stability. Various explanations have been offered for this. The difference in rates of attack at substituted and unsubstituted positions is probably best attributed to steric effects, which are expected to be negligible in attack at C-H[8], and to repulsion between the electron clouds of the entering and leaving groups[27]. A further factor contributing to the faster attack at C-3 could be ground-state resonance stabilisation of ArOR, which is lost on the formation of the C-1 adduct, but conserved when addition occurs at C-3.[13]

The greater stability of the C-1 adduct may partly be due to release of steric strain between the C-1 substituent and the ortho nitro-groups[28]: addition at C-1 changes the

hybridisation to sp^3, and rotates the substituents out of the plane of the ring[19,29]. The electron-withdrawing effect of the methoxyl group at C-1 should favour nucleophilic attack at that position[28]. The stabilisation of sp^3 hybridised carbon by multiple alkoxy substitution[30] will also contribute to the stability of the C-1 adduct.

There is evidence[31] to suggest that aliphatic amines behave in a similar way, forming first a C-H adduct of relatively low stability, and then isomerising to form a more stable adduct at a substituted ring position.

Picramide and its N-substituted derivatives undergo proton abstraction as well as base addition[32,33].

Multiple base interactions are also known, forming, for example, 1:2 adducts.

EXAMPLES OF σ-COMPLEXES FROM SUBSTITUTED 1,3,5-TRINITROBENZENES

1. Complexes from Oxygen Bases

The addition of hydroxide ion to substituted trinitrobenzenes results in the formation of σ-adducts at C-3, 1.10[34] (see Chapter Four). The 1:1 adduct with trinitrobenzene is isolable[35]. There is also evidence[34,36,37] for the ionisation of added hydroxyl groups in the C-3 adducts of some 1-X-2,4,6-trinitrobenzenes, 1.11 (see Chapter Four). 1:2 adducts, 1.12, are known to be formed from trinitrobenzene[38], picrate ion[39], and N,N-dimethylpicramide[40,41]; in all of these, both additions occur at unsubstituted ring positions. With picramide, both amino-proton abstraction, 1.13, and addition at C-3, 1.14, occur as 1:1 interactions, while N-methylpicramide undergoes amino-proton loss followed by base addition at C-3, to form 1.15.[40,41]

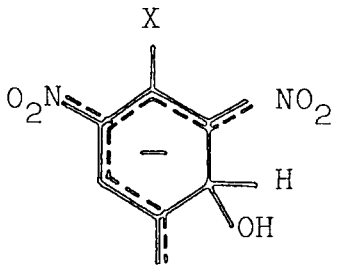

1.10

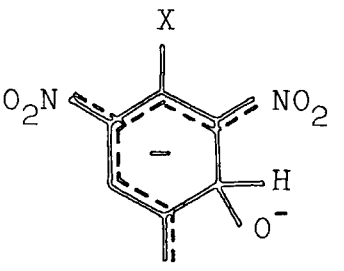

1.11

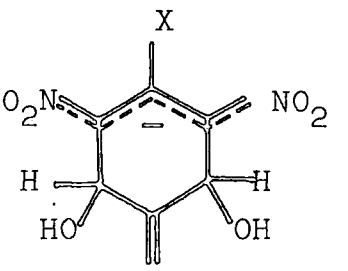

1.12

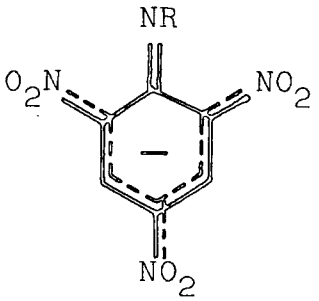

1.13

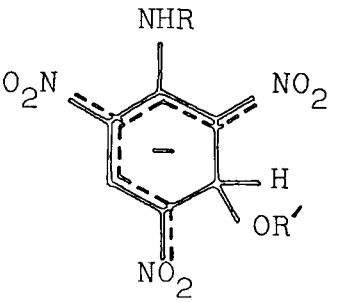

1.14

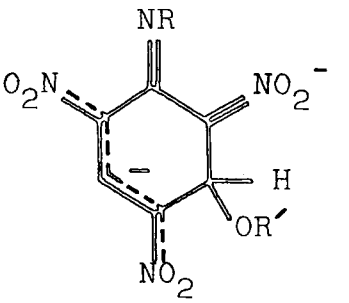

1.15

The addition of methoxide ion to 1-X-3,5-dinitrobenzenes can produce adducts at C-2, 1.16, or at C-4, 1.17. Previous results[42,43] were interpreted in terms of rapid formation of 1.17, followed by slower isomerisation to 1.16. However, flow n.m.r. studies[44] have shown that both 1.16 and 1.17 are present in both the kinetically- and thermodynamically-controlled mixtures.

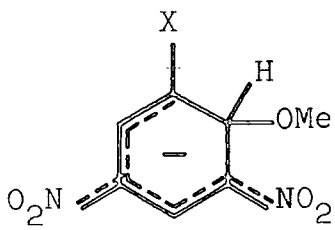

1.16

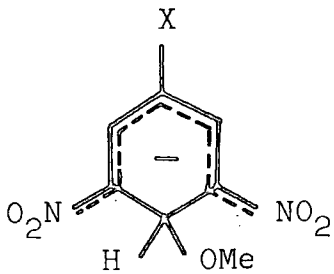

1.17

Methoxide ion addition to trinitroanisole produces first the C-3 adduct, 1.18 and then the thermodynamically more stable C-1 adduct, 1.19[26]. A 1:2 adduct, 1.20, is formed by methoxide addition at both C-1 and C-3.[8]

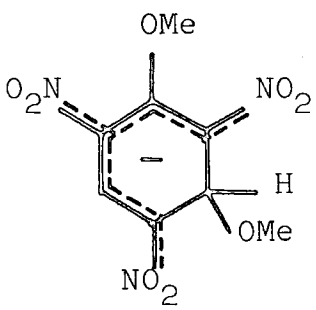

1.18

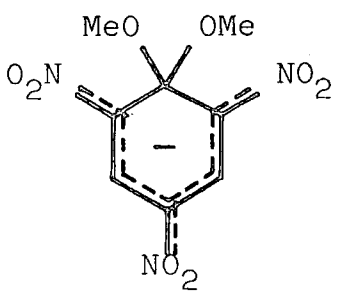

1.19

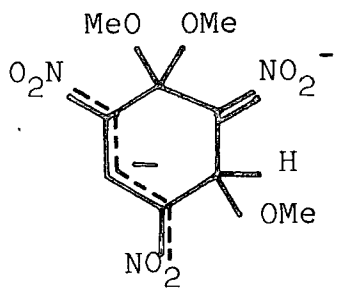

1.20

Addition of ethoxide[45], n-propoxide[46], or iso-propoxide[47] to the appropriate 1-alkoxy-2,4-dinitro-6-X-benzenes in the corresponding alcohol solution shows that, in each case, addition at C-1 is slower than that at C-3, but forms the more stable adduct.

The reaction of methoxide ion with N-substituted picramides[23,32,33,48,49] causes both amino-proton loss and base addition at C-3 (see Chapter Five).

Only C-3 adducts are obtained on the addition of methoxide[50] or ethoxide[51] ion to picryl chloride. The C-1 adduct is presumably unstable with respect to loss of chloride ion, as the only subsequent observable process forms the picryl ether.

2. Complexes from Nitrogen Bases

The addition of aliphatic amines to activated aromatic compounds in a variety of solvents gives rise to the intense colours characteristic of σ-adducts. Reactions of substituted polynitrobenzenes with primary and secondary aliphatic amines have been of considerable interest in studies of the mechanism of S_NAr reactions.[13,52] The reaction is believed to occur in two stages; first, formation of the zwitterion, 1.21 (which is probably stabilised by intramolecular hydrogen-bonding[8]), and then removal of the amino-proton and the leaving group, X(see Chapter Seven).

Low-temperature n.m.r. studies in flowing systems[31] have provided evidence of C-3 adducts, 1.22, from n-butylamine with N-n-butylpicramide and with trinitroanisole in 50% DMSO-methanol. Conventional n.m.r. studies in liquid ammonia[53] suggest that amide ion attacks preferentially at an unsubstituted position, 1.23, while the structure of the 1:2 adduct depends upon the substrate. When X, in 1-X-2,4,6-trinitrobenzene, is H, Me, or Et, the 1:2 adduct has structure 1.24, while the 1:2 adduct with X = NH_2, NMe_2, NEt_2, OMe, or SEt, has structure 1.25.

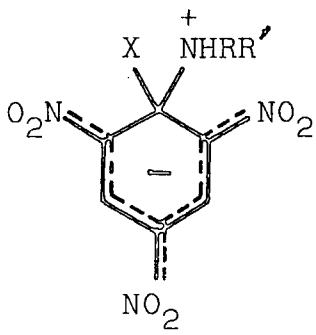

1.21

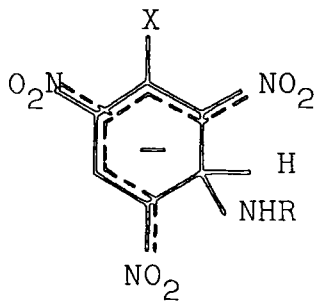

1.22

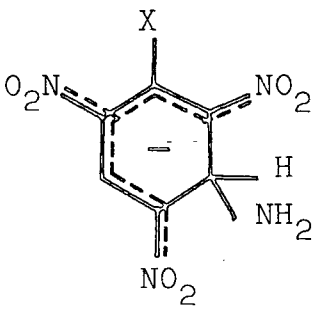

1.23

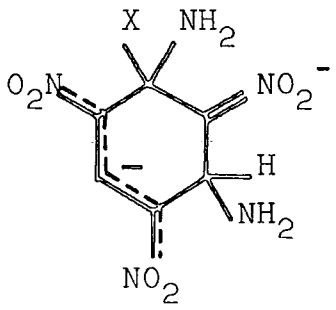

1.24

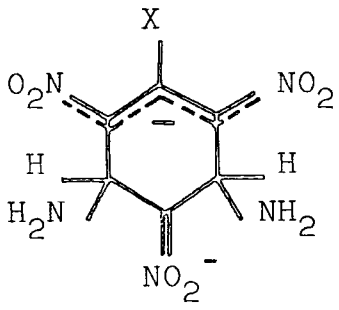

1.25

3. Complexes from Other Bases

Thioalkoxides react in a similar way to their oxygen analogues, but the formation and decomposition of the adducts are very much faster[54]. Trinitrobenzene and thioethoxide form both the 1:1 (1.26, X = H) and 1:2 (1.27, X = H) adducts. Evidence has also been found[55] for the 1:3 adduct, 1.28, in mixed solvents of high water content.

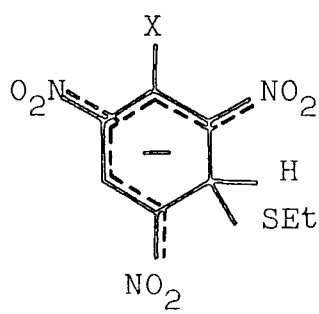

1.26

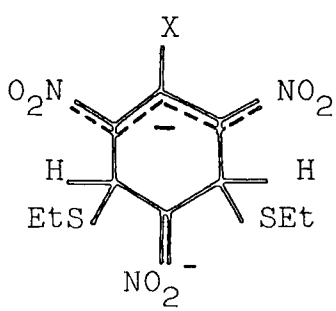

1.27

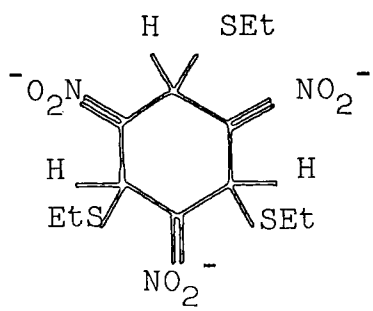

1.28

With picramide[54], virtually all of the 1:1 interaction with thioethoxide is addition at C-3 (1.26, X = NH_2), compared with the considerable degree of amino-proton abstraction found with oxygen bases. N-methylpicramide forms both the 1:1 (1.26, X = NHMe) and the 1:2 (1.27, X = NHMe) adducts by addition at C-H, again with very little amino-proton abstraction. Thus, the ratio of carbon- to proton-basicity is greater for sulphur bases than for oxygen bases.

Thioethoxide ion reacts with picryl ethyl thioether to form both the C-3 (1.26, X = SEt) and C-1 (1.29) adducts[56]. In contrast to the analogous oxygen complexes, the C-3 adduct is reported[57] to be more stable than the C-1 adduct.

Sulphite ions readily form adducts with 1-X-2,4,6-trinitrobenzenes in aqueous solution[36,39,58]. Apart from the adducts of trinitrobenzaldehyde, 1.30 and 1.31[59], both the 1:1 and 1:2 complexes are formed by addition at C-H (1.32, 1.33). The adducts from picramide and N-methylpicramide are stabilised by intramolecular hydrogen-bonding[60] between the amino-proton(s) and the ortho nitro-group(s). ^1H n.m.r.[61,62] and kinetic[63] evidence has been obtained for cis-trans isomerism in the 1:2 adduct of trinitrobenzene (1.33, X = H).

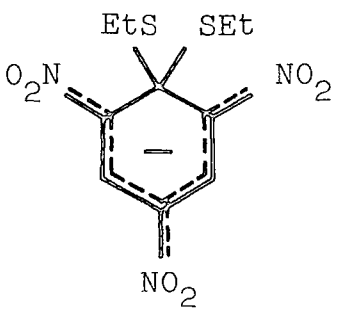

1.29

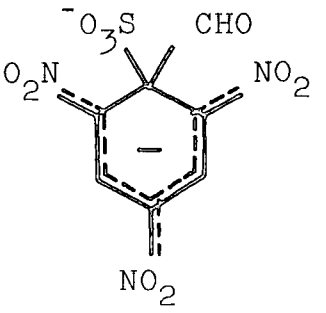

1.30

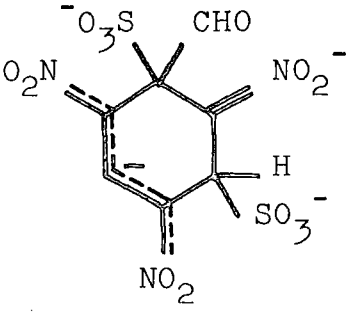

1.31

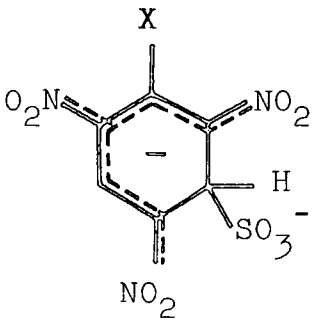

1.32

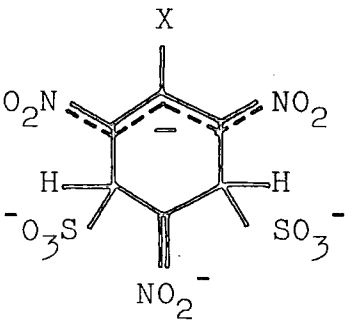

1.33

Adducts with cyanide ion have been obtained from several substrates in a variety of solvents[64,65,66].

The Janovsky reaction, between a di- or trinitroaromatic compound and the acetonate ion, has been shown by n.m.r.[67] to produce a σ-adduct. Similar reactions with ketones containing a second potentially nucleophilic site have led to the study of 'meta-bridging' reactions[68], in which the second attack occurs at a position meta to the first, i.e. at C-3. These reactions can be used in the preparation of substituted polycyclic aromatic and heteroaromatic compounds[69].

Spiro-complexes are formed when a substituent carries a nucleophilic group capable of attacking the aromatic ring at the point of substitution, i.e. at C-1, 1.34. Spiro complexes have been used as models in mechanistic studies of S_NAr reactions[52]. They also occur as intermediates in the Smiles rearrangement[70,71].

The use of tetra-alkyl borate[72] and borohydride[73] salts with trinitrobenzene produces 1.35 (R = H, alkyl).

Gem-difluoro adducts, 1.36, have also been obtained.[74]

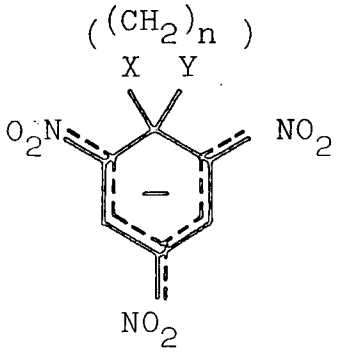

1.34

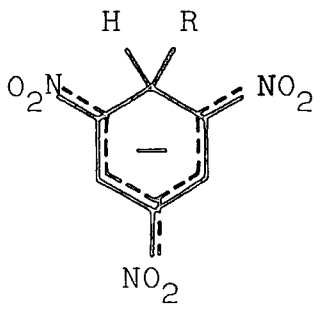

1.35

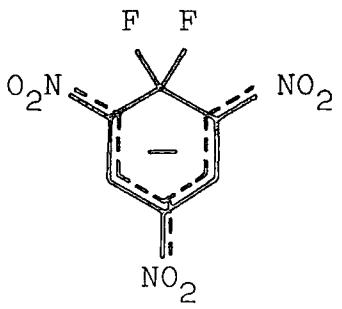

1.36

4. Complexes from Heteroaromatic and Non-benzenoid Aromatic Substrates

Substituted heteroaromatic compounds form σ-complexes analogous to those from activated aromatic substrates. The ring aza-group has a similar electron-withdrawing effect to that of the nitro-group, while its steric effect is comparable with that of a ring C-H[75]. σ-Complexes have been obtained from a wide variety of N-, O-, S-, and Se-heterocycles, with a range of nucleophiles, e.g. hydroxide ion[76], methoxide ion[77,78], and amines[79].

σ-Complexes have also been obtained from non-benzenoid homoaromatic substrates, e.g. the methoxide ion adducts of 1-nitro-azulene[80] and 2-methoxy-5-nitrotropone[81].

FACTORS AFFECTING MEISENHEIMER COMPLEX STABILITY

Because of the bright colours produced by σ-complexes in solution, the most widely-used method for determining equilibrium constants is visible spectroscopy. Measurement of the variation with base concentration of the absorption at a particular wavelength allows direct calculation of the equilibrium constant when the extinction coefficient of the coloured species is known. When it is not, a Benesi-Hildebrand plot[20], or a variant of it, must be used. When a reasonable degree of conversion to the complex is achieved in fairly dilute solution, the equilibrium constant can be expressed in terms of concentrations. However, if the substrate is not very reactive, or if the formation of higher (1:2, etc.) adducts is being considered, higher base concentrations are needed, and the basicity of the solution is no longer adequately described in terms of molar concentration. In such cases, the appropriate acidity function[82] must be introduced, the function used being dependent upon the nature of the interaction under consideration[83,84].

Although the factors governing complex stability are closely interrelated, they can be divided approximately into substrate, nucleophile and medium effects.

1. Substrate Effects

The most important condition for the formation of Meisenheimer complexes is the presence in the substrate of electron-withdrawing substituents, such as nitro-groups (or ring hetero-atoms), in positions ortho and/or para to the site of attack[2]. These groups withdraw electron density from the ring, rendering certain positions open to nucleophilic attack[3]. The more electron-withdrawing groups there are in

a substrate, the faster is σ-complex formation and nucleophilic substitution[85]. However, the effects are not additive: subsequent substituents do not exert as great an effect as the first[3].

A para nitro-group is believed[86,87] to be more strongly activating than an ortho nitro-group. The para substituent exerts only an electronic effect, while an ortho substituent can also have a steric effect[3]. However, since nucleophiles attack perpendicular to the ring, steric hindrance should only be important if the substituent and/or the nucleophile is unusually large[2].

Since most of the important activating substituents, e.g. the nitro-group, only exert their maximum electron-withdrawing effect when they are coplanar with the aromatic ring, steric interference may reduce the degree of activation by causing the activating group to rotate out of the plane of the ring. For example, the ortho nitro-groups of 2,4,6-trinitrophenetole are rotated out of the plane of the ring[88], while they are coplanar with the ring in the 1,1 diethoxy complex[19], and so help to stabilise the complex.

Whether the reaction stops at the σ-adduct or proceeds to substitution depends upon how well the negative charge is delocalised over the aromatic ring, and upon whether or not there is a good leaving group present[85].

2. Nucleophile and Leaving Group Effects

In reversible processes, the nucleophile and leaving group are interchangeable; in all cases, they are closely related. There is no unique scale of relative reactivity[27]: the reactivity of the nucleophile depends upon the leaving group, and *vice versa*. The pattern of variation of reactivity

depends upon the substrate. While there is a relationship between leaving group ability and the pK_a of the group[52], nucleophilic activity cannot be related to the Brönstead basicity of the nucleophile. This is because there is no direct link between the carbon basicity (affinity for carbon) and proton (Brönstead) basicity of a nucleophile[89].

Measurement of the equilibrium constants of formation of complexes for a series of nucleophiles with a given substrate in a particular solvent gives a scale of carbon basicities of the nucleophiles[8] in that solvent. Differences in relative carbon and proton basicities can be seen in the reaction of oxygen and sulphur bases with N-substituted picramides[8]: oxygen bases give both amino-proton abstraction and base addition, while sulphur bases give only base addition.

When there is more than one ring position available for attack, the preferred site depends upon the nucleophile. For example[8], the thermodynamically stable adduct of trinitroanisole is that at C-1 when the nucleophile is methoxide or azide ion or diethylamine, but that at C-3 with sulphite or acetonate ion.

3. Medium Effects

The solvent can play a major role in stabilising a σ-complex. Changing from a protic solvent, such as water, to a dipolar aprotic solvent, such as DMSO, tends to increase the degree of formation of a 1:1 adduct, without changing the mode of interaction[8]. This is useful in n.m.r. studies, when the use of DMSO increases the extent of conversion to complex. A few solvents, however, produce anions which interact directly with the substrate, e.g. acetonate ion from acetone.

When competing modes of interaction exist, e.g. when there are two possible sites of attack, a change of solvent can alter the balance between the two reactions[13].

Higher adducts tend to be favoured in protic solvents, e.g. water. It has been suggested[8] that this is due to their increasing resemblance to inorganic salts, which increases the degree of solvation by water. As well as changing the extent of solvation of a complex, a change of solvent can also alter the reactivity of the nucleophile[3], by altering the extent of solvation. The solvation of a species by a particular solvent depends upon its charge-type, size and polarisability[3]. Thus, the solvent effects on a σ-complex and on the transition state leading to it (i.e. on the thermodynamic stability and rate of formation of a complex) are determined by the reactants used.

The ionic strength of the solution can affect rates and complex stabilities, depending upon the charge type of the reaction[2,13]. Ion aggregation can affect both the reactivity of the nucleophile[3] and the stability of the complex[47,90,91,92].

Intramolecular hydrogen-bonding stabilises some σ-complexes[93], the nitro-group being an efficient hydrogen-bond acceptor. When the solvent is also a hydrogen-bond acceptor, this may compete with intramolecular hydrogen-bonding, so that a change of solvent may cause a change in the rate of formation or in the stability of the complex[9].

CHAPTER TWO

EXPERIMENTAL

MATERIALS

1. Solvents

(a) Water: distilled water was boiled for circa 15 minutes to expel dissolved CO_2, and stored under a soda-lime guard tube.

(b) Methanol: AnalaR grade, used without further treatment.

(c) Isopropanol: AnalaR grade, used without further treatment.

(d) Dimethyl sulphoxide: G.P.R. grade, dried over calcium hydride, fractionally distilled under reduced pressure, and stored in a desiccator.

(e) Dimethyl sulphoxide-d_6: commercial sample, used as supplied.

(f) 1,4-Dioxan: spectroscopic grade, used in making up stock solutions of substrates. Reaction solutions generally contained less than 1% dioxan, a negligible amount.

2. Substrates

(a) 1-Chloro-2,4-dinitrobenzene: commercial sample, recrystallised from ethanol. Pale yellow crystals, m.p. 51-3°C (lit.[94] 51°C).

(b) 1,3,5-Trinitrobenzene: dried reagent grade. Pale brown plates, m.p. 123°C (lit.[94] 122.5°C).

(c) Picryl chloride: recrystallised commercial sample. Small, yellow plates, m.p. 82-3°C (lit.[94] 83°C).

(d) Picric acid: recrystallised commercial sample. Light lemon-yellow plates, m.p. 122°C (lit.[94] 122.5°C).

(e) 2,4,6-Trinitroanisole: recrystallised commercial sample. Yellow-brown plates, m.p. 67°C (lit.[94] 68°C).

(f) 1-Isopropoxy-2,4,6-trinitrobenzene: prepared[47] from picryl chloride and sodium isopropoxide. Fine, pale brown crystals, m.p. 94-5°C (lit.[22] 95°C).

(g) 1,2,4,6-Tetranitrobenzene: prepared from picramide[95,96] and recrystallised from chloroform. Fine, lemon-yellow powder, m.p. 124°C (lit.[95] 126°C).

(h) Picramide: prepared by the addition of aqueous ammonia to a solution of picryl chloride in methanol. Dark-yellow crystalline powder, m.p. 195°C (lit.[94] 192-5°C).

(i) N-Methylpicramide: prepared from picryl chloride and methylamine. Yellow powder, m.p. 116°C (lit.[94] 115°C).

(j) N-Isopropylpicramide: prepared from picryl chloride and isopropylamine. Bright yellow powder, m.p. 108°C (lit.[94] 107°C).

(k) N-n-Butylpicramide: prepared by the addition of excess n-butylamine to a solution of picryl chloride in methanol, under reflux, and recrystallised from methanol. Deep yellow, fine, needle-shaped crystals, m.p. 82°C (lit.[94] 81°C). The n.m.r. spectrum was as expected, and showed no evidence of impurities.

(l) N-tert-Butylpicramide: prepared from picryl chloride and tert-butylamine. Orange, needle-shaped crystals, m.p. 95°C (lit.[97] 95°C).

(m) N-Phenylpicramide: prepared from picryl chloride and aniline. Bright orange, small, needle-shaped crystals, m.p. 183°C (lit.[94] 183°C). The n.m.r. spectrum was as expected, and showed no evidence of impurities.

(n) N,N-Dimethylpicramide: prepared by the addition of excess aqueous dimethylamine to a solution of picryl chloride in methanol, and recrystallised from glacial acetic acid. Deep yellow, needle-shaped crystals, m.p. 139°C (lit.[94] 138°C). The n.m.r. spectrum was as expected, and showed no evidence of impurities.

3. Nucleophiles

(a) Sodium hydroxide: prepared by washing AnalaR sodium hydroxide pellets, and dissolving the residual solid in boiled-out, distilled water. Stock solutions were titrated with standard acid. In a few cases, AVS standard solutions were used.

(b) Sodium methoxide: prepared by dissolving clean sodium metal in AnalaR methanol under nitrogen, and titrated with standard acid. Solutions of sodium methoxide in methanol-d were prepared in the same way.

(c) Tetramethylammonium isopropoxide: prepared by dilution of 25% aqueous tetramethylammonium hydroxide with isopropanol, and titrated with standard acid. Reaction solutions contained less than 1% water, a negligible quantity.

(d) n-Butylamine: G.P.R. grade, fractionated at atmospheric pressure; b.p. 77.5°C (lit.[94] 78°C). Some preliminary work used unpurified amine.

(e) Isopropylamine: reagent grade, fractionated at atmospheric pressure using a Fischer-Spaltrohr column; b.p. 32.5-33°C (lit.[94] 33-4°C).

(f) Benzylamine: commercial samples were used without further treatment (AnalaR grade for kinetic measurements).

(g) N-Deuterated benzylamine ($PhCH_2ND_2$): prepared by the reaction of benzylamine with deuterium oxide. After two exchange experiments, n.m.r. spectra indicated > 95% conversion to the deuterated product.

(h) Piperidine: commercial samples were used without further treatment (AnalaR grade for kinetic measurements).

(i) Diethylamine: AnalaR grade, fractionated at atmospheric pressure using a Fischer-Spaltrohr column; b.p. 55.5-56°C (lit.[94] 55.5°C). Some preliminary measurements were made using the commercial sample as supplied.

(j) Di-isopropylamine: AnalaR grade, used as supplied.

4. Salts, Catalysts, Buffers

(a) Sodium chloride: AnalaR grade, oven-dried.

(b) Sodium perchlorate: AnalaR grade monohydrate, dried by warming *in vacuo*.

(c) Tetraethylammonium chloride: commercial sample, dried by heating *in vacuo*; recrystallised[98] twice from 1:1 (v/v) toluene-acetonitrile, and dried by heating *in vacuo*. White, crystalline powder.

(d) Tetraethylammonium perchlorate: commercial sample, recrystallised[99] twice from toluene and dried by heating *in vacuo*. White, crystalline powder.

(e) n-Butylammonium chloride: prepared by bubbling hydrogen chloride gas through a solution of n-butylamine in diethyl ether, on an ice-bath. Colourless, plate-like crystals were filtered off and recrystallised from acetonitrile.

(f) Isopropylammonium perchlorate: a stock solution was prepared by mixing the appropriate weights of isopropylamine and 60% aqueous perchloric acid in a known volume of DMSO.

(g) Benzylammonium perchlorate: prepared by the addition of excess aqueous perchloric acid to a solution of benzylamine in absolute ethanol, on an ice-bath. On transfer to a dry-ice/acetone bath, near colourless crystals appeared, which were recrystallised twice from absolute ethanol, and dried by warming *in vacuo*.

(h) Piperidine hydrochloride: a commercial "pure" grade, used as supplied.

(i) Diethylammonium perchlorate: prepared[100] by the addition of excess aqueous perchloric acid to a solution of diethylamine in absolute ethanol, on an ice-bath. On transfer to a dry-ice/acetone bath, colourless crystals appeared, which were recrystallised twice from absolute ethanol and dried by warming *in vacuo*.

(j) Di-isopropylammonium perchlorate: prepared by the addition of excess aqueous perchloric acid to a solution of di-isopropylamine in absolute ethanol, on an ice-bath. On transfer to a dry-ice/acetone bath, colourless crystals appeared which were recrystallised twice from absolute ethanol and dried by warming *in vacuo*.

(k) Pyridine hydrochloride: prepared *in situ* from AnalaR pyridine and AnalaR (concentrated) hydrochloric acid.

(l) 1,4-Diazabicyclo-[2,2,2]octane (Dabco): reagent grade commercial sample, used as supplied.

(m) Borax buffers: prepared[101] from AnalaR borax (disodium tetraborate) with appropriate quantities of sodium hydroxide or hydrochloric acid.

(n) Carbonate buffers: prepared from solid sodium carbonate (decahydrate) and sodium hydrogen carbonate (anhydrous), giving a carbonate:bicarbonate ratio of 10:1.

MEASUREMENT TECHNIQUES

1. Rates

(a) Stopped-flow spectrophotometer: a 'Canterbury' SF-3A instrument, with 2 mm optical path length, was used, thermostatted at 25°C. First-order conditions were generally maintained, usually by keeping the nucleophile concentration in excess, or by buffering the base concentration. Reactions were monitored by following the change with time of the absorbance at a chosen wavelength. For small changes in absorbance, the measured difference in voltage can be assumed to be directly proportional to the change in optical density (and hence in concentration). Thus, for rate measurements, a plot of $\ln\Delta V$ vs t gives a straight line of slope k_{obs}, where $\Delta V = |V_\infty - V_t|$. In the few cases in which a reliable 'infinity' reading could not be obtained, Guggenheim[102] plots were used. Where more than one process occurred, either interference by the second reaction was avoided by choosing a suitable wavelength, or the processes were separated by visual extrapolation. The rate constants quoted are the mean of 4-6 individual runs, and are generally accurate to ca. 5%.

(b) Temperature-jump spectrophotometer: the instrument, supplied by Hartley Measurements, produced temperature jumps of ca. 7 deg.C by discharging a 0.05 μF capacitor through a heated volume of 0.5 cm^3. Tests with alkaline glycine containing phenolphthalein indicated a heating time of approximately 2 μs.

(c) Recording spectrophotometer: reactions which were too slow for the stopped-flow were followed using a Beckman S-25 instrument, thermostatted at 25°C.

2. Equilibria

Equilibrium optical density measurements were made at 25°C using either a Unicam SP500 instrument, with a path length of 1 cm, or the stopped-flow. In the latter case, the optical density is given by equation (2.1):

$$OD_s = \log \frac{V_o}{(V_o - \Delta V)} \qquad (2.1)$$

where V_o = background voltage (generally 5V),

$\Delta V = V_c - V_s$,

V_c = voltage in the absence of the absorbing species,

V_s = voltage in the presence of the absorbing species.

3. Visible Spectra

These were either recorded on a Unicam SP8000 instrument at ambient temperature, or measured point-by-point on the stopped-flow spectrophotometer.

4. Proton Magnetic Resonance Spectra

These were measured at 60 MHz on a Varian A56/60 instrument, or at 90 MHz on a Brucker HX90E instrument, modified for FT operation and using a deuterium lock. All shift measurements are relative to internal tetramethylsilane.

5. pH

The pHs of buffer solutions were measured using EIL 23A and EIL 2070 instruments, calibrated at pH 4 and pH 9.27.

6. Conductance Measurements

These were carried out using a Pye 11700 instrument with a Mullard conductivity cell.

CHAPTER THREE

THE INTERACTION OF 1,3,5-TRINITROBENZENE AND 1-ISOPROPOXY-2,4,6-TRINITROBENZENE WITH ISOPROPOXIDE ION IN ISOPROPANOL

INTRODUCTION

Crampton and Gilmore[47] investigated some reactions of aromatic nitro-compounds with sodium isopropoxide, in which ion-association is important. In some complementary experiments, the results of which are reported here, sodium isopropoxide was replaced by tetramethylammonium isopropoxide. In dilute solution, this base is expected to be largely dissociated, so that the reaction involves "free" isopropoxide ion.

In a study of the reactions of 1,3,5-trinitrobenzene in a variety of alkoxide/alcohol systems, Gan and Norris[103] found no evidence for ion-pairing in the range $0 < [^{i}PrO^{-}] \leq 7 \times 10^{-3}$ mol l^{-1}. However, the association constant for sodium isopropoxide in isopropanol is known[104] to be 1.9×10^{4} $l\ mol^{-1}$. Crampton[47] has shown that the rate of addition of sodium isopropoxide to trinitrobenzene is considerably reduced by added sodium perchlorate (which increases the amount of $Na^{+},{}^{i}PrO^{-}$ ion pair present) and increased by added 18-crown-6-polyether, an efficient complexing agent for sodium ions. This indicates that ion-paired isopropoxide is less reactive towards trinitrobenzene than is the free ion.

1,1-Dialkoxy complexes are known[90,91,92] to associate strongly with cations such as Na^{+}, K^{+}, Ba^{2+}, Ca^{2+}; the cation is believed[91] to be held by a 'cage' of electronegative atoms, 3.1, reminiscent of the way in which the oxygen atoms of crown ethers surround the central metal ion.

Crampton's results[47] for the addition of isopropoxide ion to 1-isopropoxy-2,4-dinitro-6-X-benzenes provide more evidence for ion-association between dialkoxy complexes and sodium ions. When $X = CO_2{}^{i}Pr$, the complex is better stabilised

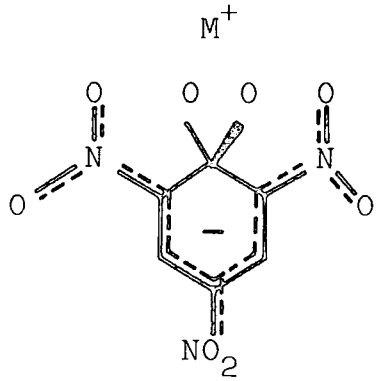

3.1

by ion-pairing than is isopropoxide ion, while the order is reversed for X = Cl or H. The rates of the forward and reverse processes are also increased by ion-association in these cases. However, complexes formed by the addition of isopropoxide ion at an unsubstituted ring position show little tendency to form ion-pairs with sodium.

In common with other alkoxide additions[8,105], addition of isopropoxide ion to an unsubstituted ring position is faster than that at a substituted position (i.e. C-O^{i}Pr), but the latter produces the more stable adduct. This is partly due to ion-association, which favours the 1,1-adduct, but the major factors are believed to be the stabilising influence of multiple alkoxy substitution[30] and/or release of steric strain at the 1-position[106], as in the case of other alkoxides.

EXPERIMENTAL

The addition of tetramethylammonium isopropoxide to trinitrobenzene and 1-isopropoxy-2,4,6-trinitrobenzene in isopropanol was studied by stopped-flow spectrophotometry. Reactions were carried out at 25°C, under first-order conditions, with the base in at least 10-fold excess over the substrate.

Optical density measurements for the trinitrobenzene reaction were made at 31°C, using the SP8000 spectrophotometer.

RESULTS AND DISCUSSION

1. 1,3,5-Trinitrobenzene

Conversion to complex 3.2 (λ_{max} 425 nm, $\varepsilon = 2.6 \times 10^4$ l mol^{-1} cm^{-1}; 500 nm, 1.8×10^4) is virtually complete at very low base concentrations, 1×10^{-4} M isopropoxide causing >90% conversion. The reaction was followed by monitoring the increase in absorption at 500 nm, using the stopped-flow spectrophotometer. Measured rate constants are given in Table 3.1, and are related to the forward and reverse rate coefficients, k_1 and k_{-1}, by equation (3.1), as is expected for the reaction shown in Scheme 3.1.

Scheme 3.1

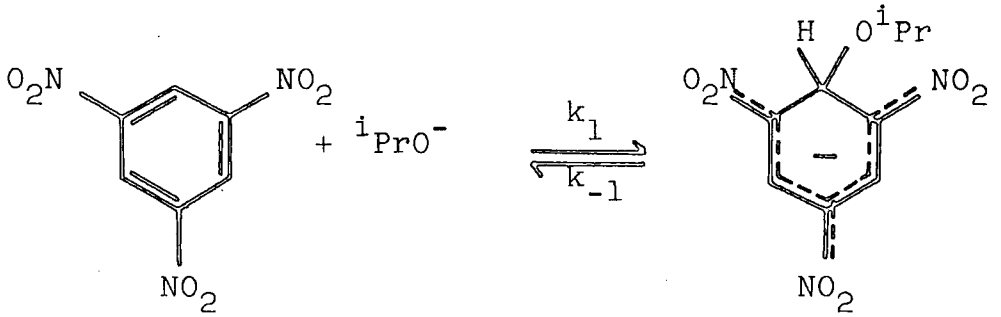

$$\frac{d[3.2]}{dt} = k_1[S][^iPrO^-] - k_{-1}[3.2]$$

$$[S]_i = [S] + [3.2]$$

$$= k_1[^iPrO^-]([S]_i - [3.2]) - k_{-1}[3.2] \qquad (i)$$

At equilibrium,

$$\frac{d[3.2]}{dt} = k_1[^iPrO^-]([S]_i - [3.2]_e) - k_{-1}[3.2]_e = 0 \qquad (ii)$$

Subtracting (ii) from (i),

$$\frac{d[3.2]}{dt} = k_1[^iPrO^-]([3.2]_e - [3.2]) + k_{-1}([3.2]_e - [3.2])$$

TABLE 3.1

Rate constants for 1:1 complex formation from 1,3,5-trinitrobenzene and isopropoxide ion in isopropanol at 25°C.

$10^4[^iPrO^-]$ M	k_{obs}^a s^{-1}
1.04	17.7
2.08	49.0
3.11	79.8
4.15	101

a. Measured on the stopped-flow spectrophotometer at 500 nm.

$$k_{obs} = \frac{1}{([\underline{3.2}]_e - [\underline{3.2}])} \frac{d[\underline{3.2}]}{dt}$$

$$k_{obs} = k_1[^iPrO^-] + k_{-1} \qquad (3.1)$$

$$K_1 = \frac{[\underline{3.2}]}{[S][^iPrO^-]} = \frac{k_1}{k_{-1}} \qquad (3.2)$$

Plotting k_{obs} vs $[^iPrO^-]$ produces a straight line of slope $k_1 = 2.5 \times 10^5$ l mol^{-1} s^{-1}, passing through the origin: i.e. k_{-1} is too small to be measured, because of the high value of K_1 (equation 3.2).

The bulky tetramethylammonium ion is not expected to associate to any significant extent with isopropoxide ion. In accordance with this, the results obtained here are in close agreement with those obtained[47] using sodium isopropoxide and crown ether. Thus, these results refer to the addition of free isopropoxide ions, which are more reactive towards trinitrobenzene than are sodium isopropoxide ion pairs.

Measurements of the optical density at the two maxima (not shown) made using the SP8000, indicate an equilibrium constant for complex formation, $K_1 \geq 3 \times 10^5$ l mol^{-1}. Because of the high degree of conversion, and the very low base concentrations used, this figure can only be treated as an estimate.

2. 1-Isopropoxy-2,4,6-trinitrobenzene

Two time-dependent processes are observable[47]; fast formation of the C-3 adduct, 3.3, and slower ionisation to the C-1 adduct, 3.4. The fast process was followed at 480nm, using the stopped-flow. The results, shown in Table 3.2, are in agreement with Scheme 3.2 and equations (3.3) and (3.4), and give a value of $k_3 = 7.6 \times 10^3$ l mol^{-1} s^{-1}. k_{-3} is too small to be determined.

TABLE 3.2

Rate constants for complex formation from 1-isopropoxy-2,4,6-trinitrobenzene and isopropoxide ion in isopropanol at 25°C.

$10^4[{}^{i}PrO^-]$	k_{fast}[a]	OD[b]	$10^4 k_{slow}$[c]
M	s^{-1}		s^{-1}
2.0	1.15	0.0244	-
4.0	2.83	0.0243	-
4.86	-	-	4.72
8.0	5.46	0.0240	-
9.66	-	-	4.15
16.0	12.7	0.0242	-
20.0	16.0	-	-

a. Measured on the stopped-flow spectrophotometer at 480 nm.

b. Measured on the stopped-flow spectrophotometer at 480 nm, after completion of the fast process. Corresponds to 9.67×10^{-6} M substrate.

c. Measured on the Beckman S-25 spectrophotometer at 480 nm. Rate constants were calculated using the Guggenheim[102] method.

SCHEME 3.2

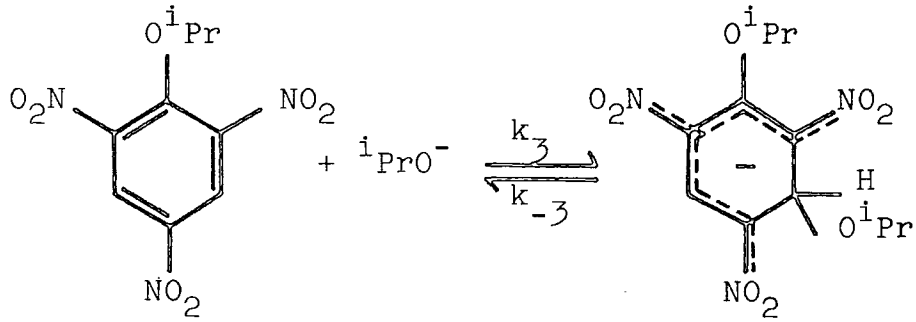

S 3.3

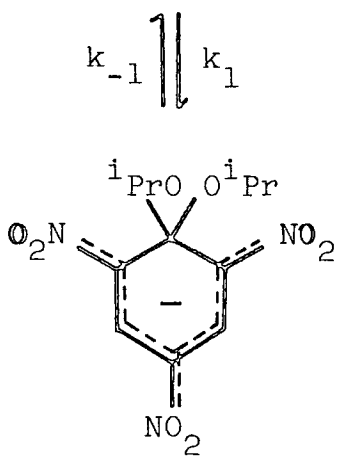

3.4

$$k_{fast} = k_3[^iPrO^-] + k_{-3} \qquad (3.3)$$

$$K_3 = \frac{[\underline{3.3}]}{[S][^iPrO^-]} = \frac{k_3}{k_{-3}} \qquad (3.4)$$

For k_{slow}:

$$[S]_i = [S] + [\underline{3.3}] + [\underline{3.4}]$$

$$[S] = [S]_i - [\underline{3.3}] - [\underline{3.4}]$$

$$= [S]_i - K_3[S][^iPrO^-] - [\underline{3.4}]$$

$$[S](1 + K_3[^iPrO^-]) = [S]_i - [\underline{3.4}]$$

$$[S] = \frac{([S]_i - [\underline{3.4}])}{(1 + K_3[^iPrO^-])}$$

$$\frac{d[\underline{3.4}]}{dt} = k_1[S][^iPrO^-] - k_{-1}[\underline{3.4}]$$

$$= \frac{k_1[^iPrO^-]([S]_i - [\underline{3.4}])}{(1 + K_3[^iPrO^-])} - k_{-1}[\underline{3.4}] \qquad (i)$$

At equilibrium,

$$\frac{d[\underline{3.4}]}{dt} = \frac{k_1[^iPrO^-]([S]_i - [\underline{3.4}]_e)}{(1 + K_3[^iPrO^-])} - k_{-1}[\underline{3.4}]_e = 0 \qquad (ii)$$

Subtracting (ii) from (i),

$$\frac{d[\underline{3.4}]}{dt} = \frac{k_1[^iPrO^-]([\underline{3.4}]_e - [\underline{3.4}])}{(1 + K_3[^iPrO^-])} + k_{-1}([\underline{3.4}]_e - [\underline{3.4}])$$

$$k_{obs} = \frac{1}{([\underline{3.4}]_e - [\underline{3.4}])} \frac{d[\underline{3.4}]}{dt}$$

$$= \frac{k_1[^iPrO^-]}{(1 + K_3[^iPrO^-])} + k_{-1} \qquad (3.5)$$

As in the case of trinitrobenzene, free isopropoxide ion is more reactive towards addition at C-H than is the sodium

isopropoxide ion pair, which gives a value[47] of $k_3 = 2.4 \times 10^3$ l mol^{-1} s^{-1}.

The optical density measurements (Table 3.2) indicate complete conversion to the C-3 adduct by circa 2×10^{-4} M base, leading to an estimated value of $K_3 \geq 1 \times 10^5$ l mol^{-1}.

The C-1 complex is expected to have high stability, and hence a small value of k_{-1}. This, together with the large value of K_3, reduces equation (3.5) to equation (3.6), leading to an estimated value of $k_1 \geq 50$ l mol^{-1} s^{-1}.

$$k_{slow} = \frac{k_1}{K_3} \qquad (3.6)$$

3. Comparison of Results

The results for the two substrates are summarised in Table 3.3.

The rate of isopropoxide ion attack at C-H is lower in isopropoxytrinitrobenzene than in trinitrobenzene. The inductive electron-withdrawing effect of the isopropoxy group is expected to favour nucleophilic attack at C-3. However, the group is very bulky, and so probably causes the ortho nitro-groups to twist out of the plane of the ring (as the ethoxy group is known[88,107] to do). This reduces their ability to delocalise the negative charge in the σ-adduct, and hence decreases the rate of adduct formation.

TABLE 3.3

Rate and equilibrium constants for the addition of free isopropoxide ion to trinitrobenzene and 1-isopropoxytrinitrobenzene in isopropanol at 25°C.

		TNB	^{i}PrO-TNB
k_3^a	($l\ mol^{-1} s^{-1}$)	2.5×10^5	7.6×10^3
K_3	($l\ mol^{-1}$)	$\geq 3.0 \times 10^5$	$\geq 1.0 \times 10^5$
k_1^b	($l\ mol^{-1}\ s^{-1}$)	-	≥ 50

a. Attack at C-H

b. Attack at C-O^{i}Pr.

CHAPTER FOUR

THE INTERACTION OF 1-X-2,4,6-TRINITROBENZENES WITH HYDROXIDE ION IN WATER

INTRODUCTION

The reaction of aqueous sodium hydroxide with 1-X-2,4,6-trinitrobenzenes may result in nucleophilic substitution of X by hydroxide ion if X is labile. The reaction probably follows the addition-elimination mechanism[3,13], involving a species of type 4.1. If, however, X is a poor leaving group, stable σ-adducts can be formed[38,39,108,109,110]: the structure of a 1:1 σ-adduct could, in principle, be either 4.1 or 4.2.

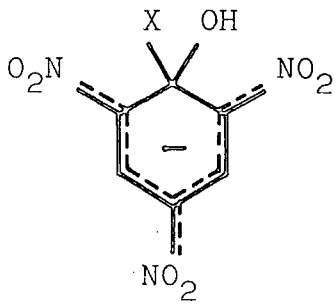

4.1

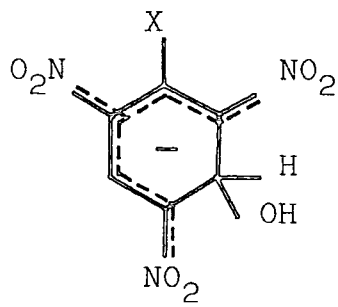

4.2

Structure 4.1 was proposed[111] for the transient coloured species observed in the alkaline hydrolyses of picryl chloride and 2,4,6-trinitroanisole. However, this would require loss of hydroxide ion from 4.1 to be considerably faster than loss of chloride or methoxide ion[105,112], which is contrary to known leaving group tendencies[113]. ^1H n.m.r. measurements[50,96,114] support the view that the transient coloured species are the C-3 adducts, 4.2.

This chapter reports on the reactions of a series of 1-X-2,4,6-trinitrobenzenes (X = O^-, OMe, Cl, NO_2, NMe_2) with aqueous sodium hydroxide. The results allow a comparison to be made between the rates of attack at C-1 and at C-3.

Eventually, the substances used undergo nucleophilic

substitution of X by hydroxide ion to form picric acid (present in aqueous solution as the picrate ion). This substitution could occur by attack on the substrate alone, but the results of this work suggest that substitution also occurs in the C-3 adduct.

Evidence has been obtained for the ionisation of added hydroxyl groups in reactions occurring in water[36,76] and in DMSO-water mixtures[37]. Further evidence for this phenomenon is presented here.

The results in this chapter have been obtained using sodium hydroxide concentrations up to 1M where activity coefficients are expected to deviate markedly from unity. One method for circumventing this problem would be to relate the basicity of the solution to the appropriate acidity function, in this case J_-[82]. An alternative, and that employed here, is to maintain the solutions at constant ionic strength, in this case using sodium chloride as the compensating electrolyte.

There is evidence[115,116] to suggest that the presence of sodium chloride in aqueous solution slightly reduces the rates of formation and decomposition of σ-complexes. Work on 1-chloro-2,4-dinitrobenzene is included in this chapter, to determine the extent of the salt effect, if any, on complex formation in the other systems studied.

EXPERIMENTAL

The reaction rates were measured by following the change in absorbance with time at a suitable wavelength, generally using the stopped-flow spectrophotometer. Slow reactions were followed in the same way, but using the Beckman S-25 and Unicam SP500 instruments. Spectra were measured on the SP8000 spectrophotometer, or determined point-by-point on the stopped-flow.

All rate measurements were carried out with the base concentration in large excess over the substrate concentration, or with the base buffered, so good first-order plots were obtained. Some typical results are shown in Table 4.1, the rate constants calculated from the integrated form of the first-order rate expression[117].

Mixing sodium hydroxide solutions above 1M with water in the stopped-flow was found to produce turbidity, which caused irregular traces on the slower timescales. This problem was overcome by mixing solutions of similar ionic strength.

TABLE 4.1

Typical results from kinetic measurements.

(i) 10^{-4}M picryl chloride, 0.02M sodium hydroxide, μ = 2.0M (with sodium chloride as compensating electrolyte), measured at 480 nm.

(ii) 10^{-4}M tetranitrobenzene, 0.005M sodium hydroxide, measured at 500 nm.

	(i)			(ii)		
t	V	ΔV^a	k^b	V	ΔV^a	k^b
s			s^{-1}			s^{-1}
0.01	5.9	3.6	-	-	-	-
0.02	5.5	3.2	11.8	6.0	4.2	-
0.04	4.9	2.6	10.8	4.9	3.1	15.2
0.06	4.3	2.0	11.8	4.1	2.3	15.1
0.08	3.9	1.6	11.6	3.5	1.7	15.1
0.10	3.6	1.3	11.3	3.1	1.3	14.7
0.12	3.3	1.0	11.6	2.7	0.9	15.4
0.14	3.1	0.8	11.6	2.5	0.7	14.9
0.16	2.9	0.6	11.9	2.3	0.5	15.2
0.18	2.8	0.5	11.6	2.2	0.4	14.7
0.20	2.7	0.4	11.6	2.1	0.3	14.7
∞	2.3	0	-	1.8	0	-
mean			11.6			15.0

a. $\Delta V = V - V_\infty$

b. $k = \frac{1}{(t-t^o)} \ln \frac{\Delta V^o}{\Delta V}$

RESULTS AND DISCUSSION

1. 1-Chloro-2,4-dinitrobenzene

This substrate was used as a 'model' system to determine the magnitude of the effect of changing the nature of the electrolyte from mainly sodium chloride (at low sodium hydroxide concentrations) to mainly sodium hydroxide, i.e. to ascertain to what extent, if any, sodium chloride exerts a specific salt effect.

As the substrate is not highly activated, a coloured intermediate is not observed, and attack at C-1 is rate-determining:

SCHEME 4.1

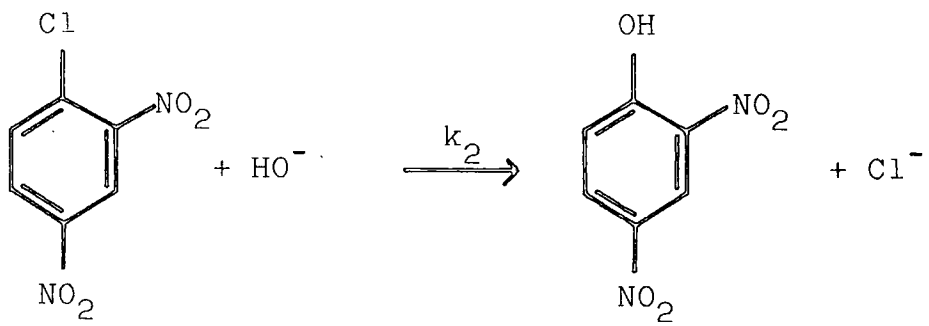

S P

$$\frac{d[P]}{dt} = k_2[S][HO^-]$$

$$k_{obs} = \frac{1}{[S]} \frac{d[P]}{dt}$$

$$= k_2[HO^-] \qquad (4.1)$$

The product, 2,4-dinitrophenol, was identified by its spectrum (λ_{max} 360 nm).

The reaction was followed by monitoring the increase in absorption at 360 nm, using the SP500. The results, shown in Table 4.2, indicate a small differential salt effect at

TABLE 4.2

Rate constants for the reaction between 1-chloro-2,4-dinitrobenzene and sodium hydroxide in water at 25°C, μ= 2.0M(NaCl)

[NaOH]	$10^5 k$	$10^4 k_1$ [a]
M	s^{-1}	1 $mol^{-1} s^{-1}$
0.05	0.568	1.14
0.10	1.17	1.17
0.30	3.57	1.19
0.60	8.14	1.36
0.99	15.4	1.56

a. $k_1 = \frac{k}{[NaOH]}$

base concentrations above circa 0.5M. This justifies the assumption, for fairly dilute base solutions, that constant values of k_1 and k_3 (for nucleophilic attack at aromatic carbon) can be obtained when the NaOH : NaCl ratio is changing.

2. Picric Acid

Because of its high dissociation constant[118], picric acid exists in aqueous solution as the picrate ion. Thus, these results apply to attack by hydroxide ion on an already negatively charged species, making ionic strength effects more important than in the case of electrically neutral substrates.

In concentrated base solution, picrate ion is known[39] to form a stable diadduct at C-3 and C-5. Stopped-flow spectrophotometry shows two separate processes. The faster process, associated with formation of the 1:1 adduct, 4.3, was measured at 500 nm using the stopped-flow spectrophotometer. The results, shown in Table 4.3, are in accord with Scheme 4.2.

TABLE 4.3

Rate and equilibrium constants for the reaction of picrate ion with sodium hydroxide in water at 25°C, μ = 2.0 M (NaCl).

$[HO^-]$ M	k_f s^{-1}	k_f[a](calc) s^{-1}	OD[b]	K_c[c] 1 mol^{-1}	K_c[d](calc) 1 mol^{-1}
0.05	19.2	19.2	0.0035	0.014	0.0135
0.10	17.6	18.5	0.0070	0.014	0.014
0.20	17.9	17.3	0.0145	0.0145	0.015
0.40	15.0	15.3	0.033	0.0165	0.017
0.60	13.6	13.7	0.060	0.020	0.019
0.80	12.0	12.4	0.080	0.020	0.021
1.00	11.6	11.4	0.137	0.027	0.023

a. Calculated from equation (4.2), using k_3 = 0.26 1 $mol^{-1}s^{-1}$; k_{-3} = 20 s^{-1}; K = 0.8 1 mol^{-1}.

b. For 5 x 10^{-4} M substrate in a 1 cm cell; measured on completion of the fast process and corrected for absorption by unreacted substrate.

c. Calculated from equation (4.3), assuming ε(4.3) = 1 x 10^4 1 mol^{-1} cm^{-1}.

d. Calculated from equation (4.4), using K_3 = 0.013 1 mol^{-1}; K = 0.8 1 mol^{-1}.

SCHEME 4.2

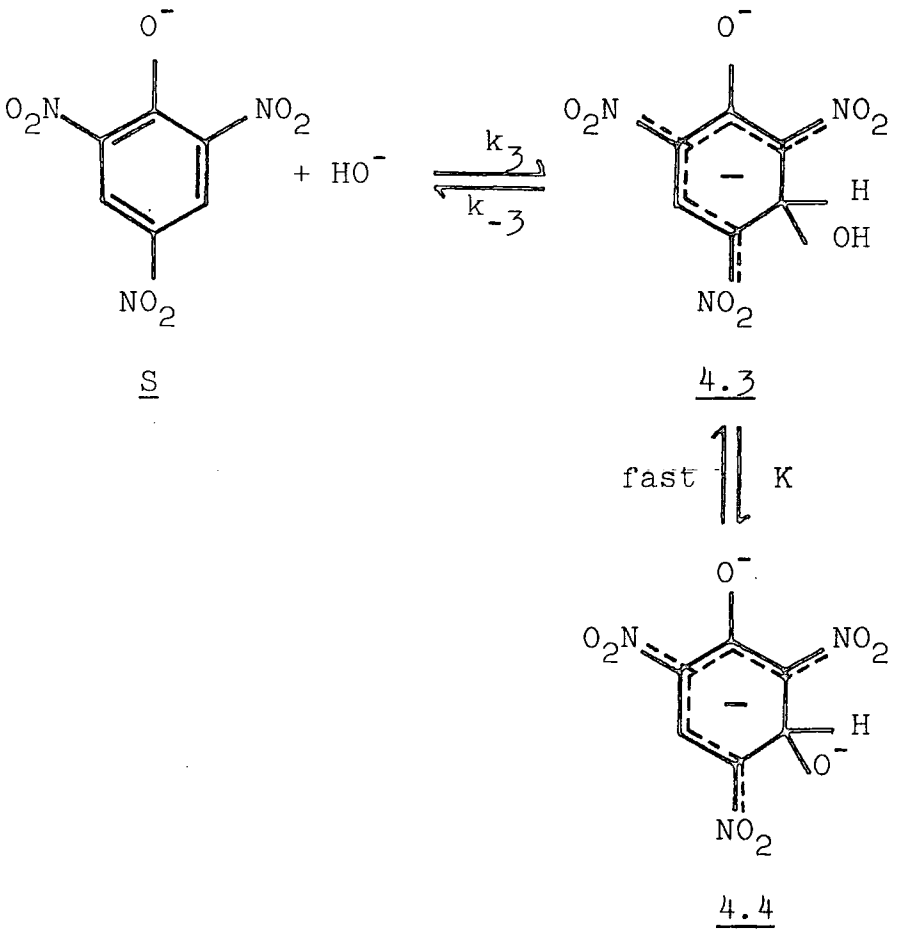

$$\frac{-d[S]}{dt} = k_3[S][HO^-] - k_{-3}[\underline{4.3}]$$

$$= k_{fast}[S]$$

$$\frac{d[S]}{dt} + \frac{d[\underline{4.3}]}{dt} + \frac{d[\underline{4.4}]}{dt} = 0$$

$$\frac{d[S]}{dt} + \frac{d[\underline{4.3}]}{dt}(1 + K[HO^-]) = 0$$

$$k_{fast}[S] = k_3[S][HO^-] - k_{-3}[\underline{4.3}]$$

$$\therefore\ k_{fast}\frac{d[S]}{dt} = k_3[HO^-]\frac{d[S]}{dt} - k_{-3}\frac{d[\underline{4.3}]}{dt}$$

$$k_{fast} = k_3[HO^-] + \frac{k_{-3}}{(1 + K[HO^-])} \qquad (4.2)$$

$$K_c = \frac{[complex]}{[S][HO^-]} = \frac{OD}{(OD_\infty - OD)[HO^-]} \qquad (4.3)$$

$$K_c = K_3(1 + K[HO^-]) \qquad (4.4)$$

The decrease in the observed rate constant with increasing base concentration can be explained in terms of ionisation of the added hydroxyl group.

The slower process observable by stopped-flow has a very small amplitude at the base concentrations used. In 1M base solution, the process causes an increase in absorption at 390 nm and a decrease at 480 nm, with a measured rate constant of 0.15 s^{-1}. This process is probably the formation of the 1:2 adduct, which is known[39] to have an absorption maximum at 390 nm.

3. 2,4,6-Trinitroanisole

Use of the stopped-flow spectrophotometer shows two processes, fast formation of the coloured adduct, and a slower decomposition to picrate ion (identified by its spectrum). The visible spectrum of the coloured species changes as the base concentration is increased, the maximum shifting to

longer wavelength (Figure 4.1). No new relaxation process is observable to correspond to this change, which is therefore attributed to ionisation of the hydroxyl adduct, 4.5 ⟶ 4.6 (Scheme 4.3).

The rate data for the fast process (Table 4.4) provide further evidence of the ionisation of the added hydroxyl group.

There is a discrepancy between the value of K_3 obtained from kinetic measurements (1.4 l mol^{-1}) and that from optical density measurements (1.2 l mol^{-1}). This probably results from the assumption that the extinction coefficients of 4.5 and 4.6 are identical. If they are not, then the (unknown) variation in the proportion of each species present in the solutions used will cause differences in the calculated value of K_3.

Picrate ion could be formed either by nucleophilic attack on the substrate only, or by attack on the 3-hydroxy adduct (in either the ionised or unionised form). If picrate ion were formed only by nucleophilic attack on the substrate (equation 4.5), then the rate of the slow process would decrease with increasing base concentration, as the amount of substrate present was reduced by conversion to the 3-hydroxy complex, 4.5, and dianion, 4.6:

$$S + HO^- \underset{}{\overset{K_3}{\rightleftharpoons}} 4.5 \overset{K}{\rightleftharpoons} 4.6$$

$$\downarrow k_A$$

$$P$$

$$\frac{d[P]}{dt} + \frac{d[S]}{dt} + \frac{d[4.5]}{dt} + \frac{d[4.6]}{dt} = 0$$

FIGURE 4.1

Spectra of the 1:1 adduct formed from 2,4,6-trinitroanisole and sodium hydroxide in water at 25°C, μ = 2.0 M (NaCl). Spectra are for 1 cm cells, and are corrected for absorption by unreacted substrate.

A. Spectrum of 10^{-5} M trinitroanisole.

B. 4×10^{-5} M trinitroanisole, 0.1 M sodium hydroxide. Spectrum attributed to the 1:1 adduct, 4.5.

C. 10^{-5} M trinitroanisole, 0.96 M sodium hydroxide. Spectrum attributed to the ionised 1:1 adduct, 4.6.

FIGURE 4.1

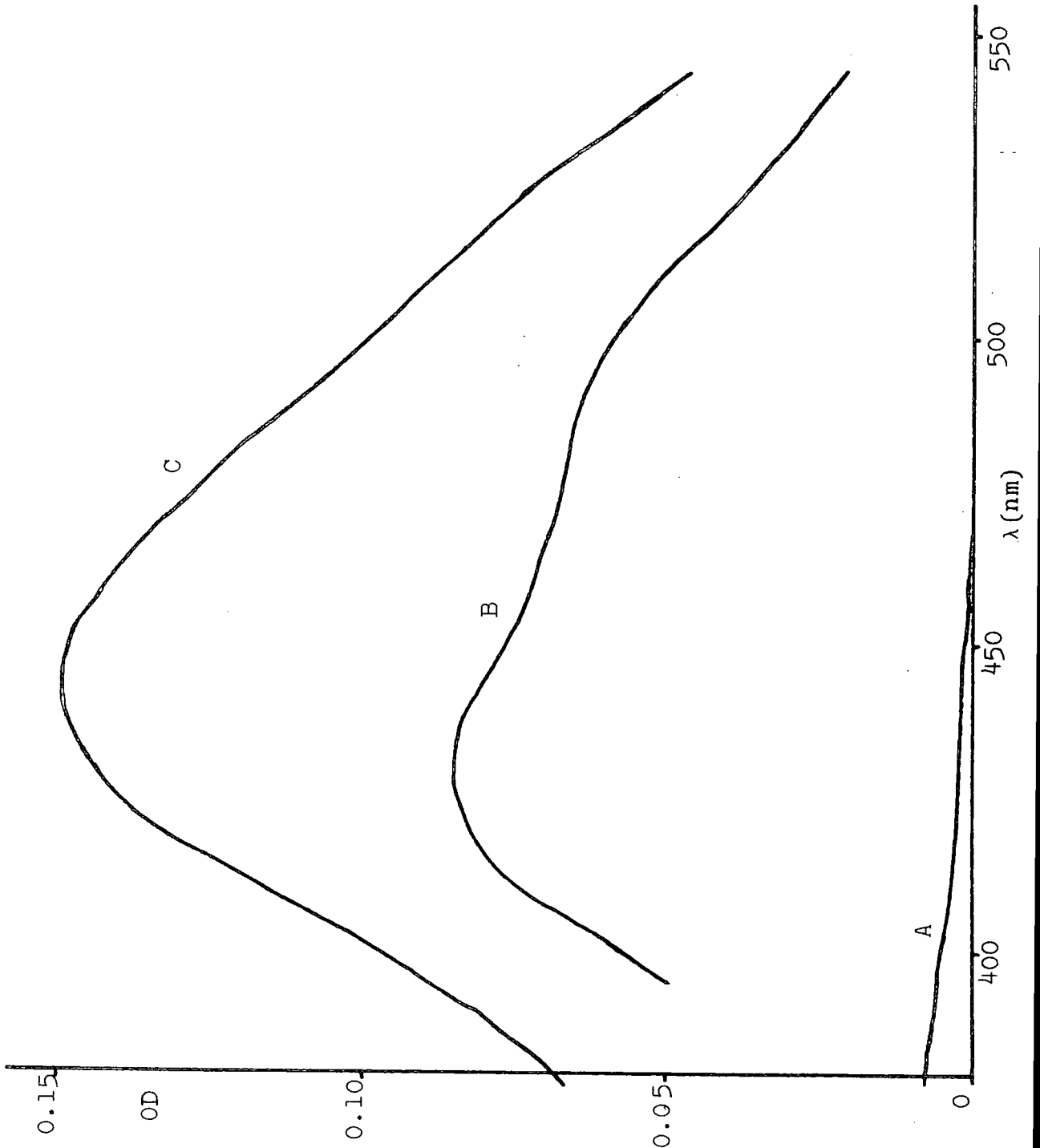

SCHEME 4.3

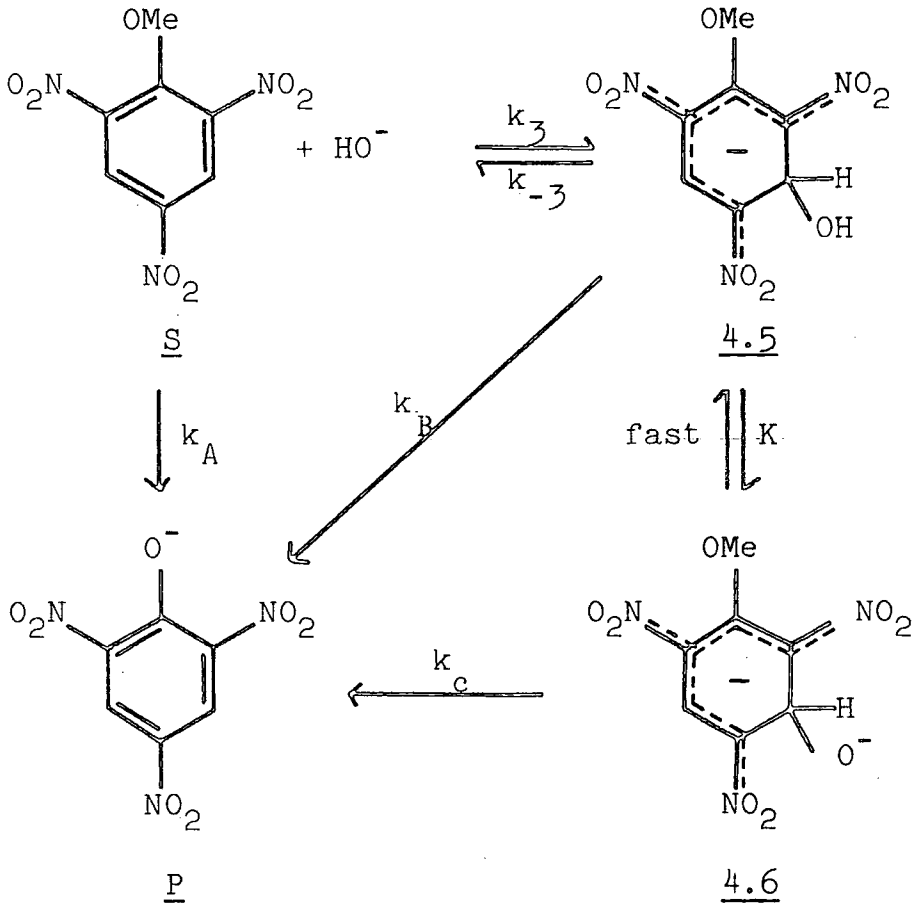
OMe
O_2N
NO_2
NO_2
+ HO^-
k_3
k_{-3}
OMe
O_2N
NO_2
H
OH
NO_2
S
4.5
k_A
k_B
fast
K
O^-
O_2N
NO_2
NO_2
k_c
OMe
O_2N
NO_2
H
O^-
NO_2
P
4.6

TABLE 4.4

Rate and equilibrium constants for the fast reaction of 2,4,6-trinitroanisole with sodium hydroxide in water at 25°C, μ= 2.0 M (NaCl).

$[HO^-]$ M	k_f[a] s^{-1}	k_f[b](calc) s^{-1}	OD[c]	K_c[d] l mol^{-1}	K_c[e](calc) l mol^{-1}
0.01	8.1	8.0	0.0015	1.25	1.3
0.02	7.9	7.7	0.0031	1.3	1.35
0.05	6.7	7.0	0.0075	1.35	1.55
0.10	6.4	6.4	0.0175	1.7	1.9
0.20	6.8	6.2	0.038	2.3	2.6
0.40	7.0	7.2	0.079	4.8	4.1
0.50	7.2	8.1	0.090	6.0	4.8
0.60	9.5	9.0	-	-	-
0.70	9.9	10.0	0.093	5.0	6.0
0.80	11.4	11.0	-	-	-

a. Measured at wavelengths chosen to avoid interference by the slow process.

b. Calculated from equation (4.2), using k_3 = 12 l $mol^{-1}s^{-1}$; k_{-3} = 8.3 s^{-1}; K = 6 l mol^{-1}.

c. Corresponds to OD after the completion of the fast colour-forming process. Measured by stopped-flow spectrophotometry at 480 nm. Values quoted are for 1 x 10^{-5} M substrate in a 1 cm cell.

d. Calculated from equation (4.3), assuming ε(4.5) = 1.13 x 10^4 l mol^{-1} cm^{-1}.

e. Calculated from equation (4.4), using K_3 = 1.2 l mol^{-1}; K = 6 l mol^{-1}.

$$[S] = \frac{[\underline{4.5}]}{K_3[HO^-]} \quad \therefore \quad \frac{d[S]}{dt} = \frac{1}{K_3[HO^-]} \frac{d[\underline{4.5}]}{dt}$$

$$[\underline{4.6}] = K[\underline{4.5}][HO^-] \quad \therefore \quad \frac{d[\underline{4.6}]}{dt} = K[HO^-] \frac{d[\underline{4.5}]}{dt}$$

$$\frac{d[P]}{dt} = k_A[S][HO^-]$$

$$= \frac{k_A}{K_3}[\underline{4.5}]$$

$$\therefore \frac{k_A}{K_3}[\underline{4.5}] + \frac{1}{K_3[HO^-]} \cdot \frac{d[\underline{4.5}]}{dt} + \frac{d[\underline{4.5}]}{dt} + K[HO^-] \frac{d[\underline{4.5}]}{dt} = 0$$

$$\frac{k_A}{K_3}[\underline{4.5}] + \frac{d[\underline{4.5}]}{dt}\left\{1 + K[HO^-] + \frac{1}{K_3[HO^-]}\right\} = 0$$

$$k_{slow} = \frac{-1}{[\underline{4.5}]} \cdot \frac{d[\underline{4.5}]}{dt}$$

$$\therefore \frac{k_A}{K_3} - k_{slow}\left\{1 + K[HO^-] + \frac{1}{K_3[HO^-]}\right\} = 0$$

$$k_{slow}\left(K_3[HO^-] + KK_3[HO^-]^2 + 1\right) = k_A[HO^-]$$

$$k_{slow} = \frac{k_A[HO^-]}{(1 + K_3[HO^-] + KK_3[HO^-]^2)} \qquad (4.5)$$

However, if picrate ion is also formed by attack on $\underline{4.5}$ and $\underline{4.6}$, as well as on the substrate, equation (4.6) results:

$$\frac{d[P]}{dt} = k_A[S][HO^-] + k_B[\underline{4.5}][HO^-] + k_C[\underline{4.6}][HO^-]$$

$$= k_A[S][HO^-] + k_B K_3[S][HO^-]^2 + k_C K_3 K[S][HO^-]^3$$

$$[S] = \frac{[\underline{4.5}]}{K_3[HO^-]} \quad \therefore \quad \frac{d[S]}{dt} = \frac{1}{K_3[HO^-]} \frac{d[\underline{4.5}]}{dt}$$

$$[\underline{4.6}] = K[\underline{4.5}][HO^-] \quad \therefore \quad \frac{d[\underline{4.6}]}{dt} = K[HO^-] \frac{d[\underline{4.5}]}{dt}$$

$$\frac{d[P]}{dt} + \frac{d[S]}{dt} + \frac{d[\underline{4.5}]}{dt} + \frac{d[\underline{4.6}]}{dt} = 0$$

$$\frac{d[P]}{dt} + \frac{1}{K_3[HO^-]} \frac{d[\underline{4.5}]}{dt} + \frac{d[\underline{4.5}]}{dt} + K[HO^-] \frac{d[\underline{4.5}]}{dt} = 0$$

$$\frac{d[P]}{dt} + \frac{d[\underline{4.5}]}{dt} \left\{ 1 + K[HO^-] + \frac{1}{K_3[HO^-]} \right\} = 0$$

$$\frac{d[P]}{dt} = k_A[S][HO^-] + k_B K_3[S][HO^-]^2 + k_C K_3 K[S][HO^-]^3$$

$$= \frac{k_A}{K_3} [\underline{4.5}] + k_B [HO^-][\underline{4.5}] + k_C K[HO^-]^2 [\underline{4.5}]$$

$$= [\underline{4.5}] \left\{ \frac{k_A}{K_3} + k_B[HO^-] + k_C K [HO^-]^2 \right\}$$

$$\therefore \left\{ \frac{k_A}{K_3} + k_B[HO^-] + k_C K[HO^-]^2 \right\} [\underline{4.5}] + \frac{d[\underline{4.5}]}{dt} \left\{ 1 + K[HO^-] + \frac{1}{K_3[HO^-]} \right\} = 0$$

$$k_{slow} = \frac{-1}{[\underline{4.5}]} \frac{d[\underline{4.5}]}{dt}$$

$$\therefore \left\{ \frac{k_A}{K_3} + k_B[HO^-] + k_C K[HO^-]^2 \right\} - k_{slow} \left\{ 1 + K[HO^-] + \frac{1}{K_3[HO^-]} \right\} = 0$$

$$\therefore k_{slow}(K_3[HO^-] + KK_3[HO^-]^2 + 1) = k_A[HO^-] + k_B K_3[HO^-]^2 + k_C KK_3[HO^-]^3$$

$$k_{slow} = \frac{(k_A[HO^-] + k_B K_3[HO^-]^2 + k_C KK_3[HO^-]^3)}{(1 + K_3[HO^-] + KK_3[HO^-]^2)} \qquad (4.6)$$

The observed rate coefficients are better correlated by equation (4.6) than by equation (4.5), as is shown in Table 4.5. This indicates that nucleophilic substitution of methoxide by hydroxide can occur in the 3-hydroxy adduct (in both forms) as well as in the substrate.

Alternatively, the experimental data could be fitted by allowing the value of k_A to increase with increasing base concentration, i.e. by considering a differential salt effect.

TABLE 4.5

Rate constants for the slow reaction of 2,4,6-trinitroanisole with sodium hydroxide in water at 25°C, μ = 2.0 M(NaCl).

$[HO^-]$ M	k_s[a] s^{-1}	k_s[b](calc) s^{-1}	k_s[c](calc) s^{-1}
0.02	0.026	0.027	0.027
0.05	0.064	0.064	0.066
0.10	0.131	0.115	0.125
0.20	0.202	0.175	0.205
0.40	0.26	0.19	0.27
0.50	0.30	0.19	0.30
0.60	0.31	0.17	0.29
0.70	0.31	0.16	0.30
0.80	0.29	0.15	0.30
1.00	0.30	0.13	0.31

a. Measured at wavelengths chosen to obtain the maximum change in OD.

b. Calculated from equation (4.5), using k_A = 1.4 l mol^{-1} s^{-1}; K_3 = 1.4 l mol^{-1}; K = 6 l mol^{-1}.

c. Calculated from equation (4.6), using k_A = 1.4 l mol^{-1} s^{-1}; k_B = 0.8 l mol^{-1} s^{-1}; k_C = 0.1 l mol^{-1} s^{-1}; K_3 = 1.4 l mol^{-1}; K = 6 l mol^{-1}.

However, the rate constant for nucleophilic attack on 1-chloro-2,4-dinitrobenzene (above) shows a much smaller variation with base concentration than that which would be needed here (1.14 - 1.56, compared with 1.4 - 3.3 over the same range of base concentration). Thus, the data suggest that nucleophilic substitution occurs within the 3-hydroxy adduct.

4. Picryl Chloride

Two processes are observed by stopped-flow spectrophotometry: fast colour formation, and a slower fading reaction which produces picrate ion (identified by its spectrum). The intermediate species has λ_{max} ca. 450 nm.

The rate coefficients for complex formation (Table 4.6) pass through a pronounced minimum as the base concentration increases. This is evidence for ionisation of the added hydroxyl group.

The value of K_3 obtained kinetically is different from that obtained from OD measurements. K_C was calculated assuming that the complex has the same extinction coefficient in both its ionised and unionised forms. As this is unlikely to be the case, and as the proportions of the two forms will vary in the different solutions, the value of K_3 obtained in this way is likely to be incorrect.

The rate coefficients for the formation of picrate ion (Table 4.7) are better correlated by equation (4.6) than by equation (4.5). This is evidence for the occurrence of nucleophilic attack in the 3-hydroxy adduct.

TABLE 4.6

Rate and equilibrium constants for the fast reaction of picryl chloride with sodium hydroxide in water at 25°C, μ = 2.0 M(NaCl).

$[HO^-]$ M	k_f[a] s^{-1}	k_f[b](calc) s^{-1}	OD[c]	K_c[d] 1 mol^{-1}	K_c[e](calc) 1 mol^{-1}
0.01	12.4	12.3	0.0012	0.78	0.70
0.02	11.8	11.1	0.0023	0.76	0.78
0.05	8.9	8.6	0.0071	0.96	1.05
0.10	7.0	6.8	0.0195	1.45	1.5
0.20	5.7	5.9	0.0485	2.3	2.4
0.40	6.2	6.8	0.0975	4.3	4.2
0.60	7.8	8.6	0.126	7.2	6.0
0.80	10.5	10.7	0.132	7.2	7.8
1.00	14.0	13.0	0.141	-	-

a. Measured at wavelengths chosen to give a maximum OD change with minimum interference by the slow process.

b. Calculated from equation (4.2), using k_3 = 12 1 $mol^{-1}s^{-1}$; k_{-3} = 14 s^{-1}; K = 15 1 mol^{-1}.

c. Corresponds to the OD after the completion of the fast colour-forming process. Measured by stopped-flow spectrophotometry at 440 nm. The values quoted are for 1 x 10^{-5} M substrate in a 1 cm cell, and are corrected for absorption by unreacted substrate.

d. Calculated from equation (4.3), assuming ε(complex) = 1.55 x 10^4 1 mol^{-1} cm^{-1}.

e. Calculated from equation (4.4), using K_3 = 0.6 1 mol^{-1}; K = 15 1 mol^{-1}.

TABLE 4.7

Rate constants for the slow reaction of picryl chloride with sodium hydroxide in water at 25°C, μ = 2.0 M(NaCl).

$[HO^-]$ M	$10^2 k_s$ [a] s^{-1}	$10^2 k_s$ [b] (calc) s^{-1}	$10^2 k_s$ [c] (calc) s^{-1}
0.02	1.01	0.79	0.79
0.05	1.76	1.85	1.88
0.10	3.27	3.3	3.4
0.20	5.0	4.8	5.4
0.40	6.8	4.8	6.3
0.60	6.0	4.0	6.4
0.80	6.0	3.3	6.4
1.00	6.9	2.7	6.4

a. Measured at wavelengths chosen to give the best OD change.

b. Calculated from equation (4.5), using k_A = 0.4 l mol^{-1} s^{-1}; K_3 = 0.85 l mol^{-1}; K = 15 l mol^{-1}.

c. Calculated from equation (4.6), using k_A = 0.4 l mol^{-1} s^{-1}; k_B = 0.21 mol^{-1} s^{-1}; k_C = 0.03 l mol^{-1} s^{-1}; K_3 = 0.85 l mol^{-1}; K = 15 l mol^{-1}.

5. 1,2,4,6-Tetranitrobenzene

Use of the stopped-flow spectrophotometer shows two processes: fast formation of a coloured species, previously identified[96] by n.m.r. as the 3-hydroxy adduct, and a slower fading process, forming the picrate ion.

Published spectra[96] show that the spectrum of the complex changes with increasing base concentration. As no trace of a second rate process associated with colour-formation could be found, this rules out formation of the 1:2 adduct, and is evidence for ionisation of the 3-hydroxy group in the 1:1 adduct. In agreement with this, OD measurements (Table 4.8) can be closely reproduced by assuming ionisation, and estimating values of ε for the ionised and unionised forms. Further support is obtained from the rate coefficients for the fast process (Table 4.8), which can be reproduced using equation (4.2).

The presence of four nitro-groups on the ring causes extensive conversion to complex in very dilute base solution. Because of this, some rate measurements (Table 4.8) were made using borax buffers. The rate measurements in Table 4.9 show that there is some catalysis by borax buffers, but little, if any, by carbonate buffers.

The rate coefficients for the formation of picrate ion (Table 4.10) are again better correlated by assuming that nucleophilic substitution occurs in the 3-hydroxy adduct, as well as in the substrate.

6. N,N-Dimethylpicramide

There is evidence[110] for the formation of a 1:2 adduct from dimethylpicramide and hydroxide ion. With aqueous sodium sulphite[58], both the 1:1 and 1:2 adducts were formed,

TABLE 4.8

Rate and equilibrium constants for the fast reaction of 1,2,4,6-tetranitrobenzene with hydroxide ion in water at 25°C.

$[HO^-]$[a] / M	OD[b]	OD[c](calc)	k_f[d] / s^{-1}	k_f[e](calc) / s^{-1}
2.0×10^{-6}	-	-	0.21	0.21
5.0×10^{-6}	-	-	0.21	0.21
1.3×10^{-5}	-	-	0.24	0.24
5.0×10^{-5}	-	-	0.34	0.34
1.1×10^{-4}	-	-	0.54	0.52
0.001	0.51	0.52	2.6	2.9
0.005	0.58	0.58	15.0	14.5
0.01	0.62	0.61	30.2	29.0
0.02	0.63	0.66	57.3	58.0
0.04	0.72	0.72	-	-
0.07	0.77	0.77	-	-
0.10	0.81	0.80	-	-
0.20	0.84	0.84	-	-
0.40	0.85	0.87	-	-
0.70	0.89	0.88	-	-

a. 0.013 M borax buffers were used for base concentrations below 10^{-3} M: $[HO^-]$ was calculated from the measured pH, assuming an activity coefficient of 0.8. Base concentrations above 10^{-3} M used NaOH, with μ=1.0 M (NaCl).

b. Measured using the SP500 spectrophotometer at 450 nm, for 4×10^{-5} M substrate, after completion of the fast colour-forming reaction.

c. Calculated assuming K = 24 l mol^{-1}; ε(complex) = 1.38×10^4 l mol^{-1} cm^{-1}; ε(ionised complex) = 2.25×10^4 l mol^{-1} cm^{-1}.

TABLE 4.8 (contd.)

d. Measured at 500 nm, using the stopped-flow spectrophotometer.

e. Calculated from equation (4.2), using k_3 = 2.9 x 10^3 l mol^{-1} s^{-1}; k_{-3} = 0.2 s^{-1}; K = 24 l mol^{-1}.

TABLE 4.9

Buffer catalysis in the fast reaction of 1,2,4,6-tetranitrobenzene and hydroxide ion in water at 25°C.

(a) Borax buffers

[buffer] M	$[HO^-]$[a] M	k_f[b] s^{-1}	k_f[c](calc) s^{-1}
0.0125	4.6×10^{-5}	0.40	0.33
0.05	5.8×10^{-5}	0.52	0.37
0.10	7.3×10^{-5}	0.71	0.41
0.0125	4.4×10^{-6}	0.21	0.21
0.05	2.4×10^{-6}	0.31	0.21

(b) Carbonate buffers

[buffer] M	$[HO^-]$[a] M	k_f[b] s^{-1}	k_f[c](calc) s^{-1}
0.011	4.4×10^{-4}	1.37	1.48
0.022	5.0×10^{-4}	1.64	1.65
0.039	6.3×10^{-4}	1.90	2.03
0.055	6.3×10^{-4}	2.09	2.03
0.077	7.0×10^{-4}	2.37	2.23
0.110	7.9×10^{-4}	2.74	2.49

a. Calculated from the measured pH, assuming an activity coefficient of 0.8.

b. Measured at 500 nm, using the stopped-flow spectrophotometer.

c. Calculated from equation (4.2), using $k_3 = 2.9 \times 10^3$ l mol^{-1} s^{-1}; $k_{-3} = 0.2$ s^{-1}; $K = 24$ l mol^{-1}.

TABLE 4.10

Rate constants for the slow reaction of 1,2,4,6-tetranitrobenzene with sodium hydroxide in water at 25°C, μ = 1.0 M (NaCl).

$[HO^-]$ M	$10^3 k_s$[a] s^{-1}	$10^3 k_s$[b](calc) s^{-1}	$10^3 k_s$[c](calc) s^{-1}
0.001	8.8	8.8	9.0
0.005	10.1	8.5	9.4
0.01	9.7	7.7	9.4
0.02	9.0	6.4	9.4
0.04	9.2	4.8	9.5
0.07	10.8	3.5	9.9
0.10	14.0	2.8	11.0
0.20	14.4	1.6	13.5
0.40	20.3	0.9	19.4
0.70	27.4	0.5	29.2

a. Measured at 450 nm, using the SP500 spectrophotometer.

b. Calculated from equation (4.5), using k_A = 140 l mol^{-1} s^{-1}; K = 24 l mol^{-1}; K_3 = 1.45 x 10^4 l mol^{-1}.

c. Calculated from equation (4.6), using k_A = 140 l mol^{-1} s^{-1}; k_B = 0.2 l mol^{-1} s^{-1}; k_C = 0.03 l mol^{-1} s^{-1}; K = 24 l mol^{-1}; K_3 = 1.45 x 10^4 l mol^{-1}.

but the 1:2 species was found to be exceptionally stable. This may explain the previous[110] failure to observe the 1:1 hydroxide adduct.

Two processes are observable by stopped-flow spectrophotometry. The faster one causes an increase in absorption at 480 nm, attributed to the formation of the 1:1 adduct. The slower, attributed to formation of the 1:2 adduct, causes fading at 480 nm, and produces an absorption maximum at 410 nm.

Observed rate constants for the fast process (Table 4.11) are fitted by equation (4.7), suggesting that K, for ionisation of the added hydroxyl group, is relatively small.

$$k_{fast} = k_3 [HO^-] + k_{-3} \qquad (4.7)$$

The value of K_3, calculated by an iterative Benesi-Hildebrand[20] treatment of measured OD values (Table 4.11) (23 l mol^{-1}) is in good agreement with that obtained from the rate data (19 l mol^{-1}).

Scheme 4.4 shows the complete reaction pattern. If K, for ionisation of the added hydroxyl group, is small (above), then a simplified scheme can be used to describe the slow process:

$$S + 2\ HO^- \underset{}{\overset{K_3}{\rightleftharpoons}} \underline{4.7} + HO^- \underset{k_{-5}}{\overset{k_5}{\rightleftharpoons}} \underline{4.8}$$

$$[S]_i = [S] + [\underline{4.7}] + [\underline{4.8}]$$

$$= \frac{[\underline{4.7}]}{K_3[HO^-]} + [\underline{4.7}] + [\underline{4.8}]$$

$$= [\underline{4.7}]\left\{1 + \frac{1}{K_3[HO^-]}\right\} + [\underline{4.8}]$$

SCHEME 4.4

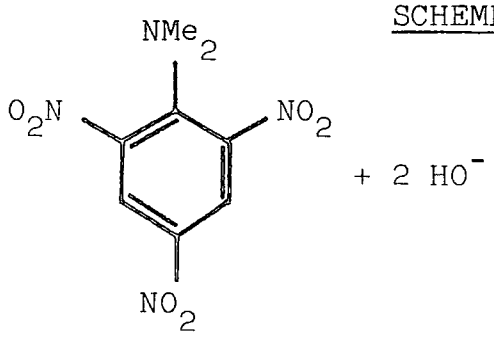

+ 2 HO^-

S

k_{-3} ⇌ k_3

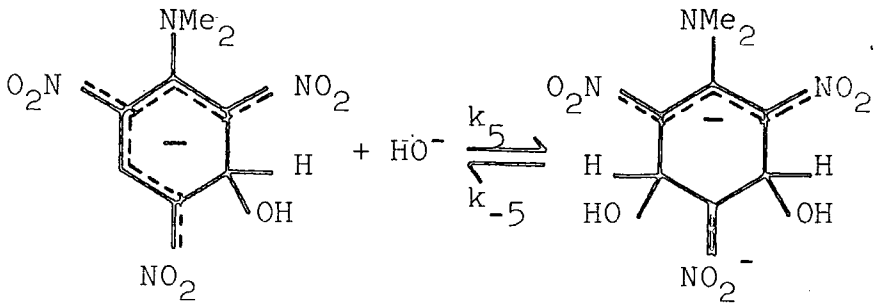

4.7 ⇌ 4.8 (k_5, k_{-5}; + HO^-)

4.7 ⇌ 4.9 (K)

4.8 ⇌ 4.10 (K)

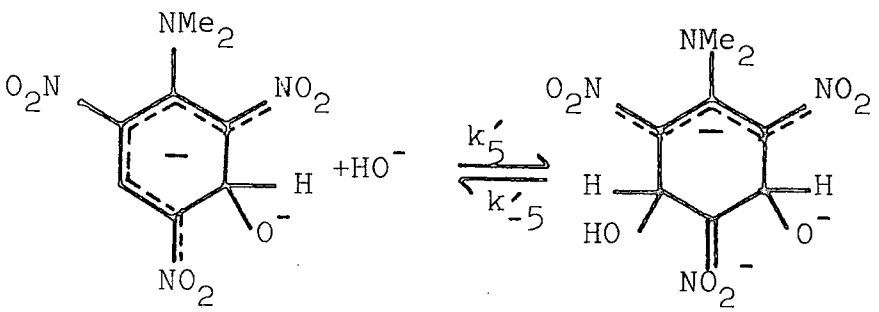

4.9 ⇌ 4.10 (k'_5, k'_{-5}; + HO^-)

4.10 ⇌ 4.11 (K)

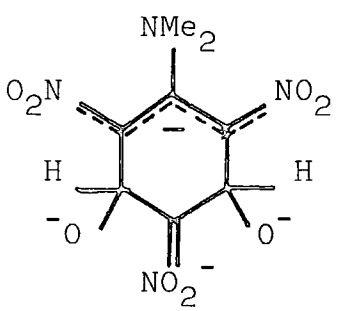

4.11

$$K_3[HO^-][S]_i = [\underline{4.7}]\ (1+K_3[HO^-]) + K_3[HO^-][\underline{4.8}]$$

$$[\underline{4.7}] = \frac{K_3[HO^-]([S]_i - [\underline{4.8}])}{(1+K_3[HO^-])}$$

$$\frac{d[\underline{4.8}]}{dt} = k_5[\underline{4.7}][HO^-] - k_{-5}[\underline{4.8}]$$

$$= \frac{k_5 K_3[HO^-]^2}{(1+K_3[HO^-])}([S]_i - [\underline{4.8}]) - k_{-5}[\underline{4.8}] \qquad (i)$$

At equilibrium,

$$\frac{d[\underline{4.8}]}{dt} = \frac{k_5 K_3[HO^-]^2}{(1+K_3[HO^-])}([S]_i - [\underline{4.8}]_e) - k_{-5}[\underline{4.8}]_e = 0 \qquad (ii)$$

Subtracting (ii) from (i),

$$\frac{d[\underline{4.8}]}{dt} = \frac{k_5 K_3[HO^-]^2}{(1+K_3[HO^-])}([\underline{4.8}]_e - [\underline{4.8}]) + k_{-5}([\underline{4.8}]_e - [\underline{4.8}])$$

$$k_{slow} = \frac{1}{([\underline{4.8}]_e - [\underline{4.8}])} \frac{d[\underline{4.8}]}{dt}$$

$$= \frac{k_5 K_3[HO^-]^2}{(1+K_3[HO^-])} + k_{-5} \qquad (4.8)$$

Rate constants for the slow process (Table 4.11) are fitted well by equation (4.8) for base concentrations below ca. 0.15 M. Above this, the calculated value is very much higher than the observed value. Similarly, calculated values of k_5 (Table 4.11) show a real decrease at higher base concentrations. Comparison with the other systems studied here suggests that, as the base concentration is raised, the 3-hydroxy adduct is increasingly ionised, so that the k_5' term (Scheme 4.4) comes into play. Because this applies to hydroxide attack on a doubly-negatively charged species, 4.9, it is expected to be smaller than k_5, for attack on the singly-

TABLE 4.11

Rate constants for the reaction of N,N-dimethylpicramide with sodium hydroxide in water at 25°C, μ = 1.0 M (NaCl).

$[HO^-]$ M	OD[a]	k_f[b] s^{-1}	k_f[c](calc) s^{-1}	$10^2 k_s$[d] s^{-1}	$10^2 k_s$[e](calc) s^{-1}	k_5[f](calc s^{-1}
0.004	-	-	-	0.134	0.13	0.97
0.005	0.040	0.199	0.208	-	-	-
0.006	-	-	-	0.161	0.17	0.89
0.008	-	-	-	0.239	0.22	1.22
0.01	0.059	0.233	0.226	0.350	0.29	1.44
0.02	0.084	0.263	0.262	1.02	0.73	1.56
0.03	0.097	0.295	0.298	-	-	-
0.04	0.113	0.318	0.334	2.59	2.02	1.36
0.05	0.131	0.334	0.370	3.70	2.77	1.41
0.06	0.122	0.378	0.406	3.71	3.58	1.08
0.07	0.144	0.401	0.442	5.10	4.42	1.20
0.08	0.150	0.478	0.478	4.66	5.28	0.91
0.09	0.154	0.474	0.514	-	-	-
0.10	-	0.600	0.550	6.7	7.07	1.09
0.15	-	-	-	11.4	11.7	0.99
0.20	0.185	0.845	0.910	14.0	16.5	0.86
0.30	-	-	-	17.3	26.3	0.66
0.50	-	-	-	24.4	46.1	0.53

a. Measured at 480 nm, using the stopped-flow spectrophotometer, after completion of the fast process. Values quoted are for 3 x 10^{-5} M substrate in a 1 cm cell.

b. Measured by stopped-flow spectrophotometry at wavelengths chosen for maximum OD change with minimum interference from the second process.

TABLE 4.11 (contd.)

c. Calculated from equation (4.7), using k_3 = 3.6 l mol^{-1} s^{-1}; k_{-3} = 0.19 s^{-1}.

d. Measured using the stopped-flow and Beckman S-25 spectrophotometers at 480 nm.

e. Calculated from equation (4.8), using k_5 = 1.0 l mol^{-1} s^{-1}; k_{-5} = 0.001 s^{-1}; K_3 = 21 l mol^{-1}.

f. Calculated from measured k_s values, using equation (4.8).

negatively charged species, 4.7.

7. Comparison of Results

Rate and equilibrium constants are collected in Table 4.12.

It has already been shown that hydroxy adducts of 2,4,6-trinitrobenzene-sulphonate ion[36] and 4,6-dinitrobenzofuran[76] in aqueous solution undergo ionisation of the added hydroxyl group, while a similar ionisation of the hydroxy adduct of N,N-dipropyl-2,6-dinitro-4-(trifluoromethyl)aniline in water-DMSO has recently been reported[37]. The work described here provides more examples of this interaction.

The value of K for a given substrate is expected to increase with increasing ionic strength of the medium, as the reaction is between two negatively charged species. The variation in K with the 1-substituent is not very great: this is not surprising, since there is no direct pathway for delocalisation of the resulting negative charge. The smallest value of K is for the picrate ion, the hydroxy adduct of which already carries two negative charges.

Nitrite, chloride and methoxide ions are better leaving groups than is hydroxide ion, so nucleophilic attack by hydroxide ion at C-1 is the rate-determining step in the substitution reaction. Thus, the values of k_A (shown in Table 4.12) are those for hydroxide ion attack at C-1 in the substrate. These are all considerably smaller than the values for attack at C-3, which forms the adducts. There are several factors involved in determining which position is favoured for nucleophilic attack. The inductive effect of electronegative X-substituents should favour attack at C-1.

TABLE 4.12

Rate and equilibrium constants for the reaction of 1-X-2,4,6-trinitrobenzenes with sodium hydroxide in water at 25°C.

X	OH	OMe	Cl	NO_2	NMe_2
μ (M)	2.0	2.0	2.0	1.0	1.0
k_3 (1 $mol^{-1}s^{-1}$)	0.26	12	12	2.9×10^3	3.6
k_{-3} (s^{-1})	20	8.3	14	0.2	0.19
K_3 (1 mol^{-1})	0.013	1.3	0.7	1.45×10^4	21
K (1 mol^{-1})	0.8	6	15	24	-
k_5 (1 $mol^{-1}s^{-1}$)	-	-	-	-	1.0
k_{-5} (s^{-1})	-	-	-	-	0.001
k_A (1 $mol^{-1}s^{-1}$)	-	1.4	0.4	140	-
k_B (1 $mol^{-1}s^{-1}$)	-	0.8	0.2	0.2	-
k_C (1 $mol^{-1}s^{-1}$)	-	0.1	0.03	0.03	-

However, the stabilising resonance interaction between X and the ring is lost when addition occurs at C-1, but retained when addition occurs at C-3[30]. There may also be an unfavourable repulsion between the entering and leaving groups when attack occurs at C-1[27].

The rate data provide evidence for nucleophilic displacement of X by hydroxide ion in the 3-hydroxy adduct (in both the ionised and unionised forms) as well as in the substrate. The intermediates will be of structures 4.12 - 4.14.

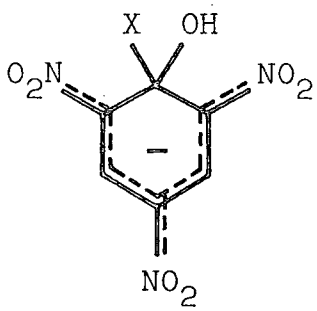

4.12

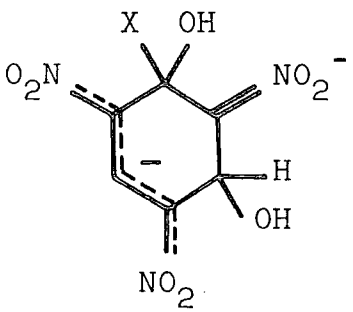

4.13

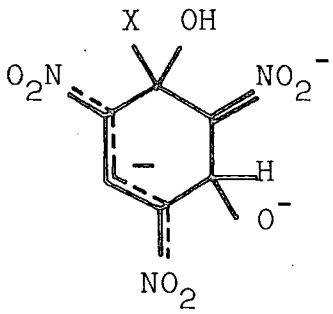

4.14

There is no evidence for a build-up in concentration of any of these species, which are expected to be unstable with respect to loss of X^- ion, decaying rapidly to picrate ion (from 4.12) or the appropriate adduct (from 4.13 and 4.14).

1:2 adducts are known to be formed by both trinitrobenzene[38] and picrate ion[39] at high base concentrations. In the case of N,N-dimethylpicramide, the 1:2 complex is considerably more stable than the 1:1 ($K_5 \approx 10^3$ l mol^{-1}, cf. K_3 = 21 l mol^{-1}). However, no evidence was found for 1:2 adducts with X = NO_2, Cl, OMe. In these substrates, nucleophilic attack at C-1, which leads to substitution, competes successfully with that at C-5, which forms the 1:2 adduct.

CHAPTER FIVE

THE INTERACTION OF N-SUBSTITUTED-2,4,6-TRINITROANILINES WITH METHOXIDE ION IN METHANOL

INTRODUCTION

The possibilities for 1:1 interaction of N-substituted-2,4,6-trinitroanilines (picramides) with base are loss of an amino-proton and σ-complex formation.

The position of base attack has been the subject of controversy, some authors favouring the formation of a "true" Meisenheimer complex by addition at C-1, and others supporting addition at the less sterically hindered C-3 position. Most recent work seems to favour the latter position.

A uv/visible spectroscopic study[48] of the reactions of picramide and N,N-dimethylpicramide with methoxide ion showed that the former undergoes only a 1:1 interaction, which could be either amino-proton loss (5.1, R=H) or base addition (5.2, R=R′=H), while the latter undergoes both 1:1 and 1:2 interactions. The 1:1 product was held to be the C-3 adduct, 5.2 (R=R′=Me).

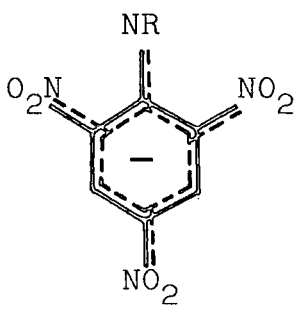

5.1

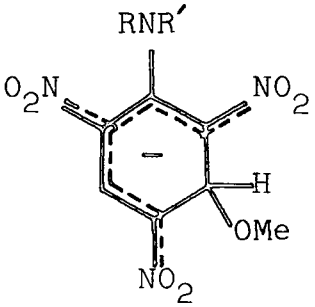

5.2

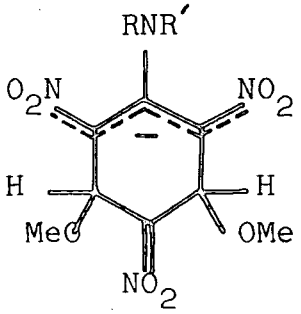

5.3

A ^{1}H n.m.r. study[23] in methanol-DMSO confirmed the structures of the 1:1 and 1:2 adducts of dimethylpicramide as being 5.2 and 5.3 (R=R′=Me) respectively, and showed that, for picramide, base addition at C-3 outweighs amino-proton abstraction. Other n.m.r. work in methanol-DMSO[32] has shown that the ratio of base addition at C-3 to amino-proton loss

in N-methylpicramide depends upon the solvent composition, an increase in the proportion of DMSO favouring amino-proton abstraction. The same author[32,33] showed that N-phenylpicramide undergoes only proton abstraction up to high base concentrations, when base addition to the anion occurs, forming 5.4 (R=Ph). N-methylpicramide also forms 5.4 (R=Me) at higher base concentrations[33].

However, some results have been taken as evidence for addition at C-1, e.g. in N-methylpicramide[119] (5.5, R=H, R′=Me). 2,4,6-Trinitroaniline-N-methylpropionamide is known[93,120] to form the C-1 adduct with methoxide ion: this complex is stabilised by intramolecular hydrogen-bonding between the amide N-H and an ortho nitro-group (5.6).

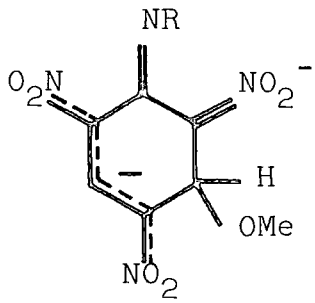

5.4

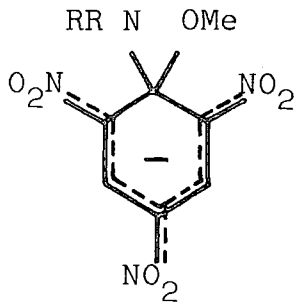

5.5

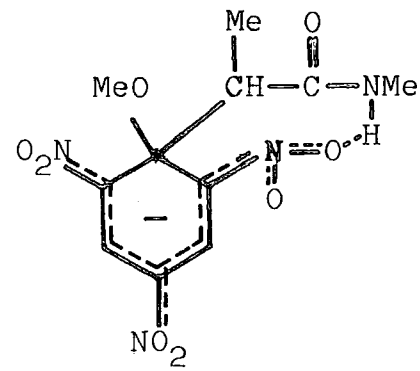

5.6

Transient intermediates formed by addition at C-1 have been observed[31,121] in reactions of picryl ethers with aliphatic amines. In the case of trinitroanisole and n-butylamine[31], the C-3 adduct is formed faster than the C-1 complex, which is the true intermediate in the substitution reaction.

EXPERIMENTAL

The work described here concerns the 1:1 interactions of a group of N-substituted picramides with sodium methoxide in methanol. The results distinguish between amino-proton loss and base addition at C-3, in accordance with Scheme 5.1. This gives rise to equation (5.1) for the observed rate constant, obtained as follows:

$$\underline{5.1} \quad \underset{\text{fast}}{\overset{K}{\rightleftharpoons}} \quad S + MeO^- \quad \underset{k_{-3}}{\overset{k_3}{\rightleftharpoons}} \quad \underline{5.2}$$

$$K = \frac{[\underline{5.1}]}{[S][MeO^-]}$$

$$[S]_i = [S] + [\underline{5.1}] + [\underline{5.2}]$$

$$= [S] + K[S][MeO^-] + [\underline{5.2}]$$

$$= [S](1 + K[MeO^-]) + [\underline{5.2}]$$

$$\therefore \quad [S] = \frac{([S]_i - [\underline{5.2}])}{(1+K[MeO^-])}$$

$$\frac{d[\underline{5.2}]}{dt} = k_3[S][MeO^-] - k_{-3}[\underline{5.2}]$$

$$= \frac{k_3[MeO^-]([S]_i - [\underline{5.2}])}{(1+K[MeO^-])} - k_{-3}[\underline{5.2}] \qquad \text{(i)}$$

At equilibrium,

$$\frac{d[\underline{5.2}]}{dt} = \frac{k_3[MeO^-]([S]_i - [\underline{5.2}]_e)}{(1+K[MeO^-])} - k_{-3}[\underline{5.2}]_e = 0 \qquad \text{(ii)}$$

Subtracting (ii) from (i):

$$\frac{d[\underline{5.2}]}{dt} = \frac{k_3[MeO^-]([\underline{5.2}]_e - [\underline{5.2}])}{(1+K[MeO^-])} + k_{-3}([\underline{5.2}]_e - [\underline{5.2}])$$

$$k_{obs} = \frac{1}{([\underline{5.2}]_e - [\underline{5.2}])} \frac{d[\underline{5.2}]}{dt}$$

$$= \frac{k_3[MeO^-]}{(1+K[MeO^-])} + k_{-3} \qquad (5.1)$$

SCHEME 5.1

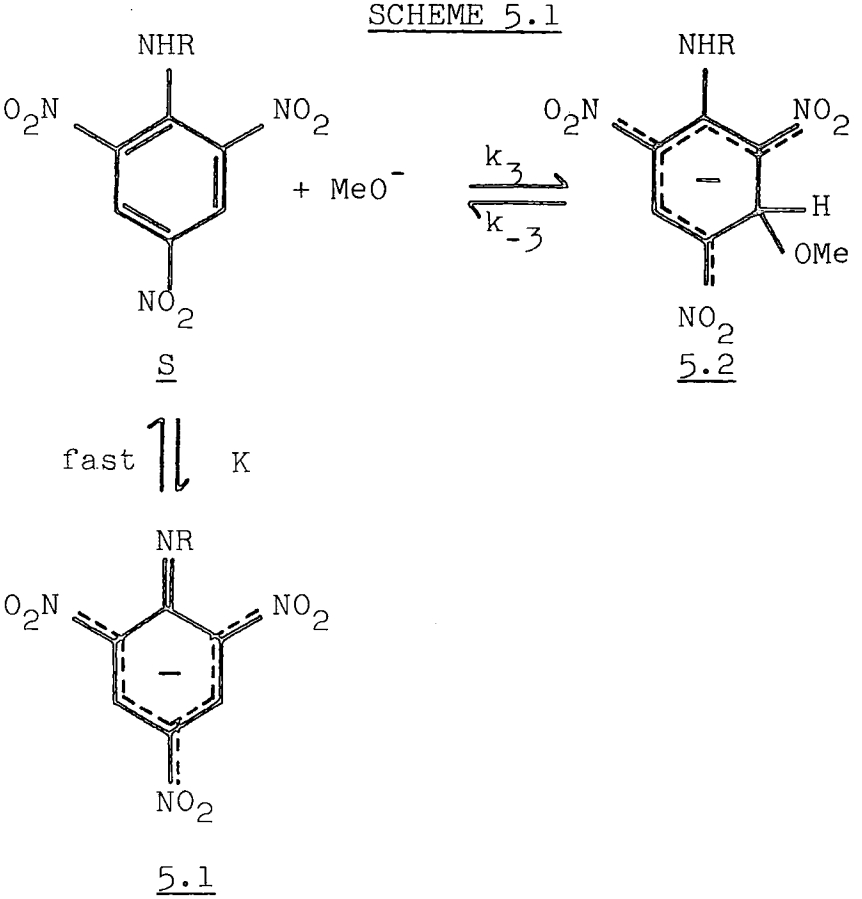

S 5.2

5.1

Rate measurements were made by following changes in the absorbance at a suitable wavelength, using the stopped-flow spectrophotometer. In all cases, first-order conditions were maintained, with the base concentration in large excess over the substrate. The very fast processes were observed using the Hartley T-jump apparatus, which has a heating time of circa 2 μs (see Chapter Two). For these tests, solutions were made up to $\mu = 0.2\,\underline{M}$ with sodium perchlorate. T-jumps of circa 7 deg.C were carried out.

Rate constants were calculated from equation (5.1), or from the 'inversion plot' of equation (5.2). When $K[MeO^-] << 1$, then (5.1) simplifies to (5.3)

$$\frac{1}{(k_{obs} - k_{-3})} = \frac{1}{k_3[MeO^-]} + \frac{K}{k_3} \qquad (5.2)$$

$$k_{obs} = k_3[MeO^-] + k_{-3} \qquad (5.3)$$

Values of K were calculated directly using equation (5.4), from stopped-flow measurements of the OD after the completion of the very rapid process. Equilibrium OD measurements at the end of the 1:1 interaction were made by either stopped-flow or conventional spectrophotometry, and used to calculate K_T, the overall equilibrium constant (5.5), from equation (5.6).

$$K = \frac{[PicNR^-]}{[PicNHR][MeO^-]} = \frac{OD_i}{(OD_\infty - OD_i)[MeO^-]} \qquad (5.4)$$

where OD_i = OD after completion of the initial, fast colour-forming reaction,

OD_∞ = OD after completion of the 1:1 interactions.

$$K_T = K + K_3 \qquad (5.5)$$

$$\frac{1}{(OD-OD_o)} = \frac{1}{(\varepsilon_c - \varepsilon_s)} \quad \frac{1}{K_T} \quad \frac{1}{[S][MeO^-]} + \frac{1}{(\varepsilon_c - \varepsilon_s)[S]} \qquad (5.6)$$

where OD_o = OD in the absence of base,

ε_c = extinction coefficient of the mixture of 1:1 complexes,

ε_s = extinction coefficient of the substrate,

$[S]$ = stoichiometric concentration of the substrate.

Spectral shapes were determined using the SP8000 and Beckman S-25 spectrophotometers.

RESULTS AND DISCUSSION

1. Picramide

Previous ^{1}H n.m.r. measurements[32,33] in methanol-DMSO indicate the formation of both 5.1 (R=H) and 5.2 (R=R'=H). Increasing the concentration of sodium methoxide in methanol in the range 0-1M is found to cause an increase in visible absorption with λ_{max} 400 nm. The spectral shape is independent of the base concentration in this range (see Figure 5.1). Above 2.0M base, further spectral changes occur (see Figure 5.2); a broad band attributed to 1:2 interaction develops at ca. 480 nm, replacing that at 400 nm. Above 4.0M base, there is virtually no absorption above 350 nm. This is consistent with 1:3 interaction.

Stopped-flow measurements at 400 nm showed two reactions. The first was too fast to follow by this method, and was also found to be faster than the heating time of the T-jump. It is therefore attributed to amino-proton abstraction. Rate constants for the slower process observable by stopped-flow are shown in Table 5.1, and agree well with equations (5.1) and (5.2). The calculated values of K_3 and K give a value for K_T = 41 l mol^{-1}, compared with a value of 38 l mol^{-1} previously obtained[48] from OD measurements.

Measurement of the OD after completion of the very fast process (Table 5.1) leads to a value of K = 8 $\pm$ 3 l mol^{-1}, in good agreement with that obtained from the kinetic measurements.

There was some spectral evidence for a further reaction above 2 Msodium methoxide (see Figure 5.2), which was not investigated kinetically, because of the high base concentrations needed.

FIGURE 5.1

Spectra recorded on the addition of sodium methoxide to 4 x 10^{-5} M picramide in methanol at 25°C (1 cm cells).

A. 0.05 M NaOMe.

B. 0.1 M NaOMe.

C. 0.5 M NaOMe.

D. 1.0 M NaOMe.

FIGURE 5.1

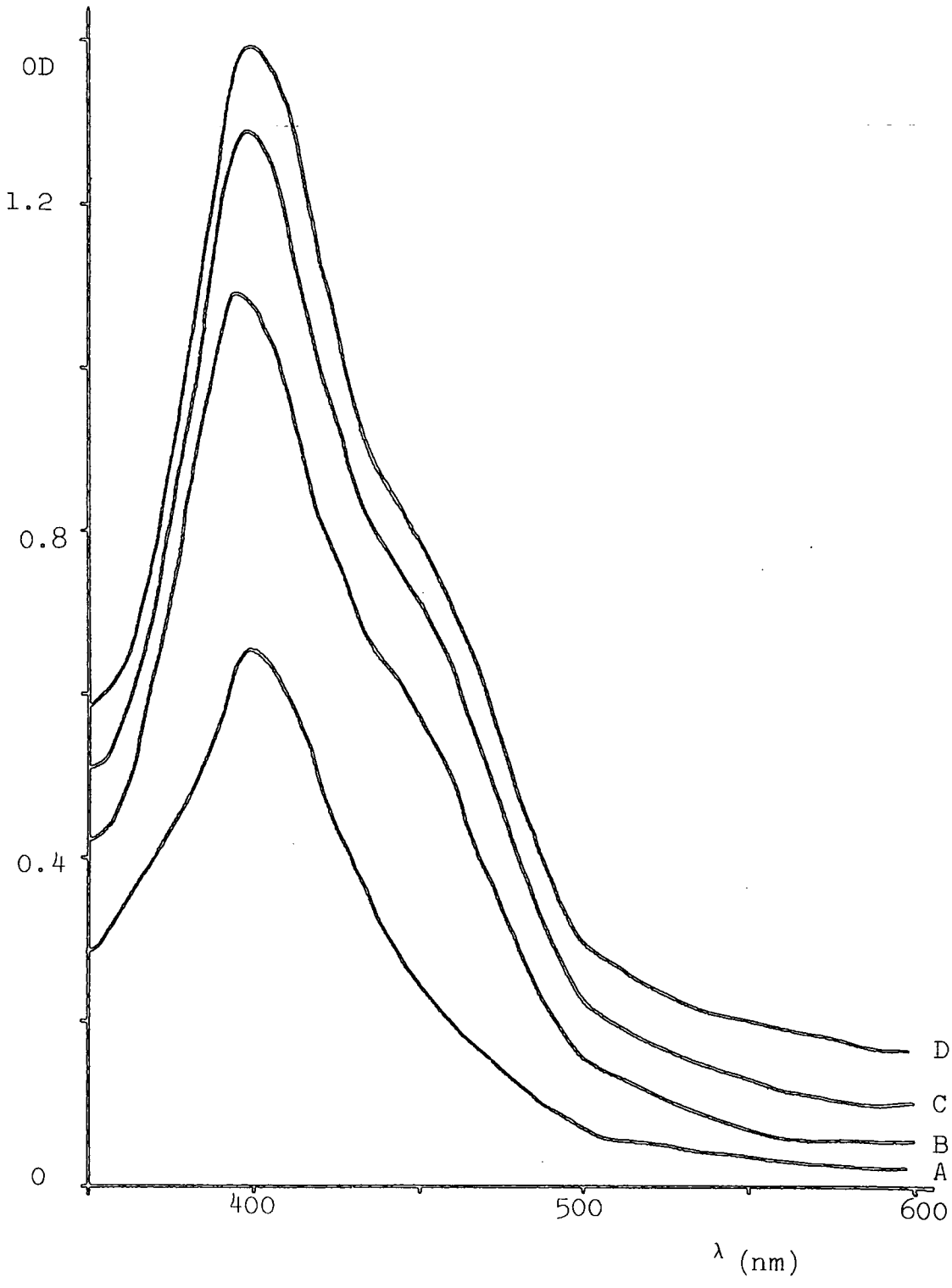

FIGURE 5.2

Spectra recorded on the addition of sodium methoxide to 4×10^{-5} M picramide in methanol at 25°C (1 cm cells).

A. 2.0 M NaOMe.

B. 3.0 M NaOMe.

C. 4.5 M NaOMe.

FIGURE 5.2

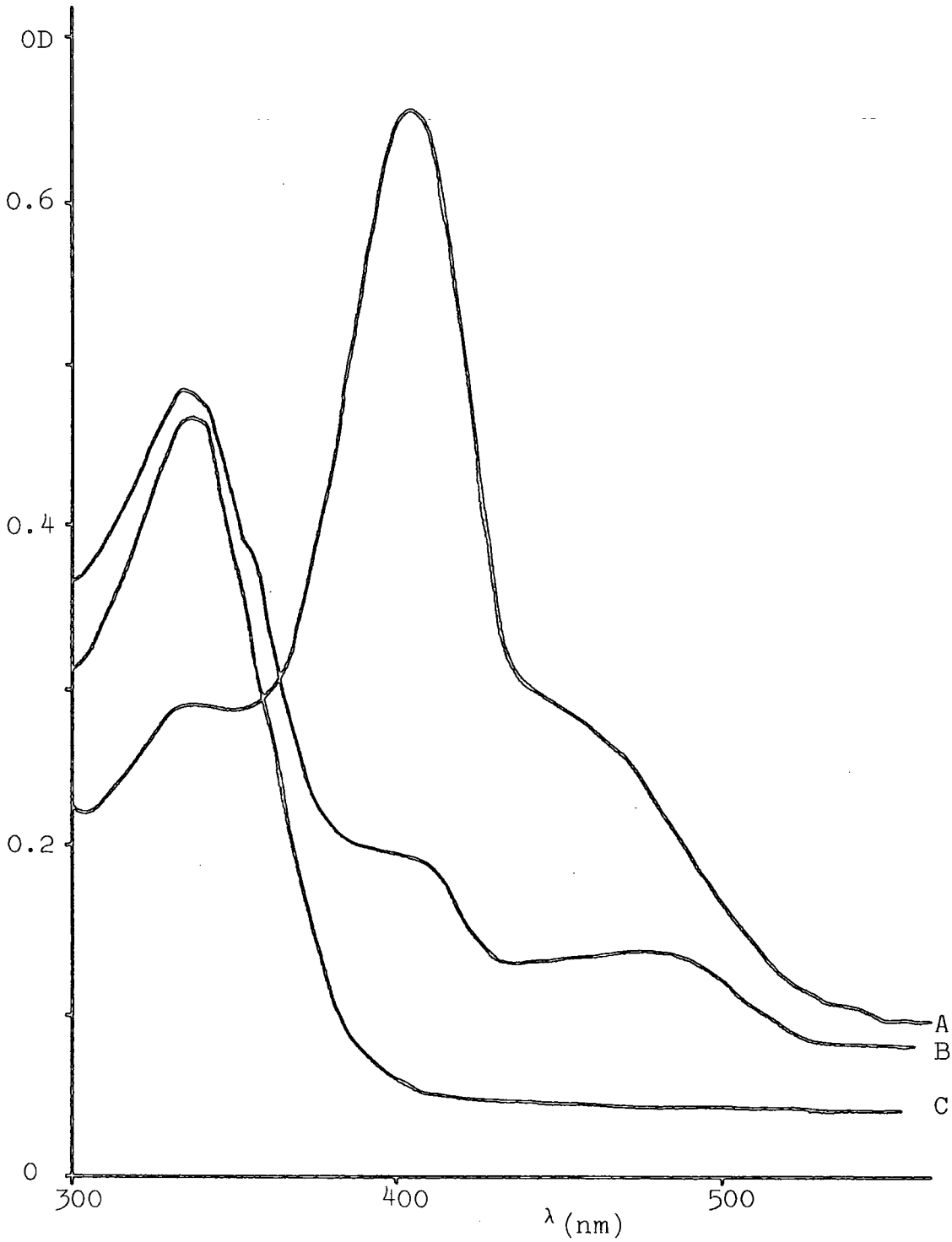

TABLE 5.1

Rate and equilibrium constants for the 1:1 reaction of picramide with sodium methoxide in methanol at 25°C.

$[MeO^-]$ M	k_{obs} s^{-1}	k_{calc} [a] s^{-1}	OD_s [b]	OD_i [c]	K [d] 1 mol^{-1}
0.002	63.7	63.8	0.285	0.300	9.6
0.004	66.7	67.2	0.285	0.305	6.4
0.006	77.0	70.8	0.300	0.365	14.7
0.008	74.8	74.2	0.300	0.365	11.1
0.010	76.9	77.4	0.295	0.370	10.3
0.02	92.1	92.2	0.205	0.335	5.6
0.03	108	105	0.290	0.415	6.2
0.04	117	116	0.195	0.310	4.2
0.05	128	126	0.295	0.520	7.2

a. Calculated from equation (5.1), using k_3 = 1900 1 mol^{-1} s^{-1}; k_{-3} = 60 s^{-1}; K = 9 1 mol^{-1}.

b. OD due to the substrate alone, at 400 nm: corresponds to an 'after mixing' concentration of 4 x 10^{-5} M in a 1 cm cell.

c. OD at the completion of the very rapid reaction; i.e. corresponding to amino-proton loss.

d. Calculated from equation (5.4), assuming ε(5.1) = 2 x 10^4 1 mol^{-1} cm^{-1}. The mean value is K = 8 ± 3 1 mol^{-1}.

2. N-Methylpicramide

^{1}H n.m.r. studies in methanol-DMSO[32,33] have shown that, in reasonably dilute base solution, both 5.1 (R=Me) and 5.2 (R=Me, R′=H) are formed. Visible spectra obtained in methanolic sodium methoxide solution[49] show evidence of several interactions. Between 0 and 0.2 M base, a band at 410 nm and an isosbestic point at 357 nm are observed, consistent with 1:1 interaction. From 0.4 to 2.0 M, the band at 410 nm decreases, and is replaced by one at 485 nm. This is attributed to 1:2 interaction. Above 2 M base, the visible absorption decreases until there is virtually no absorption above 350 nm: this is attributed to 1:3 interaction.

Stopped-flow measurements in solutions containing up to 0.2 M sodium methoxide show two colour-forming processes attributable to 1:1 interaction. The first of these was too fast for measurement by stopped-flow, and was shown by T-jump to occur within the heating time of the instrument (circa 2 μs). The slower of the two processes was followed by stopped-flow spectrophotometry at 410 nm: the rate constants, which are shown in Table 5.2, do not vary greatly with base concentration, so values obtained from them are likely to have fairly high uncertainties.

OD measurements at the end of the very fast process, and at equilibrium, were made by stopped-flow at 410 and 480 nm (Table 5.3). These give values of $K = 20 \pm 2$ l mol^{-1}, $K_T = 33 \pm 2$ l mol^{-1}, and hence $K_3 = 13 \pm 2$ l mol^{-1}. Extrapolation of the observed rate constants (Table 5.2) to zero base concentration gives $k_{-3} = 21 \pm 1$ s^{-1}. Combining this with K_3 gives a value of $k_3 = K_3 k_{-3} = 280 \pm 60$ l mol^{-1}s^{-1}.

TABLE 5.2

Rate constants for the 1:1 reaction of N-methylpicramide with sodium methoxide in methanol at 25°C.

$[MeO^-]$	k_{obs}	k_{calc}[a]
M	s^{-1}	s^{-1}
0.004	22	22
0.006	23	22.5
0.010	25	23.5
0.02	26	25
0.03	28	26.5
0.04	28	27
0.06	29	28.5
0.08	30	30
0.10	30	30.5
0.15	31	31.5
0.20	31.5	32

a. Calculated from equation (5.1), using k_3 = 280 l mol^{-1} s^{-1}; k_{-3} = 21 s^{-1}; K = 20 l mol^{-1}.

TABLE 5.3

Equilibrium measurements for the 1:1 reaction of N-methylpicramide with sodium methoxide in methanol at 25°C.

(i) Measurements at 480 nm

$[MeO^-]$ M	OD_i [a,b]	OD_e [c,d]	K [e,f] l mol^{-1}	K_T [g,h] l mol^{-1}
0	0.000	0.000	-	-
0.004	0.035	0.040	21.1	31.3
0.006	0.045	0.055	18.5	30.1
0.010	0.075	0.090	20.0	33.3
0.02	0.125	0.140	19.2	31.8
0.03	0.175	0.185	21.2	35.2
0.04	0.200	0.210	20.0	35.0
0.06	0.255	0.245	21.8	35.5
0.08	0.280	0.260	20.6	32.5
0.10	0.295	0.270	19.0	30.0
0.14	0.335	0.295	20.0	32.4
0.20	0.375	0.330	-	-

TABLE 5.3 (contd.)

(ii) Measurements at 410 nm

$[MeO^-]$ M	OD_i [a,i]	OD_e [c,j]	K [e,k] l mol^{-1}	K_T [g,l] l mol^{-1}
0	(0.225)	(0.225)	-	-
0.004	0.047	0.094	22.9	38.1
0.006	0.069	0.119	23.4	33.6
0.010	0.088	0.167	18.6	30.8
0.02	0.184	0.304	24.5	37.4
0.03	0.239	0.387	24.8	39.9
0.04	0.260	0.423	21.7	36.8
0.06	0.328	0.495	23.6	38.4
0.08	0.353	0.529	21.3	36.5
0.10	0.385	0.549	22.0	34.1
0.14	0.431	0.592	23.9	35.8
0.20	0.460	0.623	23.0	35.8

a. Measured by stopped-flow, after completion of the very fast process; 4 x 10^{-5} M substrate in a 1 cm cell.

b. A Benesi-Hildebrand[20] plot gives OD_∞ (complete conversion) = 0.45. An inversion plot according to equation (5.6) gives K = 19.6 l mol^{-1}.

c. Measured after completion of both 1:1 interactions; 4 x 10^{-5} M substrate in a 1 cm cell.

d. OD_∞ = 0.36. An inversion plot (equation 5.6) gives K_T = 31.1 l mol^{-1}.

e. Calculated from equation (5.4).

f. Mean K = 20 $\pm$ 1 l mol^{-1}.

g. Calculated from

$$K_T = \frac{[5.1 + 5.2]}{[S][MeO^-]} = \frac{OD_e}{(OD_\infty - OD_e)[MeO^-]} \qquad (5.7)$$

TABLE 5.3 (contd.)

h. Mean $K_T = 33 \pm 2$ l mol^{-1}.

i. Corrected for absorption by unreacted substrate using (5.8), with $K = 20$ l mol^{-1}. $OD_\infty = 0.56$.

$$OD' = OD - \frac{OD_s}{(1+K[MeO^-])} \qquad (5.8)$$

j. Corrected for absorption by unreacted substrate using equation (5.8), with $K_T = 30$ l mol^{-1}. $OD_\infty = 0.71$

k. Mean $K = 23 \pm 2$ l mol^{-1}.

l. Mean $K_T = 36 \pm 3$ l mol^{-1}.

3. N-iso-Propylpicramide

Two processes are observable by stopped-flow spectrophotometry: the faster one is complete within the mixing time of the instrument (ca. 2 ms) and produces a species with λ_{max} 435 nm. This is attributed to amino-proton abstraction. The slower process is attributed to formation of the methoxide ion adduct at C-3, with λ_{max} ca. 405 nm. This interpretation is in line with n.m.r. spectra obtained in 50% DMSO-methanol (the change of solvent is not expected to change the mode of interaction[8]): see Chapter Six. The visible spectra, measured point-by-point on the stopped-flow spectrophotometer, are shown in Figure 5.3.

Rate measurements (Table 5.4) were made at 450 nm (400 nm for some measurements at higher base concentration) using the stopped-flow spectrophotometer. These results give values of $K = 5.5 \pm 0.5$ l mol^{-1}; $k_3 = 450 \pm 30$ l mol^{-1}s^{-1}; $k_{-3} = 16 \pm 1$ s^{-1}, and hence $K_3 = 28 \pm 3$ l mol^{-1}, $K_T = 33.5 \pm 3.5$ l mol^{-1}. OD measurements were made after the very fast reaction, and on completion of the 1:1 processes, using the stopped-flow spectrophotometer at 450 nm (Table 5.5). These lead to values of $K = 3$ l mol^{-1} and $K_T = 30$ l mol^{-1}, respectively, giving $K_3 = 27$ l mol^{-1}. Further measurements of the equilibrium OD at 474 nm, using the SP500 instrument (Table 5.4), lead to a value of $K_T = 30 \pm 2$ l mol^{-1}.

Above 0.5M sodium methoxide, there was some evidence of a further interaction, which was not investigated.

4. N-n-Butylpicramide

In dilute sodium methoxide solution, N-n-butylpicramide gives a visible spectrum with λ_{max} 405 nm. Use of the stopped-flow spectrophotometer shows two processes; a very

FIGURE 5.3

Spectra of the anion and adduct obtained from N-isopropylpicramide and sodium methoxide in methanol at 25°C. 5×10^{-5} M substrate and 0.5 M base in a 1 cm cell. Spectra are corrected for absorption by unreacted substrate.

A. Spectrum of the substrate.

B. Spectrum attributed to the anion, 5.1 (R = ^{i}Pr).

C. Spectrum attributed to the adduct, 5.2 (R = ^{i}Pr, R′= H).

FIGURE 5.3

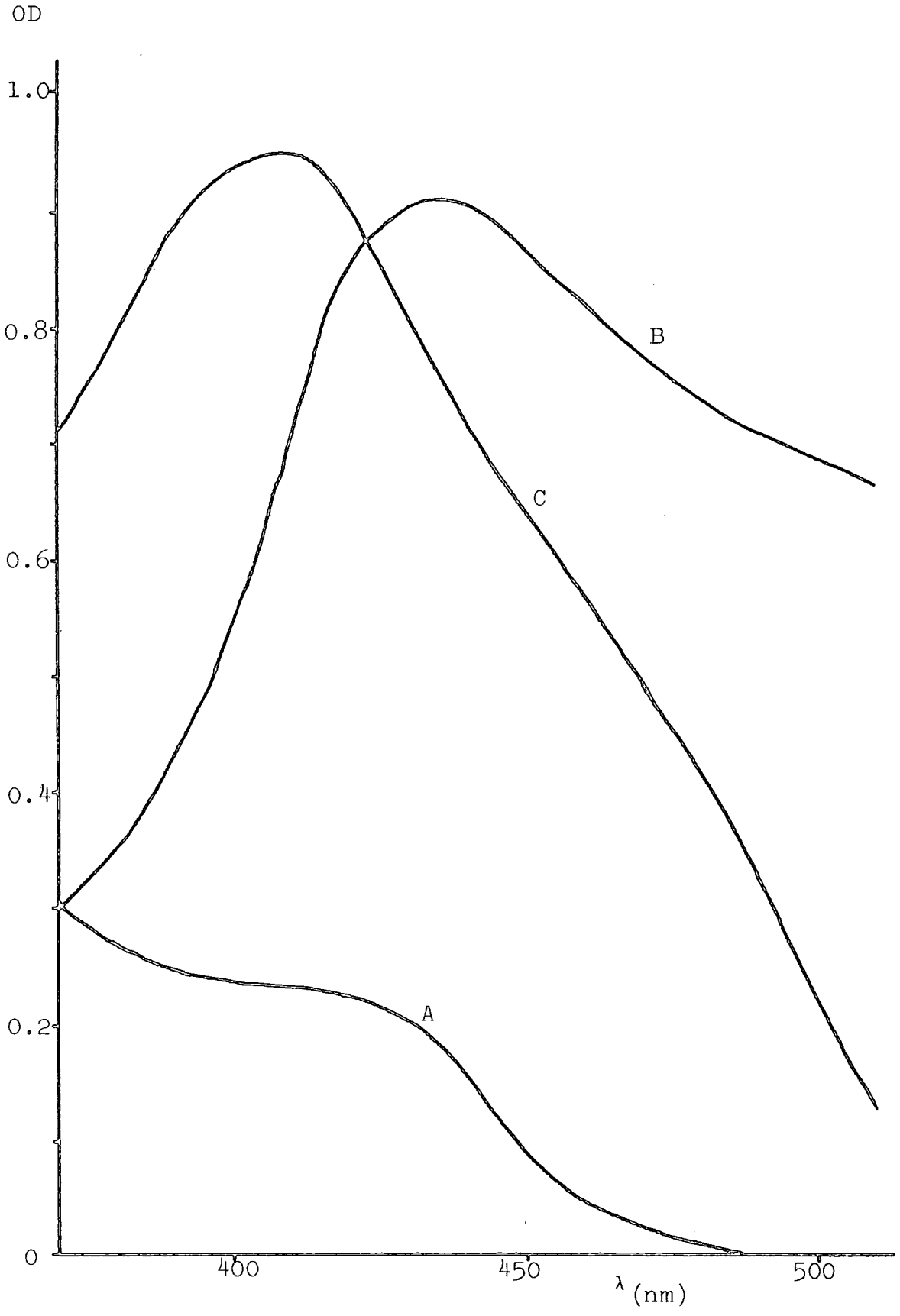

TABLE 5.4

Rate and equilibrium constants for the 1:1 reaction of N-isopropylpicramide with sodium methoxide in methanol at 25°C.

$[MeO^-]$	k_{obs} [a]	k_{calc} [b]	OD [c]	K_T [d]
M	s^{-1}	s^{-1}		$l\ mol^{-1}$
0	-	-	0.009	-
0.001	-	-	0.021	34
0.002	16.8	16.9	-	-
0.004	18.4	17.8	0.047	29
0.008	19.5	19.4	0.085	33
0.010	19.1	20.3	0.089	28
0.02	23.1	24.1	0.140	28
0.04	30.6	30.8	0.206	30
0.08	42.1	41.0	0.264	30
0.10	46.6	45.0	0.280	30
0.20	61.0	58.9	0.320	31
0.30	69.4	66.9	-	-
0.40	70.6	72.3	-	-

a. Measured by stopped-flow spectrophotometry, at 450 or 400 nm.

b. Calculated from equation (5.1), using $k_3 = 450\ l\ mol^{-1}\ s^{-1}$; $k_{-3} = 16\ s^{-1}$; $K = 5.5\ l\ mol^{-1}$.

c. Measured at 474 nm, using the SP500. 4×10^{-5} M substrate in a 1 cm cell. $OD_\infty = 0.37$.

d. Calculated from equation (5.9), with $OD_s = 0.009$; $OD_\infty = 0.37$. Mean $K_T = 30 \pm 2\ l\ mol^{-1}$.

$$K_T = \frac{(OD-OD_s)}{(OD_\infty-OD)[MeO^-]} \qquad (5.9)$$

TABLE 5.5

Equilibrium constants for the 1:1 reactions of N-isopropylpicramide with sodium methoxide in methanol at 25°C.

$[MeO^-]$ M	OD_i [a]	OD_e [b]	K [c] $l\ mol^{-1}$	K_T [d] $l\ mol^{-1}$
0.002	0.015	0.045	(6.8)	33.8
0.004	0.015	0.070	3.4	27.3
0.006	0.015	0.095	2.3	25.7
0.008	0.020	0.110	2.3	22.9
0.010	0.040	0.165	3.7	30.3
0.04	0.095	0.390	2.3	30.5
0.06	0.160	0.475	2.8	33.7
0.08	0.085	0.415	(1.0)	(17.6)
0.10	0.190	0.555	2.1	35.8
0.15	0.360	0.585	3.2	31.2
0.20	0.395	0.600	2.8	27.3
0.25	0.460	0.645	2.8	(39.7)
0.30	0.505	0.635	2.8	28.2

a. Measured by stopped-flow spectrophotometry at 450 nm, after completion of the very fast process, and corrected for absorption by unreacted substrate using equation (5.8), with $K = 5\ l\ mol^{-1}$. 5×10^{-5} M substrate in a 1 cm cell. $OD_\infty = 1.11$.

b. Measured at 450 nm after completion of both 1:1 interactions, and corrected for absorption by unreacted substrate using equation (5.8), with $K_T = 30\ l\ mol^{-1}$. 5×10^{-5} M substrate in a 1 cm cell. $OD_\infty = 0.71$.

c. Calculated from equation (5.4). Mean $K = 2.8 \pm 0.5\ l\ mol^{-1}$.

d. Calculated from equation (5.7). Mean $K_T = 30 \pm 4\ l\ mol^{-1}$.

fast colour formation (too fast to measure), and a slower process. Rate measurements for the slower reaction, made at 400 nm, are shown in Table 5.6. A plot of k_{obs} vs base concentration (not shown) gives an intercept of $k_{-3} = 20 \pm 0.5$ s^{-1}. Using this value, an inversion plot according to equation (5.2) is linear, giving $K = 8.3 \pm 1$ l mol^{-1}; $k_3 = 440$ l $mol^{-1} s^{-1}$, and hence $K_3 = 22$ l mol^{-1}, $K_T = 30.3$ l mol^{-1}.

Equilibrium OD measurements, after completion of the 1:1 interactions, were made using the SP500 instrument, at 400, 405, and 410 nm (Table 5.6). Use of equation (5.6) gives a value of $K_T = 29 \pm 3$ l mol^{-1}. OD measurements made at 470 nm using the stopped-flow spectrophotometer, on completion of the very fast process, and on completion of the 1:1 interactions (not shown) lead to values of $K = 12 \pm 6$ l mol^{-1}, $K_3 = 18 \pm 2$ l mol^{-1}, and $K_T = 30 \pm 8$ l mol^{-1}.

At higher base concentrations, further changes in the spectrum occur (Figure 5.4). Below 0.5M sodium methoxide, the spectrum shows a band at 405 nm, attributed to 1:1 interaction. Between 0.5 and 2.0M base, this decreases in intensity, and is replaced by a band at 480 nm, attributable to 1:2 interaction between the substrate and base. Above 2.0M base, this band also decreases in intensity, until there is virtually no absorption above 350 nm. This is attributed to 1:3 interaction. Because of the high base concentrations involved, these processes were not investigated further.

5. N-tert-Butylpicramide

Use of the stopped-flow spectrophotometer shows that the very fast colour-forming reaction occurs for this substrate, as for the others, but it is of very low intensity at all wavelengths (see Figure 5.5). This suggests that K,

TABLE 5.6

Rate constants for the 1:1 reaction of N-n-butyl-picramide with sodium methoxide in methanol at 25°C.

$[MeO^-]$ M	k_{obs}[a] s^{-1}	k_{calc}[b] s^{-1}	OD[c] (400nm)	OD[c] (405nm)	OD[c] (410nm)
0	-	-	0.116	0.120	0.123
0.002	21.7	20.9	-	-	-
0.004	21.7	21.7	-	-	-
0.006	22.3	22.5	-	-	-
0.008	24.3	23.3	-	-	-
0.010	24.9	24.0	0.208	0.217	0.219
0.014	25.4	25.5	-	-	-
0.02	27.4	27.5	-	-	-
0.03	30.9	30.5	0.300	0.314	0.318
0.04	34.9	33.1	-	-	-
0.05	33.7	35.4	0.339	0.355	0.362
0.06	36.5	37.5	-	-	-
0.07	39.1	39.3	0.384	0.405	0.410
0.08	39.8	41.0	-	-	-
0.09	42.4	42.5	-	-	-
0.10	42.5	43.8	0.415	0.433	0.438
0.15	-	-	0.433	0.457	0.464
0.20	-	-	0.458	0.479	0.481
0.30	-	-	0.479	0.493	0.504
0.40	-	-	0.477	0.495	0.501

a. Measured at 400 nm, using the stopped-flow spectrophotometer

b. Calculated from equation (5.1), using k_3= 440 l $mol^{-1}s^{-1}$; k_{-3} = 20 s^{-1}; K = 8.3 l mol^{-1}.

c. Measured using the SP500 instrument. 2×10^{-5} M substrate in a 1 cm cell.

Durham University SCIENCE 30 OCT 1980 SECTION Library

FIGURE 5.4

Spectra obtained on the addition of sodium methoxide to 4×10^{-5} M N-n-butylpicramide in methanol at 25°C (1 cm cell).

A. 0.5 M NaOMe.

B. 1.0 M NaOMe.

C. 2.0 M NaOMe.

D. 3.0 M NaOMe.

E. 4.5 M NaOMe.

FIGURE 5.4

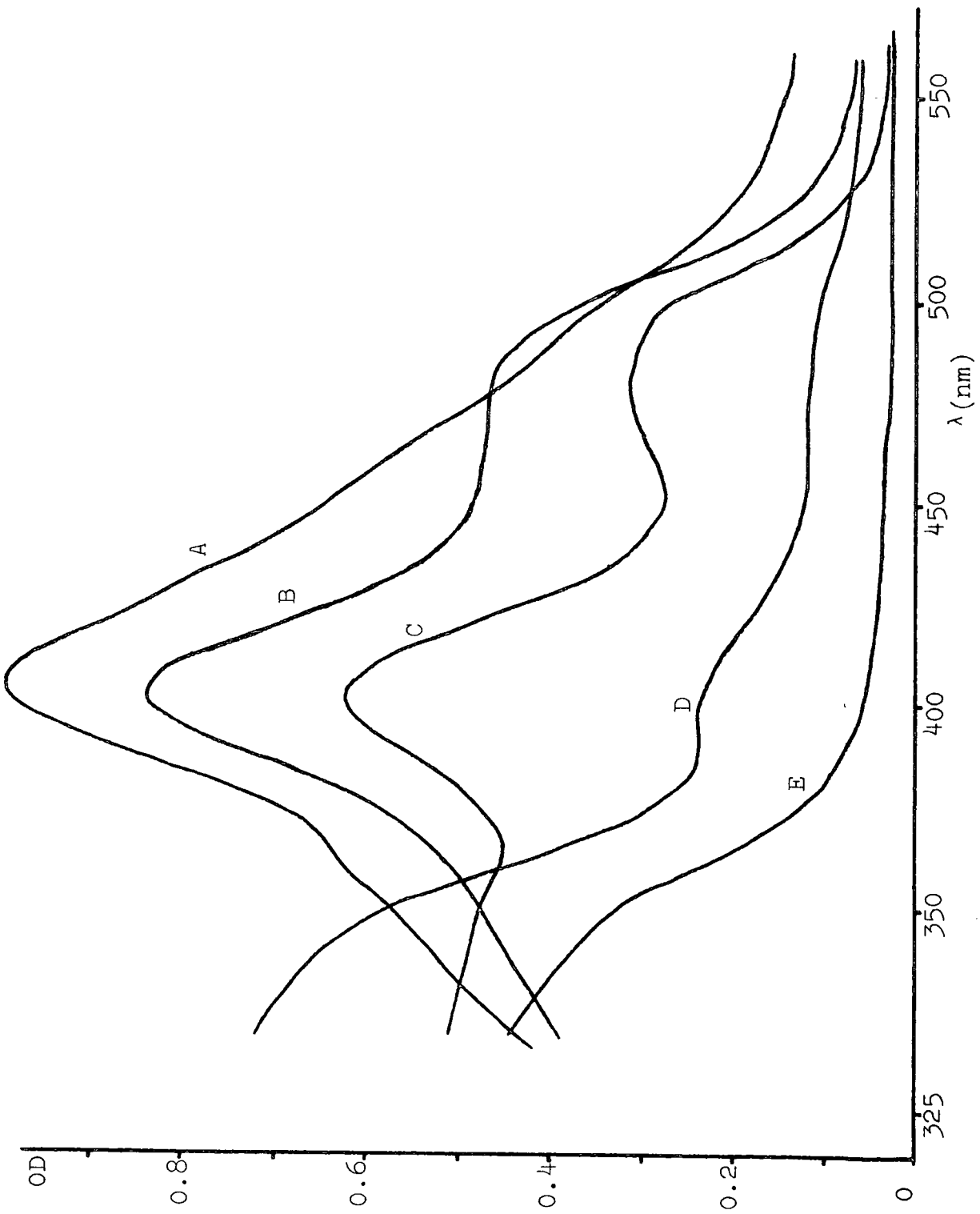

FIGURE 5.5

Spectra of the anion and adduct obtained from N-tert-butylpicramide and sodium methoxide in methanol at 25°C. 2×10^{-5} M substrate and 0.1 M sodium methoxide in a 1 cm cell. The spectrum of the adduct is corrected for absorption by unreacted substrate.

A. Spectrum of the substrate.

B. Spectrum attributed to the anion, 5.1 (R = ^{t}Bu).

C. Spectrum attributed to the adduct, 5.2 (R = ^{t}Bu, R′= H).

FIGURE 5.5

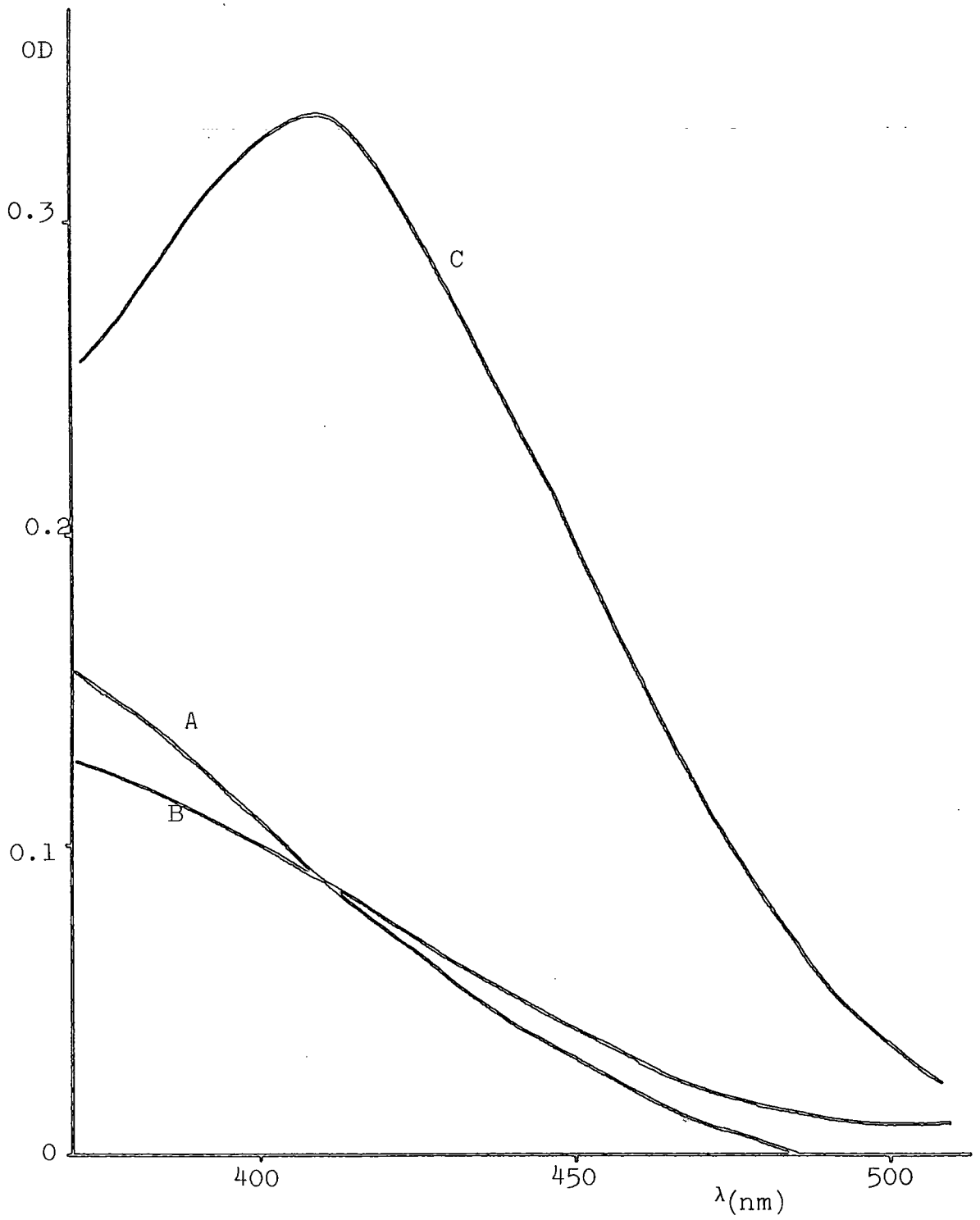

for proton abstraction, is very small. In agreement with this, a plot of k_{obs} vs base concentration (not shown)is linear; i.e. the rate data (Table 5.7) are fitted by equation (5.3), with values of $k_3 = 270 \pm 30$ l mol^{-1}s^{-1}, $k_{-3} = 10.5 \pm 0.5$ s^{-1}, and hence $K_3 = 26$ l mol^{-1}. It is estimated[49] that a value of $K \geq 1$ l mol^{-1} would cause curvature in the plot of k_{obs} vs base concentration, so this sets an upper limit on the value of K.

Equilibrium OD measurements (Table 5.7) were made using the SP500, and give a value of $K_T = 26$ l mol^{-1}, thus confirming the very small value of K.

^{1}H n.m.r. measurements (see Chapter Six) show that the two 1:1 interactions are amino-proton abstraction and C-3 adduct formation. The extent of amino-proton abstraction decreases as the proportion of methanol in the solvent increases: in 10% methanol-DMSO, 70% of the 1:1 interaction is proton abstraction, compared with approximately 35% in 50% methanol-DMSO. This is in agreement with the very small amount of proton-abstraction observed here, in pure methanol.

6. N-Phenylpicramide

In dilute base solution, this substrate undergoes a single, very fast colour-forming reaction, which produces a species with λ_{max} 435 nm. A T-jump experiment with 10^{-4} M substrate, 10^{-3} M base and 0.2 M sodium perchlorate in methanol showed that this reaction is faster than the heating time of the instrument, i.e. $t_{\frac{1}{2}} < 2$ μs, so $k > 3 \times 10^5$ s^{-1}. Measurement of the visible spectrum showed that $\geq$ 90% of the substrate is converted to the anion in a solution containing 10^{-3} M sodium methoxide. Thus, $K \geq 10^4$ l mol^{-1}. If K_3 is in the same range as those of the other substrates, i.e. of the order of 10 l mol^{-1}, then addition of methoxide ion

TABLE 5.7

Rate and equilibrium constants for the 1:1 reaction of N-tert-butylpicramide with sodium methoxide in methanol at 25°C.

$[MeO^-]$	k_{obs} [a]	k_{calc} [b]	OD_e [c]	K_T [d]
M	s^{-1}	s^{-1}		$l\ mol^{-1}$
0	-	-	0.183	-
0.01	13.3	13.2	0.350	25.7
0.02	15.8	15.9	0.417	20.1
0.04	21.1	21.3	0.591	24.9
0.06	26.1	26.7	0.682	26.2
0.08	29.3	32.1	0.751	28.5
0.10	35.2	37.5	0.789	28.7
0.15	54.0	51.0	-	-
0.20	70.5	64.5	0.925	-
0.25	80.7	78.0	-	-
0.30	90.5	91.5	-	-
0.40	-	-	0.923	-

a. Measured by stopped-flow spectrophotometry at 400 nm.

b. Calculated from equation (5.3), using k_3=270 $l\ mol^{-1}s^{-1}$; k_{-3} = 10.5 s^{-1}.

c. Measured at 405 nm, using the SP500. 4×10^{-5} M substrate in a 1 cm cell. OD_∞ = 1.00.

d. Calculated from equation (5.9), with OD_s = 0.183; OD_∞ = 1.00. Mean $K_T = 26 \pm 3$ $l\ mol^{-1}$.

is not expected to be detectable. This is in agreement with n.m.r. studies in methanol-DMSO[32,33], which showed 5.1 (R = Ph) to be the only observable product of a 1:1 reaction.

In base solutions above 2M, an absorption at 480 nm appears (Figure 5.6), attributed to methoxide addition (5.4, R = Ph). Above 3M base, an absorption at 345 nm is observed, attributed to 1:3 interaction. Because of the high base concentrations needed, these reactions were not investigated further.

7. N,N-Dimethylpicramide

Previous investigations[48] have produced evidence of 1:1 and 1:2 interactions with sodium methoxide in methanol. ^1H n.m.r. studies[33] in methanol-DMSO have shown that both complexes are formed by addition at unsubstituted ring positions.

In accord with the absence of an amino proton, stopped-flow measurements do not show a very fast colour-forming reaction. Stopped-flow measurements of the observed fast process were carried out both in the absence of added salt (Table 5.8) and with $\mu = 0.4$M using sodium perchlorate (Table 5.9). The rate constants in both cases show a linear dependence on the base concentration, as expected (equation 5.3). The two sets of results differ slightly, the presence of salt causing an increase in k_3 and a decrease in k_{-3}, with a consequent increase in K_3.

A second, much slower, process was observable using the stopped-flow, and is attributed to the formation of the 1:2 adduct, 5.8 (Scheme 5.2). The results (Table 5.10) are in accord with equation (5.10) (derived as equation (4.8): see Chapter Four).

FIGURE 5.6

Spectra obtained on the addition of sodium methoxide to 4×10^{-5} M N-phenylpicramide in methanol at 25°C (1 cm cell).

A. 1.0 M NaOMe.

B. 2.0 M NaOMe.

C. 3.0 M NaOMe.

FIGURE 5.6

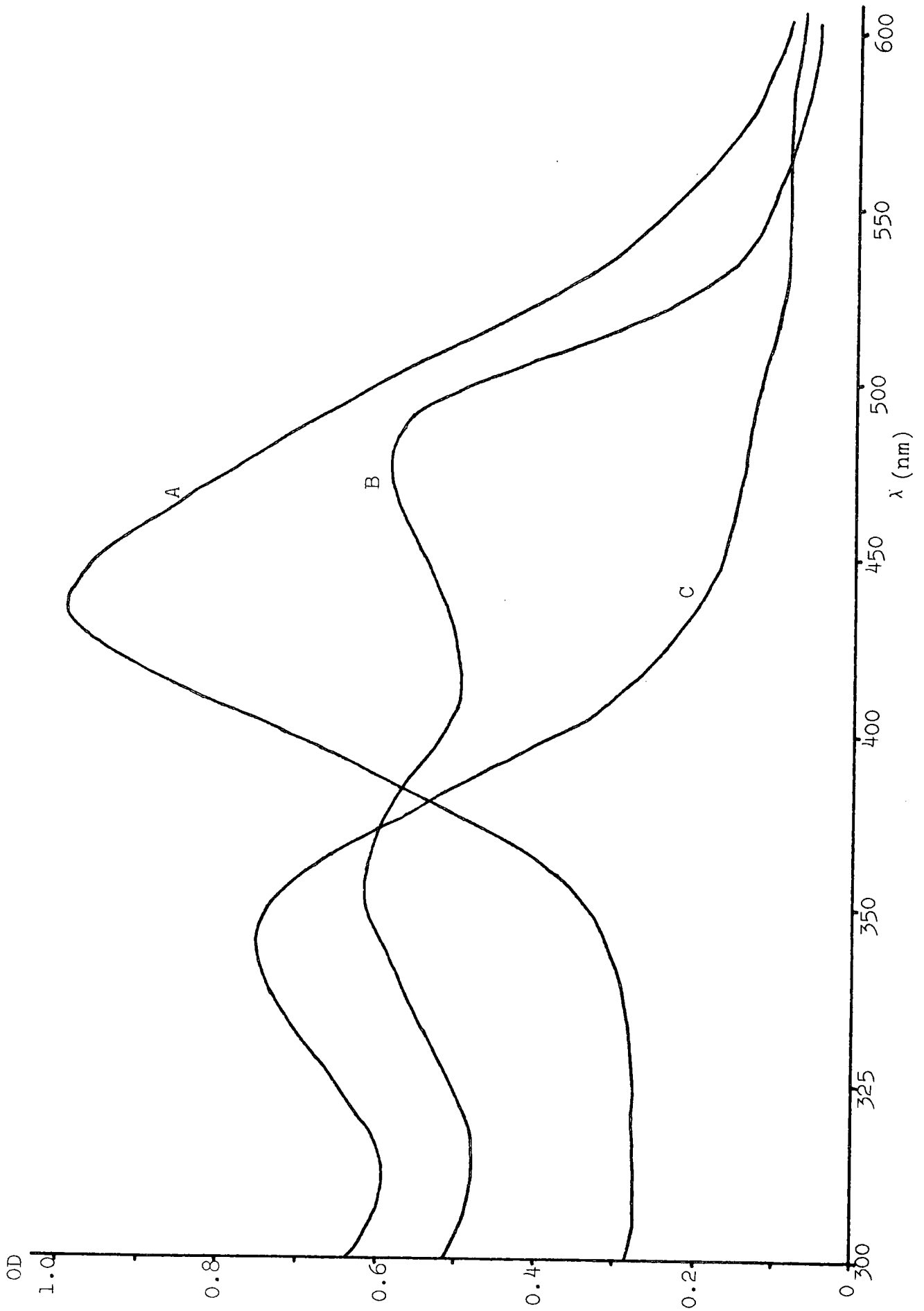

TABLE 5.8

Rate and equilibrium constants for the 1:1 reaction of N,N-dimethylpicramide with sodium methoxide in methanol at 25°C.

$[MeO^-]$ / M	k_{obs}[a] / s^{-1}	k_{calc}[b] / s^{-1}	OD[c]	K_3[d] / 1 mol^{-1}
0	-	-	0.008	-
0.02	38	35	0.055	3.6
0.04	43	38	0.085	3.1
0.06	40	42	0.125	3.3
0.08	42	45	0.165	3.6
0.10	52	49	0.200	3.8
0.20	68	67	0.300	3.6
0.30	84	85	0.370	3.5
0.40	108	103	0.440	4.0

a. Measured by stopped-flow spectrophotometry at 470 nm.

b. Calculated from equation (5.3), using k_3 = 180 1 mol^{-1} s^{-1}; k_{-3} = 31 s^{-1}; giving K_3 = 6 1 mol^{-1}.

c. Measured by stopped-flow spectrophotometry at 470 nm, after completion of the fast process.

d. Calculated from equation (5.9), with OD_s = 0.008; OD_∞ = 0.71. The mean value is $K_3 = 3.6 \pm 0.3$ 1 mol^{-1}.

TABLE 5.9

Rate constants for the 1:1 reaction of N,N-dimethylpicramide with sodium methoxide in methanol at 25°C, μ = 0.4 M($NaClO_4$).

$[MeO^-]$	k_{obs} [a]	k_{calc} [b]
M	s^{-1}	s^{-1}
0.02	27	27
0.04	27	31
0.06	37	36
0.08	39	40
0.10	39	44
0.20	64	65

a. Measured by stopped-flow spectrophotometry at 470 nm.

b. Calculated from equation (5.3), using k_3 = 210 l mol^{-1} s^{-1}; k_{-3} = 23 s^{-1}; giving K_3 = 9 ± 2 l mol^{-1}.

SCHEME 5.2

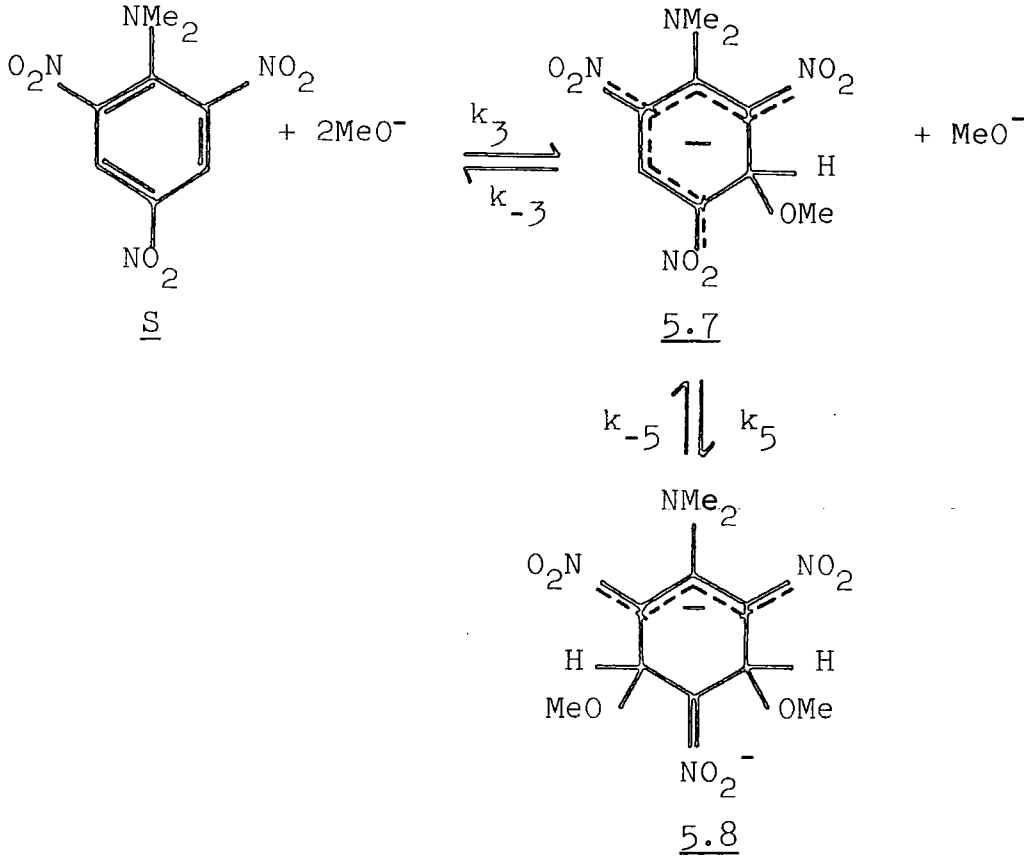

TABLE 5.10

Rate constants for the 1:2 reaction of N,N-dimethylpicramide with sodium methoxide in methanol at 25°C.

$[MeO^-]$	k_{obs} [a]	k_{calc} [b]	k_{obs} [a,c]	k_{calc} [d]
M	s^{-1}	s^{-1}	s^{-1}	s^{-1}
0.04	-	-	0.20	0.22
0.06	0.39	0.35	0.26	0.24
0.08	0.35	0.38	0.31	0.27
0.10	0.38	0.41	0.31	0.29
0.20	0.56	0.63	0.46	0.46
0.30	0.86	0.88	0.58	0.64
0.40	1.35	1.15	-	-

a. Measured by stopped-flow spectrophotometry at 410 nm.

b. Calculated from equation (5.10), using $K_3 = 6$ l mol^{-1}; $k_5 = 3$ l mol^{-1} s^{-1}; $k_{-5} = 0.3$ s^{-1}.

c. $\mu = 0.4$ M, with sodium perchlorate.

d. Calculated from equation (5.10), using $K_3 = 9$ l mol^{-1}; $k_5 = 2$ l mol^{-1} s^{-1}; $k_{-5} = 0.2$ s^{-1}.

$$k_{slow} = \frac{k_5 K_3 [MeO^-]^2}{(1+K_3[MeO^-])} + k_{-5} \qquad (5.10)$$

8. Comparison of Results

Rate and equilibrium constants are collected and shown in Table 5.11.

Those substrates which contain an amino proton undergo a very fast colour-forming reaction. T-jump measurements on picramide and its N-methyl and N-phenyl derivatives show that this reaction is faster than the heating time of the instrument (ca 2 μs). This is in accordance with the reaction's being transfer of a proton from the amino group to a methoxide ion, a process of which the forward and reverse rates are expected to be virtually diffusion-controlled[122]. Rates of methoxide ion attack at ring carbon atoms are expected[30,86,123,124] to be considerably slower than this. Therefore, the very fast process is ascribed to amino-proton abstraction.

The measurable process is assumed to be methoxide ion addition, which could occur at either C-1 or C-3. A comparison of the rate constants with those for related reactions indicate that addition occurs at C-3. For example, the rate constants for the formation and decomposition of the C-3 adduct of 2,4,6-trinitroanisole with methoxide ion[26] are 950 l $mol^{-1}s^{-1}$ and 350 s^{-1} respectively, compared with 17.3 and 10^{-3} respectively for the C-1 adduct. Thus, the values obtained here are closer to those expected for addition at an unsubstituted ring position.

^1H n.m.r. spectra also support the view that methoxide addition occurs first at C-3 and then at C-5, e.g. in the

TABLE 5.11

Collected rate and equilibrium data for the reactions of N-substituted picramides with sodium methoxide in methanol at 25°C.

X[a]	k_3 l mol^{-1}s^{-1}	k_{-3} s^{-1}	K l mol^{-1}	K_3 l mol^{-1}	K_T l mol^{-1}	K/K_T
NH_2	1900	60	9	32	41	0.22
NHMe	280	21	20	13	33	0.60
NH^iPr	450	16	5.5	28	33.5	0.16
NH^nBu	440	20	8.3	22	30	0.27
NH^tBu	270	10.5	< 1	26	26	~ 0.02
NHPh	-	-	> 10^4	-	-	~ 1.0
NMe_2	180	31	-	6	-	-
NMe_2[b]	210	23	-	9	-	-
H[c]	7050	305	-	23	-	-

a. Substrates are regarded as 1-X-2,4,6-trinitrobenzenes.

b. μ = 0.4 M ($NaClO_4$).

c. Reference 30.

reaction of trinitroanisole with methoxide ion in methanol-DMSO[32,33,125] (see also Chapter Six).

Thus, the major 1:1 interactions of picramide and its N-substituted derivatives are taken to be as in Scheme 5.1. This may be compared with the reaction of trinitrotoluene with methoxide ion[126], in which both addition at C-3 and proton abstraction (from $-CH_3$) occur.

The values of K, for amino-proton abstraction, decrease in the order Me>^{n}Bu>^{i}Pr>^{t}Bu. This can be understood in terms of differences in the inductive effect of the alkyl groups. Steric interaction between the alkyl group and the ortho nitro group may also be important. The maximum charge delocalisation in anions of structure 5.1 is achieved when the =N-R group is coplanar with the aromatic ring. The effect of the size of the alkyl group on the stability of 5.1 could well be related to the degree of difficulty encountered in achieving planarity. The high value of K when R = Ph is due to the delocalisation over two aromatic rings of the negative charge in the anion. Ground-state stabilisation of the substrates arises from resonance with 5.9. The loss of this stabilisation on forming the anion could be the cause of the relatively low value of K found for picramide itself. The extent of such ground-state stabilisation may well be less in the case of N-alkyl picramides.

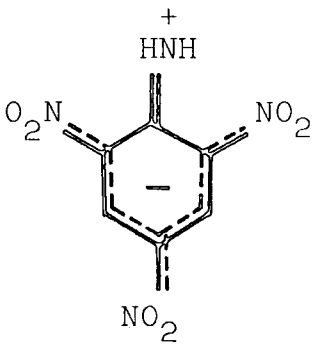

5.9

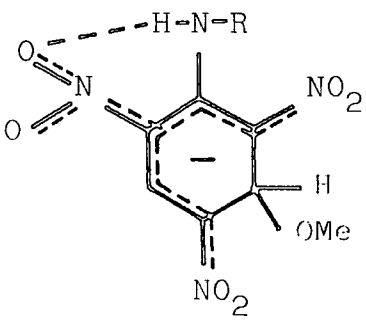

5.10

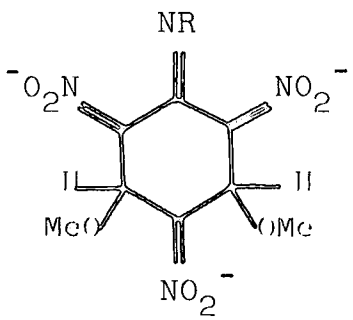

5.11

The values of K_3, for formation of the methoxide adduct at C-3, are of a similar magnitude to that for 1,3,5-trinitrobenzene[30] (Table 5.11), while the values of k_3 and k_{-3} are about an order of magnitude smaller than those for trinitrobenzene. The similarity in the values of K_3 indicates that the (substituted) amino group does not exert a substantial electronic effect at the position of attack. The smaller value of K_3 found for dimethylpicramide may be due to a reduction in the ability of the 2- and 6-nitro groups to delocalise negative charge when they are twisted out of the ring plane by steric interference from the dimethylamine group[127]. The stability of complexes containing an amino proton may be increased by intramolecular hydrogen bonding, 5.10.

The ratio K/K_T gives the fraction of substrate ionising by proton loss: the two processes are fairly well balanced in all cases. The ratios for picramide and N-methylpicramide agree well with those determined[23,41] by n.m.r. in methanol-DMSO. These ratios are expected to depend upon the solvent composition; increasing the concentration of methanol should favour the formation of the methoxide adduct.

The spectra of the adducts (Table 5.12) show that the anions formed by proton abstraction (5.1) absorb at about 440 nm, while the 1:1 adducts, 5.2, absorb near 400 nm. Increasing the base concentration produces an absorption near 480 nm, at the expense of those at shorter wavelengths. By comparison with n.m.r. data[23,41], this is probably due to formation of the 1:2 adduct, 5.4. At high base concentrations (>2M), there is little absorption above 350 nm. This change is believed to be due to a 1:3 species, 5.11[128,129].

Values of the rate and equilibrium constants for the

TABLE 5.12

Absorption maxima of species produced from N-substituted picramides with sodium methoxide in methanol at 25°C.

X[a]	λ_{max} nm			
	5.1	5.2	1:2	1:3
NH_2	~450	400	480	~340
NHMe		~410	485	<350
NH^iPr	435	~405		
NH^nBu		405	480	<350
NH^tBu		400		
NHPh	435	-	480	345
NMe_2	-	~390		

a. Substrates are regarded as 1-X-2,4,6-trinitrobenzenes.

reaction of dimethylpicramide with methoxide ion and with hydroxide ion (see Chapter Four) are compared in Table 5.13.

Both nucleophiles form the first adduct by addition at C-3, and the second by addition at C-5. In neither case is there any evidence for addition at C-1. This agrees with evidence from ^{1}H n.m.r. spectra[40,41].

That the rates of formation and decomposition of the complexes are higher with methoxide ion than with hydroxide ion is in agreement with previous results for a variety of substrates obtained in both pure[30,130] and mixed[38,113,131] solvents. The observed rate order for base addition may be partly due to the high degree of solvation of hydroxide ion by water[132], which recuces its reactivity. The observed rate order for complex decomposition may be due to intramolecular hydrogen-bonding in the complex[30], 5.12, holding the hydroxide ion more firmly than expected. A similar mechanism could operate in the 1:2 adduct, e.g. 5.13.

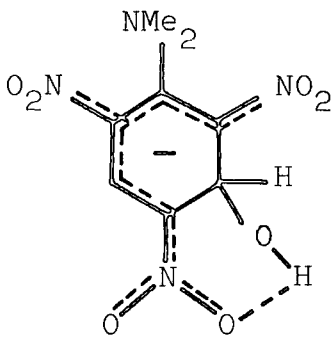

5.12

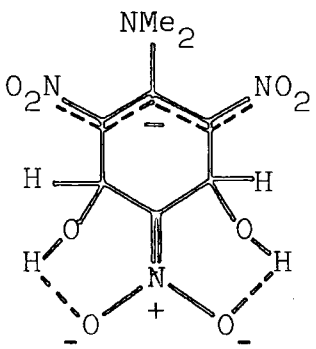

5.13

TABLE 5.13

Rate and equilibrium constants for the reaction of N,N-dimethylpicramide with sodium hydroxide in water and with sodium methoxide in methanol at 25°C.

	HO^-		MeO^-
μ M	1.0	-	0.4
k_3 l $mol^{-1}s^{-1}$	3.6	180	210
k_{-3} s^{-1}	0.19	31	23
K_3 l mol^{-1}	21	6	9
k_5 l $mol^{-1}s^{-1}$	1.0	3.0	2.0
k_{-5} s^{-1}	0.001	0.3	0.2
K_5 l mol^{-1}	10^3	10	10

CHAPTER SIX

THE INTERACTION OF N-SUBSTITUTED 2,4,6-TRINITROANILINES WITH BASES IN DIMETHYLSULPHOXIDE-METHANOL MIXTURES

INTRODUCTION

Proton magnetic resonance spectroscopy is a very useful technique for determining the structures of σ-adducts[8,105]. Probable 1:1 interactions of N-substituted picramides with nucleophiles are amino-proton abstraction to form the conjugate base, 6.1, and formation of the σ-adduct at C-3, 6.2. ^1H n.m.r. spectra for the reaction of picramide, N-methylpicramide and N,N-dimethylpicramide with sodium methoxide in DMSO indicate that both 6.1 and 6.2 are formed from the first two, and 6.2 from the last[23,33,41]. Reactions of aliphatic amines with picryl ethers[31,121] give rise to adducts at C-1, 6.3. Addition of hydroxylamine to N-methylpicramide has also been reported[119] as producing the C-1 adduct.

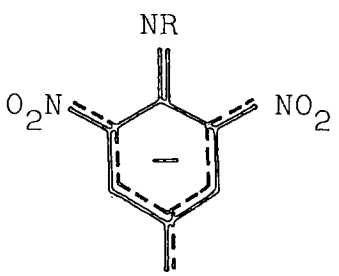

6.1

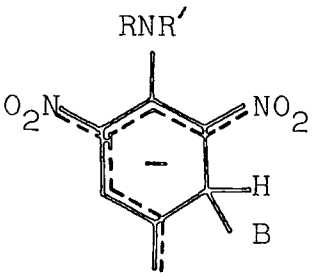

6.2

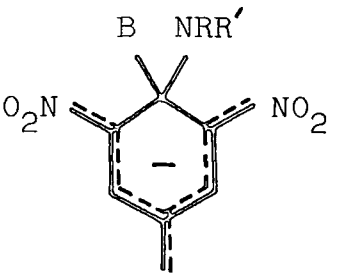

6.3

Amide adducts at C-H have been obtained from trinitrobenzene with primary and secondary aliphatic amines in DMSO[133]. Catalysts are required for the formation of trinitrobenzene adducts with aromatic amines; for example, the adduct with aniline can be formed from the methoxide adduct[134], or directly from trinitrobenzene in the presence of Dabco or triethylamine[135]. Spin-coupling has been observed[134] between the amino-proton and the adjacent ring-proton in the trinitro-

benzene-aniline complex. 1:1 and 1:2 adducts of picramide and N,N-dimethylpicramide with amide ion in liquid ammonia have been found[53] to result from addition at C-H.

The work described in this chapter is a ^{1}H n.m.r. study of the reactions of some trinitroaromatic compounds with sodium methoxide, piperidine and benzylamine in DMSO-methanol mixtures.

EXPERIMENTAL

^{1}H n.m.r. measurements were made at 60 MHz on a Varian A56/60 instrument, and at 90 MHz on a Brucker HX90E instrument modified for F.T. operation, and using a deuterium lock. All shift measurements are quoted relative to internal tetramethylsilane.

Reaction solutions were made up using weighed amounts of substrate, the appropriate volume of concentrated base solution being added by syringe immediately before running the spectrum.

RESULTS AND DISCUSSION

1. Reactions with Sodium Methoxide in DMSO-Methanol Solutions

(a) N-Isopropylpicramide in 50% d_6-DMSO-methanol

Chemical shift data are shown in Table 6.1. The ring proton resonance in column (a) shows a gradual progression from δ8.96 in the substrate, to δ8.33 above one equivalent of base. This time-averaged signal is indicative of rapid exchange between the two species, suggesting that the process involved is transfer of the amino-proton to methoxide ion, forming the conjugate base, 6.1 (R = ^{i}Pr). In contrast, the resonances listed in columns (b) and (c) show no such progression with increasing base concentration, indicating that the species concerned is in slow equilibrium with the substrate. The resonance in column (c) is shifted strongly upfield from the aromatic ring-proton position, indicating a change of hybridisation at this carbon atom. That in column (b), however, remains in the region expected for an aromatic ring-proton. These resonances suggest the formation of the C-3 adduct, 6.2, that in column (c) corresponding to the proton at the position of addition.

The relative intensities of the resonances (not shown) indicate that 6.1 and 6.2 are formed in roughly equal concentrations. This is supported by the calculated values of the chemical shift of the ring proton in the conjugate base (Table 6.3), which are in good agreement with the observed values, when calculated assuming 50% base addition. This contrasts with the finding[136] that, in 83% DMSO-methanol, virtually all of the 1:1 reaction is amino-proton abstraction, forming the conjugate base, 6.1.

TABLE 6.1

Chemical shift data for the reaction of N-isopropylpicramide with sodium methoxide in 50% d_6-DMSO-methanol. 0.2 M substrate; measured at 90 MHz.

$[MeO^-]/[S]$	δ (ring)				δ (^iPr)	
	(a)	(b)	(c)	(d)	(e)	(f)
0	8.96	-	-	1.28(d)	-	-
0.2	8.91	-	-	1.23(d)	-	-
0.5	8.76	8.50	6.20	1.26(d)	1.15(d)	1.44(d)
0.7	8.60	8.52	6.25	-	1.12(d)	1.38(d)
1.0	8.33	8.56	6.23	1.02(d)	1.15(d)	1.39(d)
1.5	8.33	8.56	6.21	1.04(d)	1.11(d)	1.39(d)
2.0	8.33	8.56	6.16	1.03(d)	1.12(d)	1.35(d)

a. Ring-proton resonance in the substrate and conjugate base, 6.1.

b. Resonance of ring-proton H_a (sp^2C) in the C-3 adduct, 6.2.

c. Resonance of ring-proton H_b (sp^3C) in the C-3 adduct, 6.2

d. Resonance of the N-alkyl group in the substrate and conjugate base, 6.1 (doublets).

e, f. Resonances of the N-alkyl group in the C-3 adduct, 6.2 (doublets).

The isopropyl group gives rise to two resonances in the C-3 adduct, indicating that the two methyl groups are non-equivalent, and hence that rotation about the ring-carbon to nitrogen bond is restricted.

(b) N-tert-Butylpicramide in 50% d_6-DMSO-methanol

Chemical shift data are shown in Table 6.2. The resonances listed in column (a) are very similar to those for N-isopropylpicramide (above), and show a similar progression. These are attributed to formation of the conjugate base, 6.1 (R = ^{t}Bu), by amino-proton abstraction, as above. The resonances in columns (b) and (c) are fairly static, as before, and are assigned to the C-3 adduct, 6.2 (R = ^{t}Bu), that in column (c) being due to the proton at the point of addition.

The relative intensities of the signals (not shown) suggest that ca 75% of the interaction occurs by base addition. Calculation of the ring-proton resonance (Table 6.3) indicates a value of approximately 55% base addition.

Separate bands are observed for the amino-proton of the substrate and adduct. The chemical shift of the amino-proton in the adduct suggests that it is hydrogen-bonded to the adjacent nitro-group.

TABLE 6.2

Chemical shift data for the reaction of N-tert-butylpicramide with sodium methoxide in 50% d_6-DMSO-methanol. 0.2 M substrate; measured at 90 MHz.

$[MeO^-]/[S]$	δ(ring)			δ(^{t}Bu)		δ(NH)
	(a)	(b)	(c)	(d)	(e)	(f)
0	8.96	-	-	1.33	-	7.88
0.2	8.91	8.44	6.19	1.33	-	-
0.5	8.81	8.47(d)	6.23(d)	1.30	1.45	10.8
0.7	8.64	8.43(d)	6.24(d)	1.29	1.45	10.9
1.0	8.37	8.51(d)	6.26(d)	1.20	1.45	-
1.5	8.24	8.50(d)	6.26(d)	1.17	1.46	-
2.0	8.24	8.51(d)	6.25(d)	1.17	1.45	-

a. Ring-proton resonance in the substrate and conjugate base, 6.1.

b. Resonance of ring-proton H_a (sp^2C) in the C-3 adduct, 6.2 (doublets).

c. Resonance of ring-proton H_b (sp^3C) in the C-3 adduct, 6.2 (doublets).

d. Resonance of the N-alkyl group in the substrate and conjugate base, 6.1.

e. Resonance of the N-alkyl group in the C-3 adduct, 6.2.

f. Resonance of the amino-proton in the substrate (δ 7.88) and in the C-3 adduct (δ10.9) (hydrogen-bonded to the ortho nitro-group).

TABLE 6.3

Calculated chemical shifts of the ring-proton in the rapid exchange between the substrate and the conjugate base.

$[MeO^-]/[S]$	PicNH^{i}Pr		PicNH^{t}Bu	
	δ	δ_{calc}[a]	δ	δ_{calc}[a]
substrate	8.96	-	8.96	-
0.2	8.91	8.89	8.91	8.89
0.5	8.76	8.75	8.81	8.75
0.7	8.60	8.62	8.64	8.63
1.0	8.33	-	8.37	8.37
conjugate base	8.33	-	8.24	-

a. Calculated from equation (6.1), assuming 50% proton abstraction for PicNH^{i}Pr and 45% for PicNH^{t}Bu.

$$\delta_{calc} = \delta_s - \frac{(\delta_s - \delta_b)}{(1 - f_N)} \cdot f_N \qquad (6.1)$$

where δ_s = chemical shift in the substrate,

δ_b = chemical shift in the conjugate base,

f_N = (% proton abstraction) x (mole fraction of base).

The ring-proton resonances of the adduct, 6.2, are doublets, due to spin-coupling between the two non-equivalent protons. However, the ring-proton resonance in the conjugate base, 6.1, is a sharp singlet, indicating that the two ring-protons are magnetically equivalent. Thus, there must be rapid rotation about the ring-carbon to nitrogen bond in the conjugate base, 6.1. In agreement with this is the single resonance found for the tert-butyl group in 6.1.

(c) N-tert-Butylpicramide in 90% d_6-DMSO-methanol

Chemical shift data are shown in Table 6.4. In this case, there is no rapid exchange between the substrate and its conjugate base, so separate resonances are seen for the ring-protons in the two species. The C-3 adduct shows two coupled resonances (columns (c) and (d)), as before, emphasising the non-equivalence of the protons at C-3 (the point of addition, and hence sp^3 hybridised) and at C-5 (an aromatic, sp^2 position). This is in contrast with the equivalence of the ring-protons in the conjugate base, 6.1, which give rise to a single resonance (column (b)).

Consideration of the relative intensities of the signals (not shown) suggest that ca 70% of the 1:1 interaction occurs by amino-proton abstraction, compared with 25-45% in 50% DMSO-methanol. Thus, formation of the adduct is favoured by a higher proportion of methanol in the solvent. This can be understood from equation (6.2), which shows that the conjugate base, 6.1, and the adduct, 6.2, differ from each other by one molecule of methanol.

$$PicNR^- + MeOH \rightleftharpoons PicNHR\cdot OMe^- \qquad (6.2)$$

TABLE 6.4

Chemical shift data for the reaction of N-tert-butylpicramide with sodium methoxide in 90% d_6-DMSO-methanol. 0.2 M substrate; measured at 90 MHz.

$[MeO^-]/[S]$	δ (ring)							δ (^tBu)			δ(NH)	
	(a)	(b)	(c)	(d)	(e)	(f)	(g)	(h)	(i)	(j)	(k)	(l)
0	8.91	-	-	-	-	-	1.30	-	-	-	7.68	-
0.2	8.89	-	-	-	-	-	1.26	-	-	-	7.67	-
0.5	8.91	8.18	8.41	6.42	-	-	-	1.15	1.36	-	7.76	-
0.7	8.90	8.17	8.43(d)	6.21(d)	-	-	-	1.14	1.40	-	7.70	10.65
1.0	-	8.19	8.46(d)	6.19(d)	-	-	-	1.15	1.40	-	-	10.68
1.5	-	8.18	-	-	8.41	6.02	-	1.17	-	1.32	-	-
2.0	-	8.16	-	-	8.41	5.98	-	1.13	-	1.30	-	-

TABLE 6.4 (contd.)

a. Ring-proton resonance in the substrate.

b. Ring-proton resonance in the conjugate base, 6.1.

c. Resonance of ring-proton H_a (sp^2C) in the C-3 adduct, 6.2 (doublets).

d. Resonance of ring-proton H_b (sp^3C) in the C-3 adduct, 6.2 (doublets).

e. Resonance of ring-proton H_a (sp^2C) in the ionised adduct, 6.4 (the conjugate base of 6.2).

f. Resonance of ring-proton H_b (sp^3C) in the ionised adduct, 6.4.

g. Resonance of the N-alkyl group in the substrate.

h. Resonance of the N-alkyl group in the conjugate base, 6.1.

i. Resonance of the N-alkyl group in the C-3 adduct, 6.2.

j. Resonance of the N-alkyl group in the ionised adduct, 6.4.

k. Resonance of the amino-proton in the substrate.

l. Resonance of the amino-proton in the C-3 adduct, 6.2.

The alkyl groups in the conjugate base, adduct and ionised adduct each give rise to single resonances, indicating that the three methyl groups in the tert-butyl group are equivalent, as expected.

The amino-protons of the substrate and adduct give resonances separate from those of the hydroxylic proton of the solvent. This suggests that the equilibria between the adduct, substrate and conjugate base are slow. The position of the amino-proton resonance of the adduct indicates that the amino-proton is hydrogen-bonded to the adjacent nitro-group.

At higher base concentrations, the H_b ring-proton resonance of the C-3 adduct undergoes a shift to higher field, while that of H_a is virtually unchanged. Because the change in chemical shift is small, and no new resonances appear, this is attributed to removal of the amino-proton from the C-3 adduct, forming the "ionised adduct", 6.4.

(d) Comparison of results

Chemical shift data for the various species are listed in Table 6.5. The data are consistent with Scheme 6.1.

The results provide evidence for addition at C-3 and amino-proton abstraction, but not addition at C-1. Formation of the C-3 adduct is indicated by the large shift to high field shown by the resonance of one ring proton: this is consistent with a change of hybridisation from sp^2 to sp^3. If the other interaction were addition at C-1, then the N-alkyl resonance would be expected to change much more than it does. The time-averaged signal for the ring-proton, due to rapid exchange between the substrate and the product also

TABLE 6.5

Chemical shifts for the reactions of N-isopropyl- and N-tert-butylpicramides with sodium methoxide in d_6-DMSO-methanol (measured at 90 MHz).

	$PicNH^iPr$	$PicNH^tBu$	
DMSO-MeOH (v/v)	50/50	50/50	90/10
substrate			
ring-proton	8.96	8.96	8.91
N-alkyl	1.28(d)	1.33	1.30
N-H	-	7.86	7.68
conjugate base, 6.1			
ring-proton	8.33	8.24	8.18
N-alkyl	1.05(d)	1.17	1.15
C-3 adduct, 6.2			
ring-proton H_a (sp^2C)	8.55	8.50(d)	8.45(d)
ring-proton H_b (sp^3C)	6.23	6.25(d)	6.20(d)
N-alkyl	1.16(d)	1.45	1.40
N-H	-	10.85	10.65
[6.1]:[6.2]	45:55	35:65	70:30

SCHEME 6.1

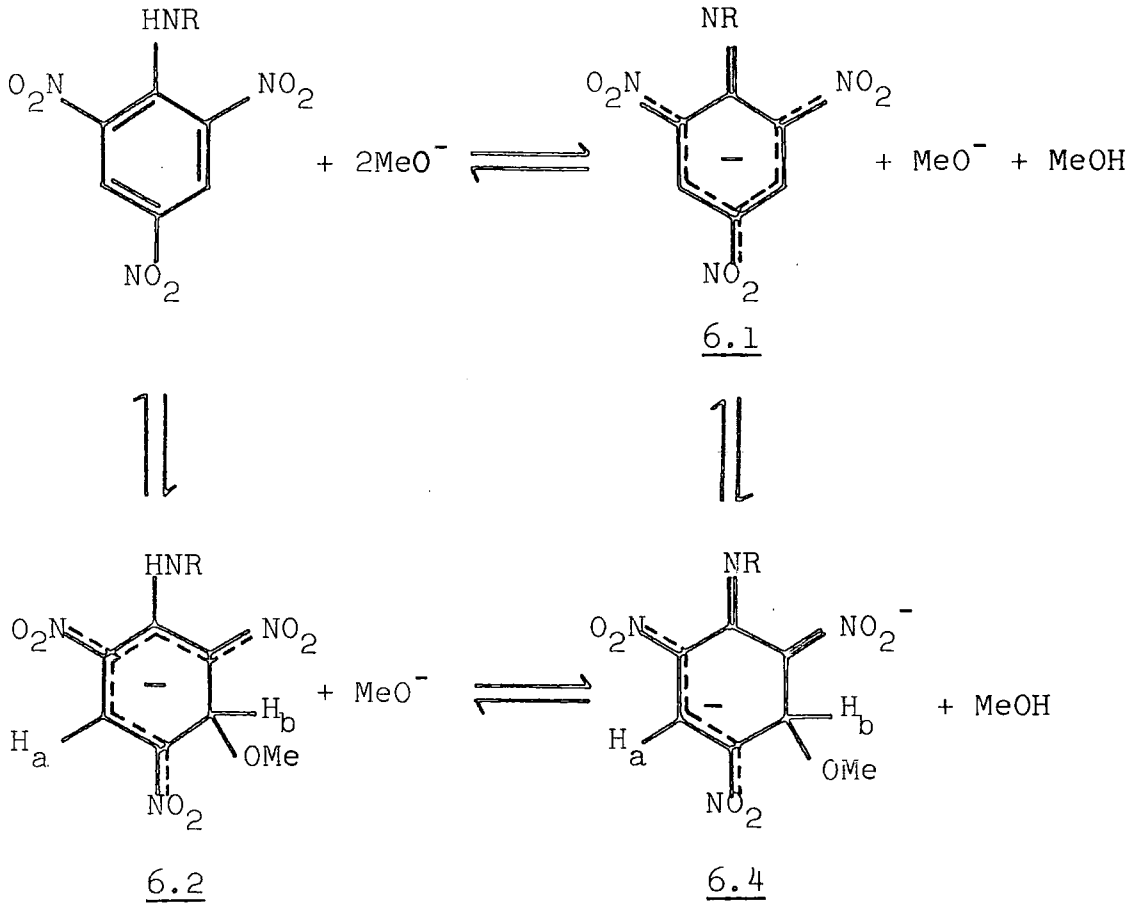
HNR
O_2N
NO_2
NO_2
+ $2MeO^-$
NR
O_2N
NO_2
NO_2
+ MeO^- + MeOH
6.1
HNR
O_2N
NO_2
H_a
H_b
OMe
NO_2
+ MeO^-
NR
O_2N
NO_2^-
H_a
H_b
OMe
NO_2
+ MeOH
6.2
6.4

supports proton transfer, as base addition would be a slow process on the n.m.r. timescale. The observation[136] that the reactions of N-methylpicramide with methoxide and isopropoxide ions produce identical spectra provides further evidence for the removal of the amino-proton. Base addition at C-1 would be expected to give quite different spectra.

Base addition is favoured over proton abstraction in 50% DMSO-methanol for both substrates, but to a slightly greater degree in the case of tert-butylpicramide. This may be due to the bulky alkyl group hindering methoxide (or methanol) attack on the amino-proton. The slow interconversion of the substrate and its conjugate base in 90% DMSO-methanol can also be explained in this way. The observation that proton abstraction is favoured in solvents containing a smaller proportion of methanol can be explained in terms of equation (6.2) (above): the conjugate base, 6.1, and adduct, 6.2, differ from each other by one molecule of methanol.

2. Reactions with Piperidine and Sodium Methoxide in 90% (v/v) DMSO-Methanol

Sodium methoxide was used to form piperidide ions (equation 6.3), which produced sharper spectra than were obtained using piperidine only.

$$pipNH + MeO^- \rightleftharpoons pipN^- + MeOH \qquad (6.3)$$

(a) N-Isopropylpicramide

Chemical shift data are shown in Table 6.6. The addition of piperidine to solutions containing a 1:1 ratio of substrate to methoxide ion causes new resonances to appear, at the expense of those due to the conjugate base of the substrate, 6.1. These new resonances are ascribed to the C-3 piperidide adduct, 6.5 (Scheme 6.2).

TABLE 6.6

Chemical shift data for the reaction of N-isopropylpicramide with piperidine and sodium methoxide in 90% DMSO-methanol. 0.2 M substrate; measured at 60 MHz.

[S]:[MeO^-]:[am]	δ(ring)			δ($^iPrO^-$)	
	(a)	(b)	(c)	(d)	(e)
1:1:0	8.22, 8.52	-	-	0.98(d)	-
1:1:0.5	8.15, 8.52	8.63	5.68	1.00(d)	1.2(m)
1:1:1	-	8.65	5.75	-	1.3(m)
1:1.5:1	-	8.75	5.60	-	1.3(m)
1:2:1	-	8.78	5.55	-	1.3(m)
1:2:2	-	8.77	5.53	-	1.4(m)

a. Ring-proton resonances in the conjugate base, 6.1.

b. Resonance of ring-proton H_a (sp^2C) in the amide adduct, 6.5.

c. Resonance of ring-proton H_b (sp^3C) in the amide adduct, 6.5.

d. Resonance of the N-alkyl group in the conjugate base, 6.1 (doublets).

e. Resonance of the N-alkyl group in the amide adduct, 6.5 (multiplets).

SCHEME 6.2

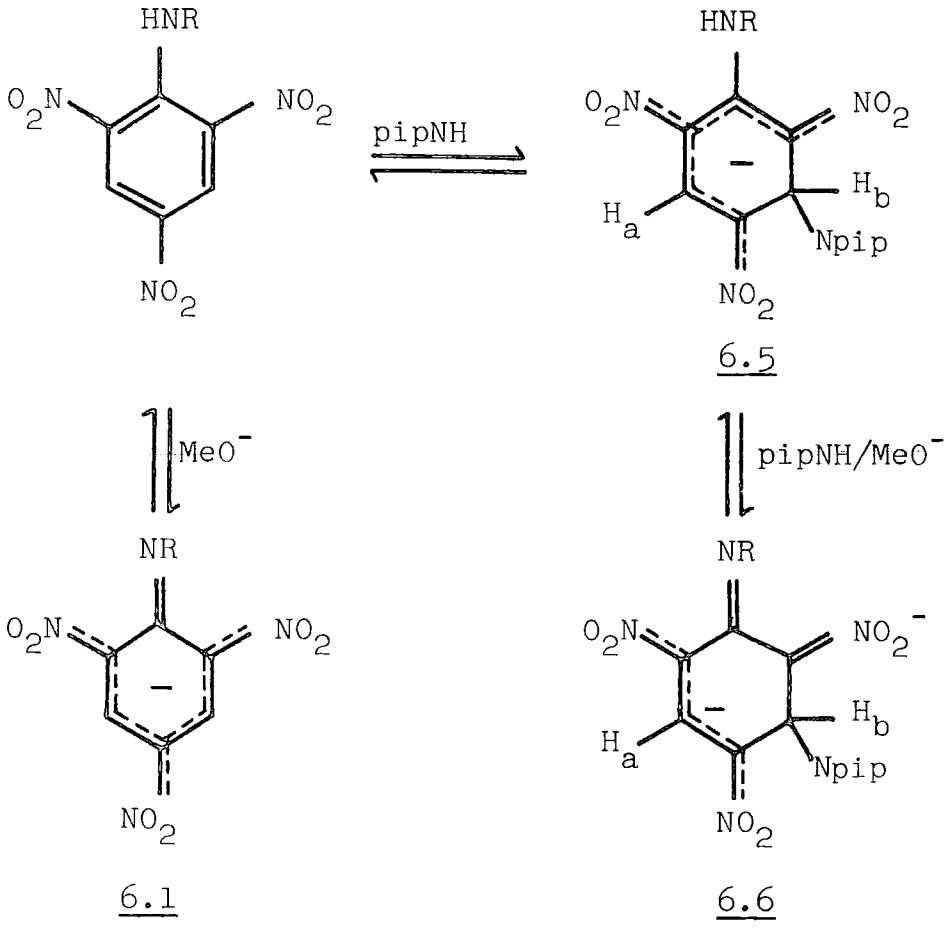

6.5

6.1

6.6

The chemical shift of H_b (sp^3C) is ca δ 5.7, similar to those found[133] for amine adducts of trinitrobenzene, but distinct from the value of ca δ 6.2 found for methoxide adducts (Table 6.5).

The ring-protons in the conjugate base, 6.1, are not equivalent, because of slow rotation about the ring-carbon to nitrogen bond, and so produce two separate signals.

The isopropyl resonance in the conjugate base is a doublet (J ~6Hz), due to spin-coupling between the methyl groups and the central C-H. In the amine adduct, 6.5, the alkyl resonance is a multiplet, indicating that the methyl groups are no longer equivalent. This suggests that rotation about the ring-carbon to nitrogen bond is restricted in the C-3 adduct.

As the proportion of methoxide and/or piperidine is raised, the resonance at δ 8.6 moves to lower field and that at δ 5.7 to higher field, indicating that a further reaction is occurring. From the relatively small shifts, and the fact that no new resonances appear, this seems to be removal of the amino-proton, forming the conjugate base of the adduct, 6.6. The 1:2 reaction with piperidide ion could also result in the formation of the 1:2 adduct, 6.7, (cf. the reaction of picramide and N,N-dimethylpicramide with amide ion in liquid ammonia[53]), but no evidence for this was found under the conditions used.

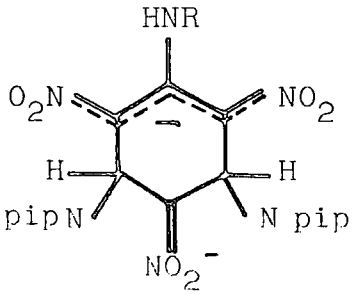

6.7

(b) N-tert-Butylpicramide

Chemical shift data are shown in Table 6.7. The addition of piperidine causes new resonances to appear, due to the formation of the C-3 adduct, 6.5. As the amount of base is increased, the separation between the ring-proton resonances increases slightly, but no new signals appear: this is again ascribed to ionisation of the adduct, 6.5, to form 6.6.

(c) Comparison of results

The major 1:1 interaction of piperidide ion with these substrates is formation of the adduct at C-3. Similar results have been obtained[136] for N-methyl- and N,N-dimethyl-picramide. The 1:2 reaction seems to result in amino-proton abstraction to form 6.6, rather than formation of the 1:2 adduct, 6.7. However, both methoxide ion and piperidine are in excess over the substrate, so there are several competing equilibria to be taken into account (6.4-6.6):

$$pipNH + MeO^- \rightleftharpoons pipN^- + MeOH \qquad (6.3)$$

$$PicNHR\cdot Npip^- + MeO^- \rightleftharpoons Pic\bar{N}R\cdot Npip^- + MeOH \qquad (6.4)$$

$$PicNHR\cdot Npip^- + pipN^- \rightleftharpoons Pic\bar{N}R\cdot Npip^- + pipNH \qquad (6.5)$$

$$PicNHR\cdot Npip^- + pipN^- \rightleftharpoons PicNHR\cdot (Npip)_2^{2-} \qquad (6.6)$$

The reaction observed will depend upon the relative magnitudes of the equilibrium constants for these processes.

3. Reactions with Benzylamine and Sodium Methoxide in ca. 80% (v/v) DMSO-Methanol

As in the reactions with piperidine, use of sodium methoxide to generate the benzylamide ion resulted in sharper spectra.

TABLE 6.7

Chemical shift data for the reaction of N-tert-butylpicramide with piperidine and sodium methoxide in 90% DMSO-methanol. 0.2 M substrate; measured at 60 MHz.

[S]:[MeO^-]:[am]	δ (ring)			δ (^tBu)	
	(a)	(b)	(c)	(d)	(e)
1:1:0	8.33	-	-	1.17	-
1:1:0.5	8.25	8.53	-	1.15	1.40
1:1:1	-	8.60	5.78	-	1.33
1:1.5:1	-	8.62	5.65	-	1.37
1:2:1	-	8.67	5.63	-	1.35
1:2:2	-	8.63	5.60	-	1.35

a. Ring-proton resonance in the conjugate base, 6.1.

b. Resonance of ring-proton H_a (sp^2C) in the amide adduct, 6.5.

c. Resonance of ring-proton H_b (sp^3C) in the amide adduct, 6.5.

d. Resonance of the N-alkyl group in the conjugate base, 6.1.

e. Resonance of the N-alkyl group in the amide adduct, 6.5.

(a) 1,3,5-Trinitrobenzene

Chemical shift data are shown in Table 6.8. The spectra indicate the formation of benzylamide complexes by addition at C-H. In the absence of methoxide ion, the signals are rather broad. Ring-proton resonances are observed corresponding to amine addition at C-H, that at higher field (due to the proton at the point of attack) being of half the intensity of the signal at lower field (due to the two remaining "aromatic" protons). The benzylamine ring and $-CH_2-$ resonances are those for the "free" amine, since the amine is present in large excess. As the concentration of benzylamine is increased, the proportion present in the protonated form, arising from equilibrium (6.7), decreases, and so the amino-proton resonance moves upfield.

$$TNB + 2RNH_2 \rightleftharpoons TNB{\cdot}NHR^- + RNH_3^+ \qquad (6.7)$$

When methoxide ion is the only nucleophile present, the C-3 adduct, 6.9 (X = H), is formed. Addition of benzylamine to a 1:1 mixture of trinitrobenzene and methoxide produces a mixture of the two adducts, 6.8 and 6.9. Conversion to the benzylamine adduct is not complete when the reactants are present in a 1:1:1 ratio, so the equilibria for the two complex formations (Scheme 6.3) must be quite closely balanced in the solvent system used.

In the amine adduct, the ring-proton at the position of addition (H_b) is a doublet (J= 5Hz). When deuterated amine is used (Table 6.8(ii)), this splitting is no longer observed. Similarly, the (bound) amine - CH_2 - signal is a doublet (J = 7Hz), but becomes a singlet when deuterated amine is used. The line separations of both these signals are independent of the field strength, as shown by measure-

TABLE 6.8

Chemical shift data for the reaction of 1,3,5-trinitrobenzene with (i) benzylamine, (ii) N-deuterated benzylamine, and sodium methoxide in 90% d_6-DMSO-methanol. 0.2 M substrate; measured at 90 MHz.

	[S]:[MeO^-]:[am]	δ (substrate)				δ (amine)				
		(a)	(b)	(c)	(d)	(e)	(f)	(g)	(h)	(i)
(i)	1:0:5	8.37	5.89	-	-	7.31	-	3.82	-	4.03
	1:0:10	8.45	5.81	-	-	7.30	-	3.74	-	2.87
	1:1:0	-	-	8.50	6.15	-	-	-	-	-
	1:1:0.5	8.37	5.71(d)	8.53	6.18	7.32	7.19	-	-	-
	1:1:1	8.37	5.73(d)	8.50	6.18	7.30	7.17	3.76	3.51(d)	-
	1:1:2	8.38	5.71(d)	8.48	6.18	7.28	7.16	3.73	3.50(d)	-
(ii)	1:1:0	-	-	8.47(d)	6.16	-	-	-	-	-
	1:1:0.5	8.36	5.73	8.48(d)	6.17	7.30	7.17	-	3.50	-
	1:1:1	8.37	5.74	8.50	6.18	7.28	7.18	3.70	3.48	-
	1:1:2	8.39	5.74	8.52	-	7.32	7.17	3.70	3.48	-

TABLE 6.8 (contd.)

a. Resonance of ring-protons H_a (sp^2C) in the amine adduct, 6.8.

b. Resonance of ring-proton H_b (sp^3C) in the amine adduct, 6.8.

c. Resonance of ring-protons H_a (sp^2C) in the methoxide adduct, 6.9.

d. Resonance of ring-proton H_b (sp^3C) in the methoxide adduct, 6.9.

e. Resonance of the Ph group in the free amine.

f. Resonance of the Ph group in the bound amine in 6.8.

g. Resonance of the $-CH_2-$ group in the free amine.

h. Resonance of the $-CH_2-$ group in the bound amine in 6.8.

i. Amino-proton resonance.

SCHEME 6.3

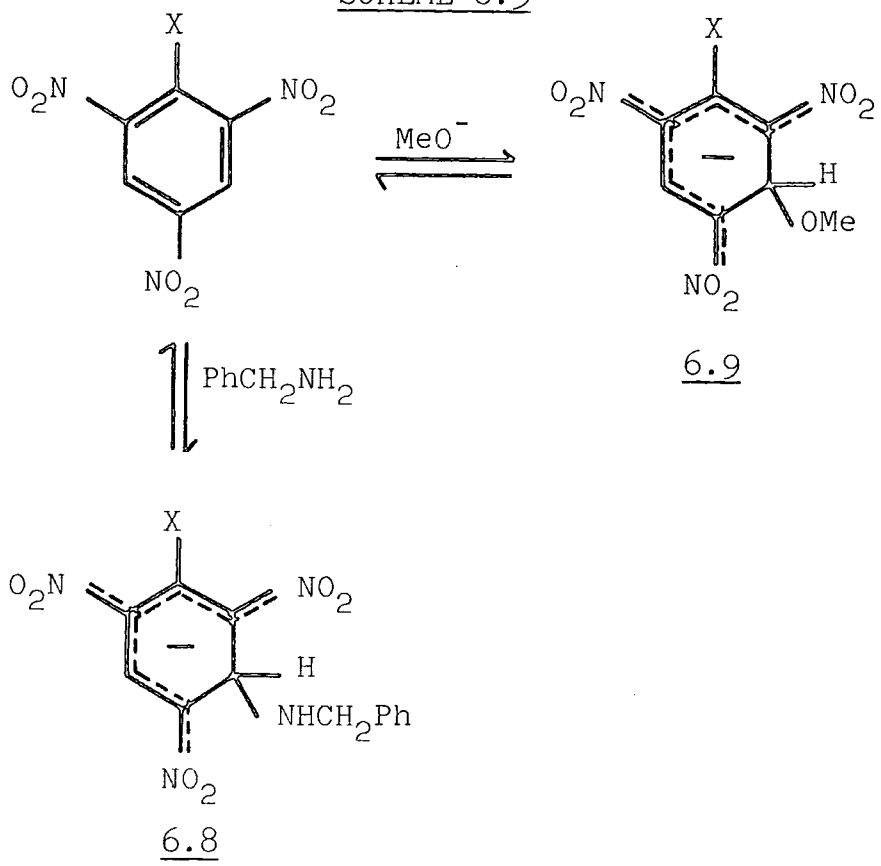

6.9

6.8

ments at 60 MHz (not shown) and at 90 MHz (Table 6.8). Thus, these splittings are due to spin-coupling with the amino-proton in the adduct, 6.8. This has previously been observed[134] in the trinitrobenzene-aniline σ-complex, and suggests that exchange of the amino-proton in 6.8 is slow, perhaps because of hydrogen-bonding to the adjacent nitro-group (6.10).

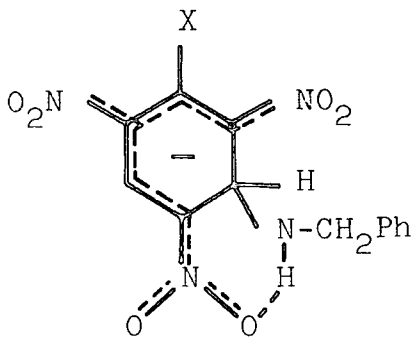

6.10

(b) Picramide

Chemical shift data are listed in Table 6.9. The spectra provide clear evidence for the formation of an adduct by amine addition at C-3, both in the presence and in the absence of sodium methoxide. When both bases are present, formation of the amine adduct, 6.8, is favoured over that of the methoxide adduct, 6.9. With only methoxide present, there is no evidence of amino-proton abstraction: C-3 adduct formation is the only interaction observed. In this case, there is no evidence for spin-coupling of the benzylamine amino-proton with the adjacent ring or methylene protons.

(c) N-Methylpicramide

Chemical shift data are listed in Table 6.10. The position in the absence of sodium methoxide is not very clear,

TABLE 6.9

Chemical shift data for the reaction of picramide with benzylamine and sodium methoxide in 80% d_6-DMSO-methanol. 0.2 M substrate; measured at 90 MHz.

[S]:[MeO$^-$]:[am]	δ(substrate)				δ(amine)				
	(a)	(b)	(c)	(d)	(e)	(f)	(g)	(h)	(i)
1:0:1	8.67	-	-	-	-	7.29	-	3.72	-
1:0:2	-	5.58	-	-	-	7.30	-	3.72	-
1:0:5	8.52	5.80	-	-	3.95	7.30	-	3.77	-
1:1:0	-	-	8.62(d)	6.18(d)	4.66(b)	-	-	-	-
1:1:1	8.50(b)	5.67(b)	-	-	4.40(b)	7.30	7.17	-	-
1:1:2	8.49	5.71	-	-	4.17(b)	7.27	7.14	3.72	3.38
1:1:5	8.51	5.71	-	-	-	7.28	7.19	3.72	-

TABLE 6.9 (contd.)

a. Resonance of ring-proton H_a (sp^2C) in the amine adduct, 6.8.

b. Resonance of ring-proton H_b (sp^3C) in the amine adduct, 6.8.

c. Resonance of ring-proton H_a (sp^2C) in the methoxide adduct, 6.9.

d. Resonance of ring-proton H_b (sp^3C) in the methoxide adduct, 6.9.

e. "Exchangeable" H: amino-protons of substrate and amine, and hydroxylic proton of methanol (broad signal).

f. Resonance of the Ph group in the free amine.

g. Resonance of the Ph group in the bound amine in 6.8.

h. Resonance of the $-CH_2-$ group in the free amine.

i. Resonance of the $-CH_2-$ group in the bound amine in 6.8.

TABLE 6.10

Chemical shift data for the reaction of N-methylpicramide with (i) benzylamine, (ii) N-deuterated benzylamine, and sodium methoxide in 80% d_6-DMSO-methanol. 0.2 M substrate; measured at 90 MHz.

	[S]:[MeO^-]:[am]	δ(substrate)							δ(amine)			
		(a)	(b)	(c)	(d)	(e)	(f)	(g)	(h)	(i)	(j)	(k)
(i)	1:0:1	8.70(b)	-	-	-	2.83	-	5.45	7.32	-	3.81	-
	1:0:2	8.53	-	-	-	2.84	-	4.95	7.30	-	3.78	-
	1:0:5	-	-	-	-	2.84	-	-	7.25	-	3.76	-
	1:1:0	-	-	-	8.18(d), 8.57(d)	-	2.81	4.12	-	-	-	-
	1:1:1	8.37	5.71	-	-	2.90	-	4.14	7.28	7.20	3.70	3.57(d)
	1:1:2	8.40	5.69(d)	6.16	8.49	2.90	-	4.21	7.28	7.22	3.72	3.59(d)
	1:1:5	8.41	5.73	-	-	2.90	-	-	7.32	7.24	3.74	3.61(d)
(ii)	1:1:0	-	-	6.14	8.17, 8.57	2.97	2.80	4.14	-	-	-	-
	1:1:0.5	8.41	5.70	6.14	8.18, 8.54	2.93	2.84	4.13	7.30	7.22	3.87	3.52
	1:1:1	8.41	5.72	6.14	8.18, 8.51	2.92	2.80	4.14	7.29	7.21	3.70	3.56
	1:1:5	8.41	5.71	6.15	8.51	2.87	-	-	7.28	7.21	3.70	3.58

TABLE 6.10 (contd.)

a. Resonance of ring-proton H_a (sp^2C) in the amine adduct, 6.8.

b. Resonance of ring-proton H_b (sp^3C) in the amine adduct, 6.8.

c. Resonance of ring-proton H_b (sp^3C) in the methoxide adduct, 6.9.

d. Ring-proton resonances in the conjugate base, 6.1.

e. Resonance of the N-alkyl group in the C-3 adduct, 6.8 or 6.9.

f. Resonance of the N-alkyl group in the conjugate base, 6.1.

g. "Exchangeable" H: amino-protons of the substrate and amine, and hydroxylic proton of methanol.

h. Resonance of the Ph group in the free amine.

i. Resonance of the Ph group in the bound amine in 6.8.

j. Resonance of the $-CH_2-$ group in the free amine.

k. Resonance of the $-CH_2-$ group in the bound amine in 6.8.

as the spectra were broad and rather weak. However, it is not unreasonable to assume that the amine forms the C-3 adduct, as with the other substrates. When methoxide is present alone, it produces both the conjugate base, 6.1, and the C-3 adduct, 6.9. When both methoxide ion and benzylamine are present, both adducts and the conjugate base are formed (Scheme 6.4).

The signals observed for the proton at the point of addition and the methylene group in the amine adduct, 6.8, are doublets. That this is due to spin-coupling with the amino-proton of the benzylamine is shown by the fact that the corresponding signals are singlets when deuterated amine is used.

(d) N-tert-Butylpicramide

Chemical shift data are shown in Table 6.11. In the absence of methoxide ion, benzylamine forms the C-3 adduct: only one of the ring-protons could be seen, the resonance of that at the site of addition being submerged under the broad amino-proton signal. Methoxide ion causes both amino-proton abstraction and addition at C-3. When both nucleophiles are present, all three species (two C-3 adducts and the conjugate base of the substrate) are formed. As the benzylamine concentration is raised, the conjugate base becomes undetectable, and the amount of methoxide adduct is reduced in favour of the amine adduct. However, even with a five-fold excess of amine, the methoxide adduct is still detectable. The ring-proton at the position of addition in the amine adduct gives rise to a doublet, presumably due to spin-coupling with the adjacent amino-proton. A signal at δ 11.0 is attributed to the amino-proton of the tert-butylamine

SCHEME 6.4

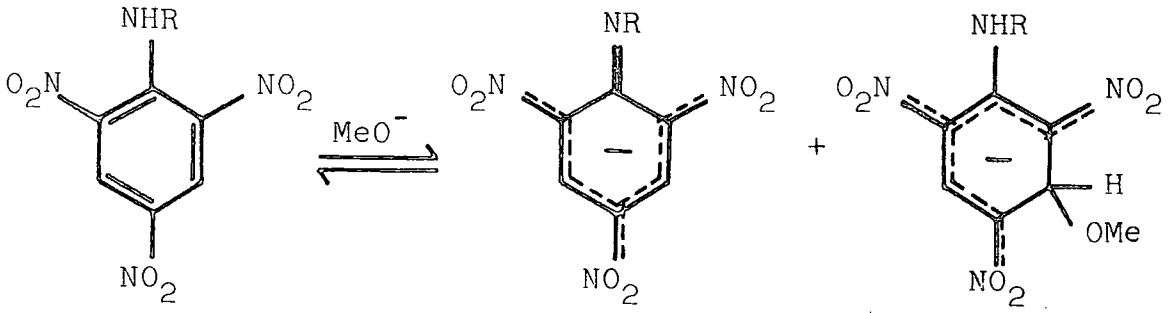

6.1 6.9

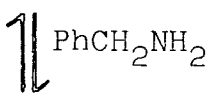

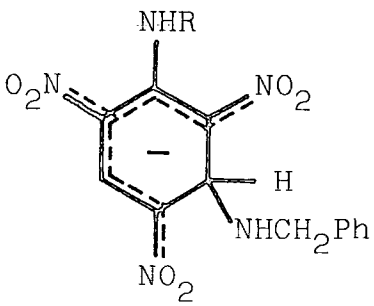

6.8

TABLE 6.11

Chemical shift data for the reaction of N-tert-butylpicramide with benzylamine and sodium methoxide in 85% d_6-DMSO-methanol. 0.15 M substrate; measured at 90 MHz.

[S]:[MeO$^-$]:[am]	δ (substrate)									δ (amine)			
	(a)	(b)	(c)	(d)	(e)	(f)	(g)	(h)	(i)	(j)	(k)	(l)	(m)
1:0:1	8.45	-	-	-	-	1.23	-	6.25	-	7.28	-	3.76	3.98
1:0:2	8.46	-	-	-	-	1.21	-	5.20	-	7.28	-	3.74	3.97
1:0:5	8.35	-	-	-	-	1.17	-	5.68	-	7.28	-	3.72	-
1:1:0	-	-	8.46	-	8.20	1.34	1.13	4.10	-	-	-	-	-
1:1:1	8.34	5.76(d)	8.44	6.19	8.17	1.42	1.14	4.13	10.99	7.31	7.26	3.72	3.61
1:1:2	8.35	5.77(d)	8.46	6.21	-	1.43	-	4.16	10.99	7.29	7.23	3.70	3.62
1:1:5	8.40	5.79(d)	8.49	6.22	-	1.44	-	4.25	11.02	7.30	7.24	3.72	3.65

TABLE 6.11 (contd.)

a. Resonance of ring-proton H_a (sp^2C) in the amine adduct, 6.8.

b. Resonance of ring-proton H_b (sp^3C) in the amine adduct, 6.8.

c. Resonance of ring-proton H_a (sp^2C) in the methoxide adduct, 6.9.

d. Resonance of ring-proton H_b (sp^3C) in the methoxide adduct, 6.9.

e. Ring proton resonance in the conjugate base, 6.1.

f. Resonance of the N-alkyl group in the C-3 adduct, 6.8 or 6.9.

g. Resonance of the N-alkyl group in the conjugate base, 6.1.

h. "Exchangeable" H: amino-protons of the substrate and amine, and hydroxylic proton of methanol.

i. Resonance of (substrate) amino-proton in the C-3 adduct, hydrogen-bonded to the ortho nitro-group.

j. Resonance of the Ph group in the free amine.

k. Resonance of the Ph group in the bound amine in 6.8.

l. Resonance of the $-CH_2-$ group in the free amine.

m. Resonance of the $-CH_2-$ group in the bound amine in 6.8.

group in the C-3 adduct. This is probably hydrogen-bonded to the adjacent ortho nitro-group, and so will not undergo rapid exchange with other acidic protons in the system.

(e) N,N-Dimethylpicramide

Chemical shift data are listed in Table 6.12. The spectra in the absence of methoxide ion are broad, but suggest that benzylamine forms an adduct at C-3. When both benzylamine and methoxide ion are present, both of the C-3 adducts, 6.8 and 6.9, are formed. There is some evidence of spin-coupling between the amino-proton of the benzylamine and the ring-proton at C-3, the site of addition. A signal which moves to higher field as the amine concentration is increased, in the absence of methoxide ion, is attributed to the amino-protons of the benzylamine. The upfield shift is due to the decreasing proportion of amine present in the protonated form (equilibrium 6.7).

(f) Comparison of results

Chemical shift data for the various species are listed in Table 6.13. The results are in accord with Scheme 6.4 (above), the relative amounts of each species depending upon the system considered. When only benzylamine is used, the spectra are broad. The addition of sodium methoxide sharpens the spectra, but causes complications by producing the conjugate base of the substrate, 6.1, where this is possible, and the methoxide adduct at C-3. In each system used, benzylamine forms the adduct at C-3, i.e. at an unsubstituted ring position. Spin-coupling of the amino-proton of the benzylamine with the ring-proton at the site of addition, and with the methylene protons of the benzylamine, is observed. Similar coupling

TABLE 6.12

Chemical shift data for the reaction of N,N-dimethylpicramide with benzylamine and sodium methoxide in 80% d_6-DMSO-methanol. 0.3 M substrate; measured at 90 MHz.

[S]:[MeO^-]:[am]	δ(substrate)				δ (amine)					
	(a)	(b)	(c)	(d)	(e)	(f)	(g)	(h)	(i)	(j)
1:0:1	8.67(b)	-	-	-	2.86	7.32	-	3.80	-	4.95
1:0:3	-	-	-	-	2.82	7.32	-	3.78	-	4.36
1:0:7	8.68	5.93	-	-	2.81	7.31	-	3.76	-	3.46
1:1:0	-	-	-	6.05(d)	2.83	-	-	-	-	-
1:1:1	8.43	5.74(d)	8.51	6.18	2.78,2.84	7.28	7.22	3.67	3.61	-
1:1:3	8.44	5.81	-	-	2.80	7.30	-	3.70	-	-
1:1:7	8.50	5.86	8.57	6.25(d)	2.79,2.88	7.30	7.25	3.73	-	-

TABLE 6.12 (contd.)

a. Resonance of ring-proton H_a (sp^2C) in the amine adduct, 6.8.

b. Resonance of ring-proton H_b (sp^3C) in the amine adduct, 6.8.

c. Resonance of ring-proton H_a (sp^2C) in the methoxide adduct, 6.9.

d. Resonance of ring-proton H_b (sp^3C) in the methoxide adduct, 6.9.

e. Resonance of the N-alkyl group in the C-3 adduct, 6.8 or 6.9.

f. Resonance of the Ph group in the free amine.

g. Resonance of the Ph group in the bound amine in 6.8.

h. Resonance of the $-CH_2-$ group in the free amine.

i. Resonance of the $-CH_2-$ group in the bound amine in 6.8.

j. Resonance of the amino-proton in the free amine.

TABLE 6.13

Chemical shifts of the benzylamide adducts, 6.8.

X	ring-protons		N-alkyl	benzylamide	
	H_a	H_b [a]		Ph	$-CH_2-$ [b]
H	8.37	5.73	-	7.17	3.50
NH_2	8.50	5.71	-	7.15	3.38
NHMe	8.41	5.71	2.90	7.21	3.55
NH^tBu	8.35	5.77	1.43	7.24	3.63
NMe_2	8.44	5.74	2.80	7.22	3.61

a. Signals are doublets, J = 5Hz.

b. Signals are doublets, J = 7Hz.

has been observed[134] in the trinitrobenzene-anilide adduct. It suggests that exchange of the amino-proton in the adduct, 6.8, is slow. This may be due to hydrogen-bonding with an adjacent nitro-group (6.10, above).

CHAPTER SEVEN

THE INTERACTION OF 1,3,5-TRINITROBENZENE WITH SOME PRIMARY AND SECONDARY ALIPHATIC AMINES IN DIMETHYLSULPHOXIDE

INTRODUCTION

Kinetic studies of the reactions of activated aromatic substrates with aliphatic amines have provided some of the most important evidence in support of the intermediate complex mechanism of nucleophilic aromatic substitution[3,13,137]. The reactions are often subject to base catalysis (especially when the substrate contains a poor leaving group[7]), which occurs in the second stage of the reaction shown in Scheme 7.1[13,144].

The base-catalysed step, $k_3[B]$, may involve rate-limiting proton-transfer from the zwitterion, 7.1; a rapid equilibrium between 7.1 and the deprotonated adduct, followed by rate-determining, general acid catalysed removal of the leaving group (the specific base - general acid, SB-GA, mechanism); or concerted expulsion of H and the leaving group[13]. Rate-limiting proton-transfer is generally believed to hold in protic solvents, and the SB-GA mechanism in aprotic solvents[52]. The uncatalysed step, k_2, probably involves intramolecular proton transfer from the amino-nitrogen atom to the leaving group, via a hydrogen-bond which may or may not involve a solvent molecule[13].

The work reported in this chapter is a study of the reactions of trinitrobenzene with aliphatic amines in DMSO. The formation of σ-adducts in such reactions is well established[133,138].

The probable mechanism is shown in Scheme 7.2. Results obtained in 10% dioxan-water[139] were interpreted on the assumption that proton transfer between 7.2 and 7.3 is fast compared with the formation of 7.2. Further results in 10%

SCHEME 7.1

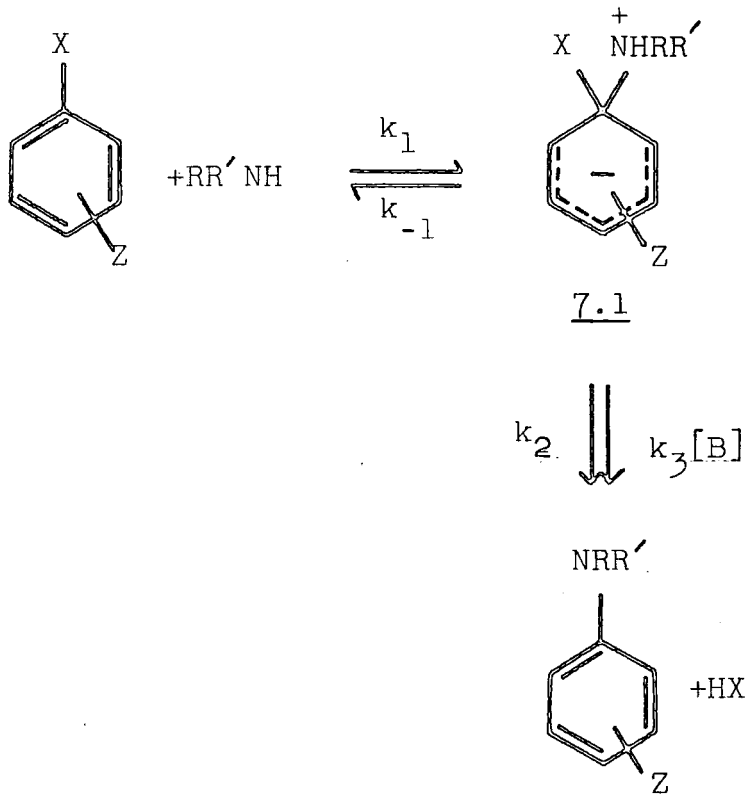

SCHEME 7.2

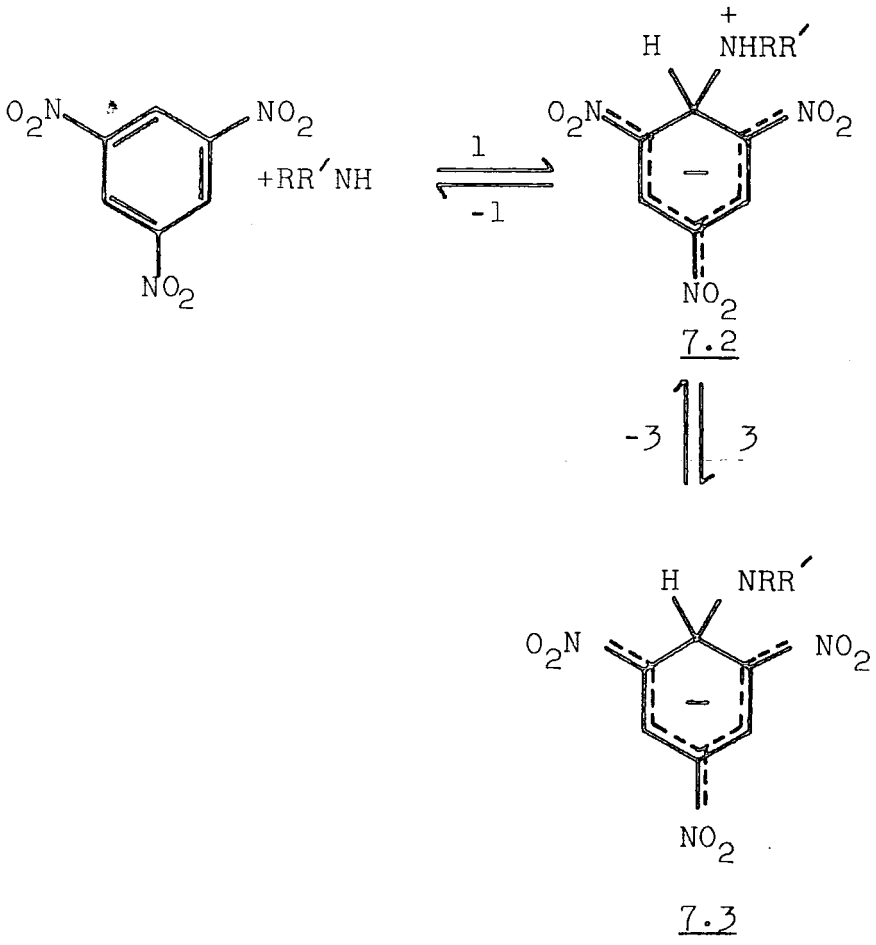

dioxan-water and in 30% DMSO-water[140], however, have shown that proton-transfer may be rate-limiting. Rate-limiting proton-transfer has also been demonstrated in spiro-complex formation[141,142,143], and in the formation of the trinitrobenzene-aniline σ-complex in DMSO, in the presence of Dabco (1,4-diazabicyclo- 2,2,2 -octane).[98]

The results in this chapter show that proton-transfer is kinetically significant in DMSO, and allow a comparison to be made of the effects of the solvents (dioxan-water, DMSO-water, DMSO) on the reaction. The results obtained for the bulky secondary amines, diethylamine and di-isopropylamine, indicate that there are significant steric effects on proton-transfer in DMSO.

EXPERIMENTAL

The reaction between 1,3,5-trinitrobenzene and a variety of primary and secondary aliphatic amines in DMSO was studied by stopped-flow spectrophotometry. Spectra of relatively stable species were obtained using the Unicam SP8000 spectrophotometer, and some equilibrium OD measurements were made on the SP500 instrument. Reaction rates and equilibria were measured in the presence and absence of salt (tetraethylammonium perchlorate or chloride) and Dabco. The reverse rate was studied by forming the complex, and then monitoring its decomposition in the presence of the appropriate amine perchlorate or hydrochloride.

The results are interpreted in terms of Scheme 7.2 (above).

Step 1 involves direct attack by a molecule of amine on trinitrobenzene. Step 3, proton removal from 7.2, can be effected by the amine, A, an added base, B (such as Dabco), or the solvent, S. Correspondingly, the species which may protonate 7.3 in the reverse step, -3, are the protonated amine, AH^+, the protonated base, BH^+, or the protonated solvent, SH^+.

$$V_3 = (k_A[A] + k_B[B] + k_S)\,[7.2] \qquad (7.1)$$

$$V_{-3} = (k_{AH^+}[AH^+] + k_{BH^+}[BH^+] + k_{SH^+}[SH^+])\,[7.3] \qquad (7.2)$$

Assuming that there is no appreciable build-up in concentration of 7.2, i.e. treating 7.2 as a steady-state intermediate,

$$\frac{d[7.3]}{dt} = \frac{k_1[TNB][A]V_3}{(k_{-1}[7.2]+V_3)} - \frac{V_{-3}k_{-1}[7.2]}{(k_{-1}[7.2]+V_3)} \qquad (7.3)$$

$$= \frac{k_1[TNB][A](k_A[A] + k_B[B] + k_S)}{(k_{-1} + k_A[A] + k_B[B] + k_S)}$$

$$- \frac{k_{-1}(k_{AH^+}[AH^+]+k_{BH^+}[BH^+]+k_{SH^+}[SH^+])\,[7.3]^2}{(k_{-1}+k_A[A]+k_B[B]+k_S)\,([AH^+]+[BH^+]+[SH^+])} \qquad (7.4)$$

The overall process for complex formation can be written as (7.5), where B may or may not be the amine:

$$TNB + A + B \underset{k_r}{\overset{k_f}{\rightleftharpoons}} \underline{7.3} + BH^+ \qquad (7.5)$$

All experimental measurements were made with A and B in excess over the substrate, giving an experimental rate law of the form

$$V = \frac{d[\underline{7.3}]}{dt} = k^1_f [TNB] - k^2_r [\underline{7.3}]^2 \qquad (7.6)$$

where k^1_f = first-order forward rate constant,

k^2_r = second-order reverse rate constant.

Equation (7.6) can be integrated by standard methods[117], giving (7.7).

$$\ln \left\{ \frac{[TNB]_o [\underline{7.3}]_e + [\underline{7.3}] ([TNB]_o - [\underline{7.3}]_e)}{[TNB]_o ([\underline{7.3}]_e - [\underline{7.3}])} \right\} = \frac{(2[TNB]_o - [\underline{7.3}]_e) k^1_f t}{[\underline{7.3}]_e} \qquad (7.7)$$

where o denotes initial concentration,

e denotes equilibrium concentration.

In most cases, the reaction was > 95% complete, so that $[\underline{7.3}]_e \simeq [TNB]_o$, giving (7.8); i.e. a normal first-order plot was linear.

$$\ln \frac{[\underline{7.3}]_e}{([\underline{7.3}]_e - [\underline{7.3}])} = k^1_f t \qquad (7.8)$$

Comparing equations (7.4) and (7.6), and using equations (7.9) and (7.10) gives equations (7.11) and (7.12).

$$K_{BH^+} = \frac{[B][SH^+]}{[BH^+]} \qquad (7.9)$$

$$K_{AH^+} = \frac{[A][SH^+]}{[AH^+]} \qquad (7.10)$$

$$k^1_f = \frac{k_1[A](k_A[A] + k_B[B] + k_S)}{(k_{-1} + k_A[A] + k_B[B] + k_S)} \quad (7.11)$$

$$k^2_r = \frac{k_{-1}\ (k_{AH}+ K_{BH}+[A] + k_{BH}+K_{AH}+[B] + k_{SH}+K_{AH}+K_{BH}+\ )}{(k_{-1} + k_A[A] +k_B[B] + k_S)(K_{BH}+[A] +K_{AH}+[B] +K_{AH}+K_{BH}+)} \quad (7.12)$$

When the forward reaction is measured with the amine as the only base present, (7.11) gives (7.13), which can be written as (7.14).

$$k^1_f = \frac{k_1[A](k_A[A] + k_S)}{(k_{-1} + k_A[A] + k_S)} \quad (7.13)$$

$$k^2_f = \frac{k^1_f}{[A]} = \frac{k_1(k_A[A] + k_S)}{(k_{-1} + k_A[A] + k_S)} \quad (7.14)$$

At sufficiently low amine concentration, $k_{-1} + k_S > k_A[A]$, giving (7.15).

$$k^2_f = \frac{k_1\ (k_A[A] + k_S)}{(k_{-1} + k_S)} \quad (7.15)$$

In this case, a plot of k^2_f *versus* the amine concentration has an intercept $k_1k_S/(k_{-1} + k_S) \simeq K_1k_S$, assuming that $k_{-1} > k_S$. If k_S is negligible compared with $k_A[A]$, then (7.14) becomes (7.16), which, when inverted, gives (7.17).

$$k^2_f = \frac{k_1k_A[A]}{(k_{-1} + k_A\ [A])} \quad (7.16)$$

$$\frac{1}{k^2_f} = \frac{k_{-1}}{k_1k_A[A]} + \frac{1}{k_1} \quad (7.17)$$

If a base, B, is added such that it is in excess over the amine, A, then, assuming that B is a better catalyst of the reaction than A, i.e. that $k_B[B] >> k_A[A]$, equation (7.11) becomes (7.18) which, on inversion, gives (7.19).

$$k^2_f = \frac{k_1 k_B[B]}{(k_{-1} + k_B[B])} \tag{7.18}$$

$$\frac{1}{k^2_f} = \frac{k_{-1}}{k_1 k_B [B]} + \frac{1}{k_1} \tag{7.19}$$

Alternatively, when $k_B[B] + k_A[A] + k_S >> k_{-1}$, the observed rate reaches a limit, giving $k^2_f = k_1$.

The fading reaction was measured under 'buffered' conditions with A and the protonated base in excess over the substrate. Thus, the reaction (7.5) is first-order in both the forward and reverse directions. Standard methods[117] show that the approach to equilibrium is first-order, with an observed rate constant given by (7.20).

$$k^1_{obs} = k^1_f + k^1_r \tag{7.20}$$

From equation (7.4),

$$\frac{-d[\underline{7.3}]}{dt} = -k^1_f[TNB] + k^1_r [\underline{7.3}] \tag{7.21}$$

When the amine is the only base present, from equation (7.3),

$$\frac{-d[\underline{7.3}]}{dt} = \frac{-k_1 [TNB][A](k_A[A] + k_S)}{(k_{-1} + k_A[A] + k_S)} + \frac{k_{-1}\,(k_{AH^+}[AH^+] + k_{SH^+}[SH^+])[\underline{7.3}]}{(k_{-1} + k_A[A] + k_S)} \tag{7.22}$$

Hence,

$$k^1_{obs} = \frac{k_1\,[A](k_A[A] + k_S) + k_{-1}(k_{AH^+}[AH^+] + k_{SH^+}[SH^+])}{(k_{-1} + k_A[A] + k_S)} \tag{7.23}$$

The first term in equation (7.23) can be compared with the rate of the colour-forming reaction. Thus, (7.23) can be written as (7.24), or, assuming the solvent contribution to be negligible, (7.25).

$$k^{1}_{obs} = k^{1}_{f} + \frac{k_{-1}(k_{AH^+}[AH^+] + k_{SH^+}[SH^+])}{(k_{-1} + k_A[A] + k_S)} \quad (7.24)$$

$$= k^{1}_{f} + \frac{k_{-1}k_{AH^+}[AH^+]}{(k_{-1} + k_A[A])} \quad (7.25)$$

Rearranging equation (7.25) gives (7.26), which, on inversion, gives (7.27).

$$\frac{(k^{1}_{obs} - k^{1}_{f})}{[AH^+]} = \frac{k_{-1}\ k_{AH^+}}{(k_{-1} + k_A[A])} \quad (7.26)$$

$$\frac{[AH^+]}{(k^{1}_{obs} - k^{1}_{f})} = \frac{k_A[A]}{k_{-1}\ k_{AH^+}} + \frac{1}{k_{AH^+}} \quad (7.27)$$

The overall equilibrium constant for complex formation, K_{eq}, is given by equation (7.28).

$$K_{eq} = \frac{[\underline{7.3}][AH^+]}{[TNB][A]^2} \quad (7.28)$$

At equilibrium, $V_f = V_r$, i.e.

$$k_1k_A[TNB][A]^2 = k_{-1}k_{AH^+}[\underline{7.3}][AH^+] \quad (7.29)$$

Thus,

$$K_{eq} = \frac{k_1k_A}{k_{-1}k_{AH^+}} = \frac{K_1K_a}{K_{AH^+}} \quad (7.30)$$

where K_a = acid dissociation constant of 7.2,

for the reaction 7.2 $\rightleftharpoons$ 7.3 + H^+,

K_{AH^+} = acid dissociation constant of the protonated amine, $AH^+ \rightleftharpoons A + H^+$.

RESULTS AND DISCUSSION

1. Primary Amines

(a) Isopropylamine

Addition of isopropylamine to trinitrobenzene in DMSO produces a deep red species with λ_{max} 450, 528 nm. Rate and equilibrium measurements were made at 450 nm.

Rate constants for the forward reaction in the absence of added salts are given in Table 7.1. A plot of k^2_f vs [A] is curved with an intercept $K_1k_S < 1000$ l mol^{-1}s^{-1}. An inversion plot according to equation (7.17) gives values of $k_1 = 7.94 \times 10^3$ l mol^{-1}s^{-1}, and $k_A/k_{-1} = 402$ l mol^{-1} ($K_1k_A = 3.2 \times 10^6$ l^2 mol^{-2}s^{-1}). The measured OD values show that virtually complete conversion to the complex is achieved over the amine concentration range used.

Rate constants for the forward reaction with $\mu = 0.1$ M (using tetraethylammonium perchlorate) are in Table 7.2. An inversion plot (equation 7.17) gives $k_1 = 7.14 \times 10^3$ l mol^{-1}s^{-1}, and $k_A/k_{-1} = 400$ l mol^{-1} ($K_1k_A = 2.9 \times 10^6$ l^2 mol^{-2}s^{-1}), showing that there is a negligible salt effect. Again, virtually complete conversion to complex is achieved over the range of amine concentrations used.

Rate constants for the reaction catalysed by Dabco are given in Table 7.3. A plot of k^2_f vs [B] reaches a limit at $k_1 = 9.3 \times 10^3$ l mol^{-1}s^{-1}. An inversion plot (equation 7.19) gives values of $k_1 = 9.4 \times 10^3$ l mol^{-1}s^{-1}, and $k_B/k_{-1} = 85$ l mol^{-1}. Thus, $k_A/k_B \approx 5$, i.e. the amine is approximately five times as effective a catalyst as is Dabco.

The reverse reaction was studied using isopropylammonium perchlorate. The results are shown in Table 7.4.

TABLE 7.1

Rate constants for the reaction of trinitrobenzene with isopropylamine in DMSO at 25°C.

[A] M	OD[a]	k^1_f s^{-1}	$10^{-3}k^2_f$ $l\ mol^{-1}s^{-1}$	$10^4/k^2_f$ $s\ mol\ l^{-1}$
0.001	0.023	2.29	2.29	4.37
0.0015	0.024	4.41	2.94	3.40
0.002	0.024	8.07	4.04	2.48
0.003	0.025	12.8	4.27	2.34
0.004	0.025	21.2	5.30	1.89
0.006	0.025	35.0	5.83	1.71
0.008	0.025	49.9	6.24	1.60
0.010	0.025	62.3	6.23	1.61

a. Measured by stopped-flow spectrophotometry at 450 nm, after completion of the colour-forming process. 5×10^{-6} M substrate in a 2 mm cell.

TABLE 7.2

Rate constants for the reaction of trinitrobenzene with isopropylamine in DMSO at 25°C, μ = 0.1 M (Et_4NClO_4).

[A]	OD[a]	k^1_f	$10^{-3}k^2_f$	$10^4/k^2_f$
M		s^{-1}	l $mol^{-1}s^{-1}$	s mol l^{-1}
0.001	0.019	1.99	1.99	5.03
0.0015	0.021	4.48	2.99	3.33
0.002	0.023	6.33	3.17	3.16
0.003	0.024	12.1	4.03	2.48
0.004	0.024	18.9	4.73	2.12
0.006	0.024	29.2	4.87	2.05
0.008	0.024	43.3	5.41	1.85
0.010	0.024	58.7	5.87	1.70

a. Measured by stopped-flow at 450 nm, after completion of the colour-forming process. 5×10^{-6} M substrate in a 2 mm cell.

TABLE 7.3

Rate constants for the reaction between trinitrobenzene and isopropylamine in DMSO at 25°C, in the presence of Dabco.

$[B]^a$	k^1_f	$10^{-3}k^2_f$	$10^{-4}/k^2_f$
M	s^{-1}	$l\ mol^{-1}s^{-1}$	$s\ mol\ l^{-1}$
0	6.01	3.01	3.33
0.05	15.5	7.75	1.29
0.1	16.6	8.30	1.20
0.2	18.5	9.25	1.08
0.3	18.5	9.25	1.08
0.4	18.3	9.15	1.09
0.5	18.5	9.25	1.08

a. 2×10^{-3} M amine throughout.

TABLE 7.4

Rate and equilibrium constants for the fading reaction between the trinitrobenzene-isopropylamine complex and isopropylammonium perchlorate in DMSO at 25°C, μ = 0.1 M (Et_4NClO_4), 10^{-3} M amine.

$[AH^+]$	$OD_e^{a,b}$	$OD_\infty^{a,c}$	K_{eq}^{d}	k_{obs}^{1}	k_r^{1} e
M			1 mol^{-1}	s^{-1}	s^{-1}
5×10^{-4}	0.022	0.005	147	6.73	4.7
1×10^{-3}	0.024	0.004	199	11.5	9.5
2×10^{-3}	0.023	0.003	299	20.9	18.9
3×10^{-3}	0.023	0.002	283	32.8	30.8
4×10^{-3}	0.023	0.002	377	43.5	41.5
5×10^{-3}	0.023	0.001	230	53.2	51.2

a. Measured by stopped-flow at 450 nm. 5×10^{-6} M substrate in a 2 mm cell.

b. OD of the complex before starting the fading process.

c. OD after completion of the fading reaction.

d. Calculated using equation (7.28); the mean value is $K_{eq} = 250 \pm 80$ 1 mol^{-1}.

e. $k^1_r = k^1_{obs} - k^1_f$, where $k^1_f = 2.0$ s^{-1} (see Table 7.2).

A plot of k^1r vs $[AH^+]$ gives $k_{-1}k_{AH^+}/(k_{-1} + k_A[A]) = 1.02 \times 10^4$ l $mol^{-1}s^{-1}$. Using $k_A/k_{-1} = 400$ l mol^{-1} (above) allows the calculation of $k_{AH^+} = 1.43 \times 10^4$ l $mol^{-1}s^{-1}$. Substituting the values of k_1, k_A/k_{-1} and k_{AH^+} obtained here into equation (7.30) gives $K_{eq} = 200$ l mol^{-1}, compared with a value of $K_{eq} = 250$ l mol^{-1} obtained from OD measurements (Table 7.4).

(b) n-Butylamine

Measurement of the visible spectrum produced by the addition of n-butylamine to trinitrobenzene in DMSO shows that a species with λ_{max} 450, 534 nm is formed. Rate and equilibrium measurements were made at 450 nm.

Rate constants for the forward reaction in the absence of added salt are given in Table 7.5. As can be seen from the OD measurements, complete conversion to complex is achieved above 5×10^{-4} M amine. Accordingly, rate constants for the three amine concentrations below this were calculated using equation (7.7), the remainder being obtained from first-order plots.

A plot of k^2_f vs $[A]$ is curved, with an intercept $K_1k_s < 1000$ l $mol^{-1}s^{-1}$. A reciprocal plot according to equation (7.17) gives values of $k_1 = 5.6 \times 10^4$ l $mol^{-1}s^{-1}$, and $k_A/k_{-1} = 890$ l mol^{-1}, and hence $K_1k_A = 5.0 \times 10^7$ l^2 $mol^{-2}s^{-1}$.

Because of the very low amine concentrations used, the OD values are held to be unreliable. An estimate of the overall equilibrium constant was obtained using the 'half-conversion' method, in which equation (7.28) becomes

$$K_{eq} = \frac{[7.3]}{[A]^2} = \frac{[TNB]_s}{2[A]^2} \qquad (7.31)$$

where $[TNB]_s$ = stoichiometric concentration of trinitrobenzene
$= 5 \times 10^{-6}$ M.

TABLE 7.5

Rate constants for the reaction between trinitrobenzene and n-butylamine in DMSO at 25°C.

[A]	OD[a]	k^1_f	$10^{-4}k^2_f$	$10^4/k^2_f$
M		s^{-1}	l $mol^{-1}s^{-1}$	s mol l^{-1}
1×10^{-4}	0.013	0.48	0.48	2.08
2×10^{-4}	0.018	1.73	0.87	1.16
3×10^{-4}	0.019	3.30	1.10	0.91
5×10^{-4}	0.021	9.38	1.88	0.53
7×10^{-4}	0.021	15.2	2.17	0.46
1×10^{-3}	0.024	25.4	2.54	0.39
2×10^{-3}	0.022	65.4	3.27	0.31
3×10^{-3}	0.021	121	4.03	0.25
4×10^{-3}	0.023	165	4.13	0.24
5×10^{-3}	0.022	177	3.54	0.28
6×10^{-3}	0.024	253	4.22	0.24
7×10^{-3}	0.023	280	4.00	0.25
1×10^{-2}	0.023	307	3.07	0.33

a. Measured by stopped-flow spectrophotometry at 450 nm after completion of the colour-forming process. 5×10^{-6} M substrate in a 2 mm cell.

A plot of OD vs [A] (not shown) indicates that half-conversion occurs at 5×10^{-5} M amine, leading to a value of $K_{eq} = 10^3$ l mol^{-1}.

Rate constants for the forward reaction in the presence of added Dabco are given in Table 7.6. An inversion plot according to equation (7.19) gives values of $k_1 = 4.5 \times 10^4$ l $mol^{-1}s^{-1}$ and $k_B/k_{-1} = 440$ l mol^{-1}. The former is in good agreement with the value obtained in the absence of added salts (above), while the latter indicates that the amine is more effective than Dabco in removing the amino-proton from 7.2 : $k_A/k_B \approx 2$.

Rate constants for the reverse reaction were obtained at a variety of amine concentrations, using n-butylammonium chloride, and are shown in Table 7.7(i). An inversion plot according to equation (7.27) of the data for 0.002 M salt gives values of $k_{AH^+} = 5.1 \times 10^4$ l $mol^{-1}s^{-1}$, and $k_A/k_{-1} = 730$ l mol^{-1}. The latter is in reasonable agreement with the value obtained from the forward reaction in the absence of added salts (above).

Rate measurements with varying salt concentrations (Table 7.7(ii)) give a value of $k^1_r / AH^+ = 1.8 \times 10^4$ l $mol^{-1}s^{-1}$. Combining this with $k_A/k_{-1} = 730$ l mol^{-1} (above) in equation (7.25) yields a value of $k_{AH^+} = 5.1 \times 10^4$ l $mol^{-1}s^{-1}$, as above. OD measurements in the same series (not shown) give an estimated value of $K_{eq} = 1.1 \times 10^3$ l mol^{-1}.

Combining the values of k_1, k_A/k_{-1}, and k_{AH^+} in equation (7.30) gives a value of $K_{eq} = 970$ l mol^{-1}, in good agreement with those above.

TABLE 7.6

Rate constants for the reaction between trinitrobenzene and n-butylamine in the presence of Dabco, in DMSO at 25°C.

$[B]^a$	k^1_f	$10^{-4}k^2_f$	$10^4/k^2_f$
M	s^{-1}	$l\ mol^{-1}s^{-1}$	$s\ mol\ l^{-1}$
0	7.38	1.48	0.68
0.001	10.2	2.04	0.49
0.005	15.5	3.10	0.32
0.01	18.2	3.64	0.27
0.03	22.0	4.40	0.23
0.05	21.3	4.26	0.23
0.1	22.0	4.40	0.23
0.2	21.1	4.22	0.24
0.3	23.5	4.70	0.21
0.4	26.7	5.34	0.19
0.5	31.3	6.26	0.16

a. 5×10^{-4} M amine throughout.

TABLE 7.7

Rate constants for the fading reaction between the trinitrobenzene-n-butylamine complex and n-butylammonium chloride in DMSO at 25°C.

	[A]	[AH^+]	k^1_{obs}	k^1_r [a]	$10^5[AH^+]/k^1_r$
	M	M	s^{-1}	s^{-1}	s mol l^{-1}
(i)	1×10^{-4}	0.01	308	307	3.3
	5×10^{-4}	0.01	225	215	4.7
	1×10^{-4}	0.002	95.9	95.4	2.1
	2×10^{-4}	0.002	91.8	90	2.2
	4×10^{-4}	0.002	87.2	81	2.5
	5×10^{-4}	0.002	87.5	78	2.6
	6×10^{-4}	0.002	84.2	72	2.8
	5×10^{-4}	0.004	148	139	2.9
	5×10^{-4}	0.006	214	203	3.0
	5×10^{-4}	0.008	228	219	3.7
	5×10^{-4}	0.010	229	220	4.5
(ii)	0.0025	0	85	-	-
	0.0025	0.0025	135	50	5.0
	0.0025	0.0050	169	84	6.0
	0.0025	0.0075	216	131	5.7

a. $k^1_r = k^1_{obs} - k^1_f$, where k^1_f is the measured rate constant for the forward reaction at the appropriate amine concentration (see Table 7.5).

(c) Benzylamine

Addition of benzylamine to a solution of trinitrobenzene in DMSO produces a red species with λ_{max} 450, 534 nm. All kinetic and equilibrium measurements were made at 450 nm.

Rate measurements for the forward reaction in the absence of added salts are shown in Table 7.8. A plot of k^2_f against amine concentration is curved, with a maximum intercept of K_1k_S <1000 l $mol^{-1}s^{-1}$. An inversion plot according to equation (7.17) gives values of k_1 = 9.1 x 10^3 l $mol^{-1}s^{-1}$, and k_A/k_{-1} = 224 l mol^{-1} ($K_1k_A \simeq 2.0 \times 10^6$ l^2 $mol^{-2}s^{-1}$).

The equilibrium OD measurements (Table 7.8) indicate that virtually complete conversion to complex is achieved over the range of amine concentrations studied.

In the presence of 0.1 M Et_4NClO_4 (Table 7.9), the degree of conversion to complex is unchanged, but values of k_1 = 1.1 x 10^4 l $mol^{-1}s^{-1}$, and k_A/k_{-1} = 142 l mol^{-1} (K_1k_A = 1.56 x 10^6 l^2 $mol^{-2}s^{-1}$) are obtained.

Rate measurements in the presence of Dabco are given in Table 7.10. An inversion plot according to equation (7.19) gives values of k_1 = 1.47 x 10^4 l $mol^{-1}s^{-1}$, in reasonable agreement with those obtained above, and k_B/k_{-1} = 61 l mol^{-1}. Thus, $k_A/k_B \simeq 2\text{-}4$, i.e. the amine is more effective than Dabco in catalysing proton abstraction from 7.2.

Adding benzylammonium perchlorate to a solution of the complex allows the reverse process to be observed: results are given in Table 7.11. A plot of k^1_r against the salt concentration gives a value of $k_{-1}k_{AH^+}/(k_{-1} + k_A[A])$ = 1.39 x 10^4 l $mol^{-1}s^{-1}$, leading to k_{AH^+} = 1.6 x 10^4 l $mol^{-1}s^{-1}$. Use of equation (7.30) gives a calculated value of K_{eq} = 98 l mol^{-1},

TABLE 7.8

Rate constants for the reaction between trinitrobenzene and benzylamine in DMSO at 25°C.

[A] / M	OD_e^a	k^1_f / s^{-1}	$10^{-3}k^2_f$ / $l\ mol^{-1}s^{-1}$	$10^4/k^2_f$ / $s\ mol\ l^{-1}$
0.001	0.022	1.68	1.68	5.95
0.002	0.023	5.66	2.83	3.53
0.004	0.023	16.3	4.07	2.45
0.006	0.024	31.6	5.27	1.90
0.008	0.024	49.7	6.21	1.61
0.010	0.025	64.9	6.49	1.54
0.010	0.023	61.7	6.17	1.62

a. Measured by stopped-flow at 450 nm, after completion of the colour-forming process. 5×10^{-6} M substrate in a 2 mm cell.

TABLE 7.9

Rate constants for the reaction between trinitrobenzene and benzylamine in DMSO at 25°C, μ= 0.1 M (Et_4NClO_4).

[A]	OD_e^a	k^1_f	$10^{-3}k^2_f$	$10^4/k^2_f$
M		s^{-1}	l $mol^{-1}s^{-1}$	s mol l^{-1}
0.001	0.022	1.44	1.44	6.94
0.001	0.022	1.38	1.38	7.25
0.002	0.023	4.60	2.30	4.35
0.004	0.025	16.0	4.00	2.50
0.006	0.025	31.6	5.27	1.90
0.008	0.025	49.1	6.14	1.63

a. Measured by stopped-flow at 450 nm, after completion of the colour-forming process. 5×10^{-6} M substrate in a 2 mm cell.

TABLE 7.10

Rate constants for the reaction between trinitrobenzene and benzylamine in the presence of Dabco, in DMSO at 25°C.

$[B]^a$	k^1_f	$10^{-3}k^2_f$	$10^4/k^2_f$
M	s^{-1}	$l\ mol^{-1}s^{-1}$	$s\ mol\ l^{-1}$
0	5.66	2.83	3.53
0.005	9.45	4.73	2.12
0.01	12.1	6.05	1.65
0.02	15.6	7.80	1.28
0.03	19.5	9.75	1.03
0.04	21.4	10.7	0.93
0.05	23.9	12.0	0.84
0.06	23.1	11.6	0.87
0.07	24.5	12.3	0.82
0.08	25.5	12.8	0.79
0.09	26.3	13.4	0.75
0.10	28.5	14.3	0.70
0.15	29.3	14.7	0.68
0.20	30.8	15.4	0.65
0.25	30.6	15.3	0.65

a. 2×10^{-3} M amine throughout.

TABLE 7.11

Rate and equilibrium constants for the fading reaction between the trinitrobenzene-benzylamine complex and benzylammonium perchlorate in DMSO at 25°C, μ = 0.1 M (Et_4NClO_4), 10^{-3} M amine.

$[AH^+]$ M	OD_e[a]	OD_∞[b]	K_{eq}[c] l mol^{-1}	k^1_{obs} s^{-1}	k^1_r[d] s^{-1}
1×10^{-4}	0.022	0.011	99	2.96	1.5
3×10^{-4}	0.023	0.006	105	5.35	3.9
5×10^{-4}	0.021	0.004	117	8.36	6.9
7×10^{-4}	0.024	0.003	100	10.7	9.3
1×10^{-3}	0.021	0.003	-	15.1	13.7
2×10^{-3}	0.022	0.002	-	27.8	26.4
3×10^{-3}	-	-	-	41.2	39.8
4×10^{-3}	0.024	0.001	-	55.9	54.5
5×10^{-3}	-	-	-	72.8	71.4

a. OD of the complex before fading: 5×10^{-6} M substrate in a 2 mm cell.

b. OD after completion of the fading reaction.

c. Calculated using equation (7.28); the mean value is 105 $\pm$ 8 l mol^{-1}.

d. $k^1_r = k^1_{obs} - k^1_f$, where k^1_f = 1.4 s^{-1} (see Table 7.9).

compared with K_{eq} = 105 l mol^{-1} obtained from OD measurements (Table 7.11).

2. Secondary Amines

(a) Piperidine

The complex produced from trinitrobenzene and piperidine has λ_{max} 446, 524 nm. Rate and equilibrium measurements were made at 445 nm.

Equilibrium optical density measurements (Table 7.12) were made on the SP500 spectrophotometer, and used to calculate K_{eq} from equation (7.28). The value of K_{eq} appears to increase with increasing piperidine hydrochloride concentration. Over the range studied, the mean value is $(4.3 \pm 0.9) \times 10^3$ l mol^{-1}.

Rate constants in the absence of added salts are shown in Table 7.13. OD measurements indicate that conversion to complex is virtually complete over the range of amine concentrations used. A plot of k_f^2 against the amine concentration is linear, indicating that k_{-1} is the dominant term in the denominator. Thus, the intercept gives an estimate of $K_1 k_S$ = 100 l $mol^{-1} s^{-1}$, and the slopegives $K_1 k_A$ = 6.0×10^5 l^2 $mol^{-2} s^{-1}$. The absence of curvature allows the estimation of a value of k_A/k_{-1} as follows: at 0.01 M amine (near the top of the concentration range used), a reduction of 10% in the observed rate constant would cause a marked deviation from the straight line plot. Thus,

$$\frac{k_A[A]}{(k_{-1} + k_A[A])} < \frac{1}{10},$$

giving $\frac{k_A[A]}{k_{-1}} < 0.1$

and hence k_A/k_{-1} <10 l mol^{-1}, and $k_1 > 6 \times 10^4$ l $mol^{-1} s^{-1}$.

TABLE 7.12

Equilibrium measurements for the reaction between trinitrobenzene and piperidine in DMSO at 25°C, μ = 0.1 M (Et_4NClO_4) in the presence of piperidine hydrochloride.

[A]	$[AH^+]$	OD_e^a	$10^{-3}K_{eq}^b$
M	M		1 mol^{-1}
0.001	0.01	0.160	3.79
0.002	0.01	0.321	3.12
0.003	0.01	0.427	3.08
0.002	0.02	0.249	3.77
0.003	0.02	0.377	4.13
0.002	0.05	0.168	5.11
0.004	0.05	0.360	5.10
0.004	0.10	0.270	5.43
0.006	0.10	0.363	4.63
0.008	0.10	0.445	5.09

a. OD after completion of the colour-forming process. 2×10^{-5} M substrate in a 1 cm cell.

b. Calculated using equation (7.28); the mean value is $(4.3 \pm 0.9) \times 10^3$ 1 mol^{-1}.

TABLE 7.13

Rate constants for the reaction between trinitrobenzene and piperidine in DMSO at 25°C.

[A] M	OD_e[a]	k^1_f s^{-1}	$10^{-3}k^2_f$ $l\ mol^{-1}s^{-1}$
0.001	0.022	0.52	0.52
0.002	0.023	2.47	1.24
0.002	0.023	2.55	1.28
0.003	0.024	5.51	1.84
0.004	0.024	11.1	2.78
0.005	0.023	16.1	3.22
0.006	0.023	22.1	3.68
0.007	0.024	30.7	4.39
0.008	0.023	38.1	4.76
0.009	0.023	47.8	5.31
0.010	0.023	58.8	5.88
0.011	0.024	72.6	6.60

a. Measured by stopped-flow at 445 nm, after completion of the colour-forming process. 5×10^{-6} M substrate in a 2 mm cell.

Rate constants obtained in the presence of added Dabco are given in Table 7.14. A plot of k^2_f against the concentration of Dabco is a straight line, with slope K_1k_B = 1.2 x 10^5 l^2 $mol^{-2}s^{-1}$ (giving $k_B/k_{-1} < 2$ l mol^{-1}), and intercept $K_1k_S \approx 2x10^3$ l $mol^{-1}s^{-1}$. (k^2_f is independent of the amine concentration, as expected if k_{-1} is the dominant term in the denominator). Comparing the values of K_1k_A and K_1k_B, $k_A/k_B \approx 5$, so piperidine is a better catalyst for proton removal from 7.2 than is Dabco.

The reverse reaction was carried out using piperidine hydrochloride, both with and without control of the ionic strength. The results are shown in Table 7.15. A plot of k^1_r vs $[AH^+]$ for the first set (no Et_4NClO_4) gives $k_{-1}k_{AH^+}/(k_{-1} + k_A[A]) = 170$ l $mol^{-1}s^{-1}$, yielding a calculated value of $k_{AH^+} < 170$ l $mol^{-1}s^{-1}$. When $\mu = 0.1$ M, $k_{-1}k_{AH^+}/(k_{-1} + k_A[A]) = 98$ l $mol^{-1}s^{-1}$, giving $k_{AH^+} < 100$ l $mol^{-1}s^{-1}$ (these must be upper limits, as the estimated value of k_A/k_{-1} used in their calculation is an upper limit).

Substituting values into equation (7.30) gives $K_{eq} \approx 6$ x 10^3 l mol^{-1}, compared with 4.3 x 10^3 l mol^{-1} from OD measurements (Table 7.12).

(b) Diethylamine

Addition of diethylamine to trinitrobenzene in DMSO produces a red species with λ_{max} 448,524 nm. The adduct is fairly stable in the presence of amine alone, but decays to a copper-pink species, λ_{max} 515 nm, in the presence of diethylammonium perchlorate. All rate and equilibrium measurements were made at 445 nm.

Considerable difficulty was experienced in obtaining consistent sets of rate constants. The results appeared to

TABLE 7.14

Rate constants for the reaction between trinitrobenzene and piperidine in the presence of Dabco, in DMSO at 25°C.

	[A]	[B]	k^1_f	$10^{-3}k^2_f$
	M	M	s^{-1}	$l\ mol^{-1}s^{-1}$
(i)	0.001	0	0.52	0.52
	0.001	0.05	7.91	7.91
	0.001	0.1	15.0	15.0
	0.001	0.2	27.9	27.9
	0.001	0.3	38.6	38.6
	0.001	0.4	53.9	53.9
	0.001	0.5	61.2	61.2
(ii)	0.002	0	2.55	1.28
	0.002	0.01	5.52	2.76
	0.002	0.03	10.9	5.45
	0.002	0.05	15.5	7.75
	0.002	0.07	20.2	10.1
	0.002	0.10	29.1	14.6
	0.002	0.15	40.7	20.4
	0.002	0.20	52.8	26.4

TABLE 7.15

Rate constants for the fading reaction between the trinitrobenzene-piperidine complex and piperidine hydrochloride in DMSO at 25°C; (i) no control of μ ; (ii) μ = 0.1 M (Et_4NClO_4). 10^{-3} M amine throughout.

	$[AH^+]$ / M	k^1_{obs} / s^{-1}	k^1_r [a] / s^{-1}
(i)	0.005	2.15	1.63
	0.01	3.19	2.67
	0.02	4.68	4.16
(ii)	0.01	2.27	1.75
	0.02	3.31	2.79
	0.04	5.43	4.91
	0.07	7.72	7.20
	0.10	11.2	10.7

a. $k^1_r = k^1_{obs} - k^1_f$, where $k^1_f = 0.52\ s^{-1}$ (see Table 7.13).

be affected by both the batch in which the amine sample was fractionated, and the 'age' of the sample (the time between fractionating the amine and carrying out the runs). The inconsistency may be due to a decomposition reaction occurring in the amine on standing, which changes its reactivity, or to the presence of very low concentrations of highly reactive impurities.

Rate constants for the colour-forming reaction in the absence of added salts are shown in Table 7.16. Those for less than 4×10^{-3} M amine were calculated from equation (7.7). (The results are split into the sets in which they were obtained). Plots of k^2_f against the amine concentration are linear, but give widely different values for the intercept (K_1k_S) and slope (K_1k_A).

The addition of 0.01 M Et_4NCl or Et_4NClO_4 produces the results shown in Table 7.17(ii) and (iii) respectively (those in (i) were obtained in the absence of added salts, at the same amine concentrations). Plotting k^2_f against amine concentration produces the following results: (i) K_1k_S (intercept) = 0.44 l $mol^{-1}s^{-1}$, K_1k_A (slope) = 230 l^2 $mol^{-2}s^{-1}$; (ii) K_1k_S = 0.44 l $mol^{-1}s^{-1}$, K_1k_A = 150 l^2 $mol^{-2}s^{-1}$; (iii) K_1k_S = 0.24 l $mol^{-1}s^{-1}$, K_1k_A = 230 $l^2mol^{-2}s^{-1}$. The K_1k_S and K_1k_A values are much lower than those obtained previously (Table 7.16): the measured reaction rates are about three orders of magnitude smaller.

That this is a different reaction from that in Table 7.16 is supported by the behaviour of the observed rate constants in Table 7.17. 'Instantaneous' values of k^1_f were calculated at half-minute intervals, using equation (7.7). For each run, the values (not shown) dropped sharply at first,

TABLE 7.16

Rate constants for the reaction of trinitrobenzene with diethylamine in DMSO at 25°C.

	[A]	k^1_f [a]	k^2_f	k_1k_S	K_1k_A
	M	s^{-1}	$l\ mol^{-1}s^{-1}$	$l\ mol^{-1}s^{-1}$	$l^2mol^{-2}s^{-1}$
(i)	0.01	0.95	95	90	2700
	0.03	3.13	104		
	0.05	5.92	118		
	0.07	9.28	133		
	0.10	13.8	138		
(ii)	0.01	2.95	295	285	300
	0.02	5.36	268		
	0.05	14.7	294		
	0.10	31.8	318		
(iii)	0.002	0.18	90	65	19000
	0.004	0.51	128		
	0.006	1.35	225		
	0.008	1.79	224		
	0.010	2.26	226		
(iv)	0.01	2.70	270	305	800
	0.03	10.4	347		
	0.05	17.3	346		
	0.10	38.4	384		
	0.20	77.4	387		

a. Measured by stopped-flow at 445 nm.

TABLE 7.17

Rate constants for the reaction between trinitrobenzene and diethylamine in DMSO at 25°C: (i) no added salt; (ii) 0.01 M Et_4NCl; (iii) 0.01 M Et_4NClO_4.

	[A] / M	$10^3 k^1_f$ [a] / s^{-1}	k^2_f / $l\ mol^{-1} s^{-1}$
(i)	0.001	0.60	0.60
	0.002	1.90	0.95
	0.004	5.50	1.38
(ii)	0.001	0.53	0.53
	0.002	1.50	0.75
	0.004	1.90	0.48
	0.006	8.00	1.33
(iii)	0.001	0.47	0.47
	0.002	1.40	0.70
	0.004	4.80	1.20

a. Measured using the SP500 spectrophotometer, and calculated using equation (7.7).

before levelling out at the values given in the Table. This would be consistent with an initial, fast reaction (measurable by stopped-flow) followed by a slower process (measurable by conventional spectrophotometry).

If the diethylamine contains a highly reactive impurity, then this could be the nucleophile involved in the fast reaction, while the diethylamine itself is responsible for the slower process. The variations in the data for the faster reaction (Table 7.16) with the sample of diethylamine used, indicate that this may be the explanation.

Rate constants obtained with added Dabco are shown in Table 7.18; these relate to the faster of the two processes considered above. As in Table 7.16, the results are split into groups according to the sample of diethylamine used. In each run, OD measurements (not shown) indicate that virtually complete conversion to complex was achieved. Plotting k^2_f against Dabco concentration for sets (i) and (iii) give straight lines, with (i) K_1k_S (intercept) = 56 l $mol^{-1}s^{-1}$, K_1k_B (slope) = 1500 l^2 $mol^{-2}s^{-1}$; (iii) K_1k_S = 270 l $mol^{-1}s^{-1}$, K_1k_B = 1800 l^2 $mol^{-2}s^{-1}$. The values of K_1k_B are in good agreement with each other, and are an order of magnitude larger than the values of K_1k_A determined from Table 7.17, but fall within the range of K_1k_A values obtained from Table 7.16. The values of K_1k_S are in the same range as those from Table 7.16.

A plot of k^2_f versus B for set (ii) produces a curve, so values of K_1k_S and K_1k_B could not be obtained.

Measured rate constants for the fading reaction (using diethylammonium perchlorate) are shown in Table 7.19. Most of these are smaller than the measured values of the rate

TABLE 7.18

Rate constants for the reaction between trinitrobenzene and diethylamine in DMSO at 25°C, in the presence of Dabco.

	[A] / M	[B] / M	k^1_f [a] / s^{-1}	k^2_f / l $mol^{-1}s^{-1}$
(i)	0.01	0.05	1.35	135
	0.01	0.10	2.20	220
	0.01	0.20	4.43	443
	0.02	0.05	2.89	145
	0.02	0.10	3.80	190
	0.02	0.20	7.28	364
	0.05	0.05	6.58	132
	0.05	0.10	9.73	195
	0.05	0.20	14.7	294
(ii)	0.02	0.05	5.55	278
	0.05	0.05	13.7	274
	0.005	0.05	1.69	338
	0.005	0.10	2.15	430
	0.005	0.20	3.85	770
	0.005	0.30	7.01	1420
	0.005	0.40	11.3	2260
	0.005	0.50	15.5	3100
(iii)	0.02	0	5.36	268
	0.02	0.05	7.46	373
	0.02	0.10	8.96	448
	0.02	0.20	12.5	625

a. Measured by stopped-flow at 445 nm.

TABLE 7.19

Rate constants for the fading reaction between the trinitrobenzene-diethylamine complex and diethylammonium perchlorate in DMSO at 25°C.

[A]	$[AH^+]$	$k_{obs}^{1\ a}$
M	M	s^{-1}
0.005	0.01	0.431
0.01	0.01	0.457
0.01	0.02	0.848
0.01	0.02	0.821
0.01	0.03	1.10
0.02	0.04	1.53

a. Measured by stopped-flow at 445 nm.

of complex formation (see Tables 7.16, 7.17(i)). A plot of the observed rate against the salt concentration is linear, of slope $k_{-1}k_{AH^+}/(k_{-1} + k_A[A]) = 36$ l mol^{-1}s^{-1}, and intercept $k^1_f = 0.1$ s^{-1}.

Calculations of the overall equilibrium constant, K_{eq}, from OD measurements (not shown) obtained using the SP500 spectrophotometer, gave values of between 1 and 10 l mol^{-1}, depending upon the conditions used (no salt, added Et_4NCl, Et_4NClO_4, $Et_2NH_2ClO_4$, or Dabco). A conductiometric determination gave a value of $K_{eq} = 22 \pm 2$ l mol^{-1} at 20°C.

(c) Di-isopropylamine

The visible spectrum of the species resulting from the addition of di-isopropylamine to trinitrobenzene in DMSO has λ_{max} 450,520 nm. All rate and equilibrium measurements were made at 450 nm. The range of amine concentrations studied was limited at the lower end by the low rate of conversion, and at the upper end by the solubility of the amine in DMSO.

Rate constants for the forward reaction in the absence of added salts are given in Table 7.20. A plot of k^2_f against amine concentration is linear, with intercept $K_1k_S = 1.24$ l mol^{-1}s^{-1}, and slope $K_1k_A = 9.75$ l^2 mol^{-2}s^{-1}.

Rate constants for the reaction catalysed by triethylamine are shown in Table 7.21. Triethylamine slightly reduces the extent of conversion to complex, as shown by the OD values. A plot of k^2_f against the concentration of triethylamine is a straight line, of slope $K_1k_B = 12.5$ l^2 mol^{-2}s^{-1}, slightly larger than the value of K_1k_A (above). Thus, triethylamine is a slightly better catalyst of proton removal from 7.2 than is di-isopropylamine.

TABLE 7.20

Rate constants for the reaction of trinitrobenzene with di-isopropylamine in DMSO at 25°C.

[A] M	OD_e [a]	k^1_f s^{-1}	k^2_f $l\ mol^{-1}s^{-1}$
0.1	0.013	0.135	1.35
0.2	0.017	0.272	1.36
0.4	0.018	0.693	1.73
0.6	0.020	1.09	1.82
0.8	0.019	1.60	2.00

a. Measured by stopped-flow at 450 nm, after completion of the colour-forming process. 5×10^{-6} M substrate in a 2 mm cell.

TABLE 7.21

Rate constants for the reaction between trinitrobenzene and di-isopropylamine in DMSO at 25°C, in the presence of triethylamine.

[A]	[B][a]	OD_e[b]	k^1_f	k^2_f
M	M		s^{-1}	$l\ mol^{-1}s^{-1}$
0.25	0	0.018	0.394	1.58
0.25	0.05	0.016	0.549	2.20
0.25	0.10	0.015	0.825	3.30
0.25	0.20	0.015	1.00	4.00

a. The available concentration range was severely limited by the low solubility of triethylamine in di-isopropylamine-DMSO solution.

b. Measured by stopped-flow at 450 nm, after completion of the colour-forming process. 5×10^{-6} M substrate in a 2 mm cell.

Table 7.22 gives rate constants for the forward reaction with added Dabco. Plots of k^2_f against Dabco concentration for both amine concentrations produce upward curves, so values of K_1k_B cannot be obtained. However, by comparing the observed rate constants with those for the amine alone (Table 7.20), Dabco appears to be a better catalyst of proton removal from 7.2 than is the amine.

It was not possible to study the reverse reaction, as the trinitrobenzene-di-isopropylamine complex solution decomposed too rapidly to allow repeated runs on the stopped-flow, and the reaction with the amine perchlorate was very fast and of small amplitude.

Equilibrium OD measurements (not shown) made on the SP500 spectrophotometer indicate a value of $K_{eq} \simeq 2 \times 10^3$ l mol^{-1}.

3. Comparison of Results

Kinetic and equilibrium data for the three primary amines and piperidine are collected in Table 7.23. The values in the first eight rows of the Table were obtained directly from the observed quantities. The remaining values depend upon the assumption that $K_a/K_{AH^+} \simeq 500$, independent of the amine. Values of this ratio lying between 120 and 400 have been reported[140] for 10% dioxan-water and 30% DMSO-water, the latter solvent giving higher values than the former. The ratio is not expected to change very much with a change of solvent: the basicities of amines, as measured by their pK_a values, do not change very markedly on transfer from water to DMSO[146], and it seems reasonable to assume that 7.2 and AH^+ would be affected in similar ways by a change in solvent.

The spectra of the adducts are all very similar, as is

TABLE 7.22

Rate constants for the reaction of trinitrobenzene with di-isopropylamine in DMSO at 25°C, in the presence of Dabco.

	[A] M	[B] M	k^1_f [a] s^{-1}	k^2_f $l\ mol^{-1}s^{-1}$
(i)	0.1	0.01	0.217	2.17
	0.1	0.03	0.296	2.96
	0.1	0.05	0.382	3.82
	0.1	0.07	0.606	6.06
	0.1	0.10	0.862	8.62
	0.1	0.15	1.72	17.2
(ii)	0.25	0	0.394	1.58
	0.25	0.05	0.751	3.00
	0.25	0.1	1.38	5.52
	0.25	0.2	3.05	12.2
	0.25	0.3	5.52	22.1
	0.25	0.4	8.86	35.4
	0.25	0.5	12.3	49.2

a. Measured by stopped-flow at 450 nm.

TABLE 7.23

Kinetic and equilibrium data for the reaction of trinitrobenzene with some amines in DMSO at 25°C.

	$^{i}PrNH_2$	$^{n}BuNH_2$	$PhCH_2NH_2$	PipNH
λ_{max} (nm)	450,528	450,534	450,534	446,524
k_1 ($l\ mol^{-1}s^{-1}$)	$(8\pm1) \times 10^3$	$(5.0\pm0.5) \times 10^4$	$(1.2\pm0.3) \times 10^4$	$>6 \times 10^4$
K_1k_A ($l^2mol^{-2}s^{-1}$)	$(3.0\pm0.2) \times 10^6$	5.0×10^7	$(1.8\pm0.2) \times 10^6$	6.0×10^5
k_A/k_{-1} ($l\ mol^{-1}$)	400	800 ± 100	180 ± 40	<10
k_B/k_{-1}[a] ($l\ mol^{-1}$)	85	440	61	< 2
K_1k_S ($l\ mol^{-1}s^{-1}$)	<1000	<1000	<1000	≈ 100
k_{AH^+} ($l\ mol^{-1}s^{-1}$)	1.4×10^4	5.1×10^4	1.6×10^4	<100
K_{eq} ($l\ mol^{-1}$)	200 ± 50	1000 ± 100	100 ± 5	$(5\pm1) \times 10^3$
K_1[b] ($l\ mol^{-1}$)	0.4	2	0.2	10
k_{-1}[c] (s^{-1})	2×10^4	2.5×10^4	6×10^4	$> 6 \times 10^3$
k_A[d] ($l\ mol^{-1}s^{-1}$)	7×10^6	3×10^7	8×10^6	$< 5 \times 10^4$
k_B[e] ($l\ mol^{-1}s^{-1}$)	1.5×10^6	2×10^7	2×10^6	$\approx 10^4$
$pK_a(AH^+)$[f]	10.6	10.6	9.3	11.1

TABLE 7.23 (contd)

a. B = Dabco.

b. Calculated from equation (7.30), assuming $K_a/K_{AH^+} = 500$ (see text).

c. $k_{-1} = k_1/K_1$.

d. Calculated from equation (7.30): $k_A = K_{eq}k_{AH^+}/K_1$.

e. $k_B = k_A(k_B/k_{-1})(k_{-1}/k_A)$.

f. Reference 145.

to be expected of species with similar structure: the added amino groups do not form part of the chromophore (the trinitrocyclopentadienyl system)[21].

A comparison of the observed rate (k^2_f) and equilibrium constants shows that there are differences in behaviour between the primary and secondary amines, with piperidine behaving more like a primary than a secondary amine. The most obvious difference between the two groups is steric: the amino-nitrogen atom is more crowded in the secondary than in the primary amines, while that in piperidine is less crowded than those in the other secondary amines because the 'two' alkyl groups are held back in the ring.

For the primary amines, plots of the second-order forward rate constant (k^2_f) against the base concentration are curved, indicating a change in the rate-determining step as the amine concentration increases. At low concentrations, $k_{-1} > k_A[A] + k_S$, so proton-transfer from 7.2 to the amine is rate-determining, and subject to base catalysis. At higher amine concentrations, $k_{-1} < k_A[A] + k_S$, so the first step becomes rate-determining and the reaction is no longer subject to base catalysis. Eventually, a limiting rate should be reached when $k^2_f = k_1$.

k_S is small, as shown by the linearity of the reciprocal plots (equation 7.17), so $k_{-1} >> k$, and the intercept of the k^2_f vs [A] plot gives the value of K_1k_S. Because of the difficulties involved in extrapolating curves, the values given in Table 7.23 are upper limits. Since the values of k_S are much smaller than those of $k_A[A]$ and $k_B[B]$ (B = Dabco), catalysis of proton removal from 7.2 by the solvent is a very small effect, which does not effectively compete with catalysis by the amine or added base.

Values of k_A/k_{-1} are larger than those of k_B/k_{-1} for all three primary amines: thus, the amines are more effective catalysts of proton removal from 7.2 than is Dabco.

The results show that proton-transfer between nitrogen and nitrogen is not diffusion-controlled, as might have been expected[147]. Rate-limiting proton-transfer has previously been found in the formation of σ-adducts of trinitrobenzene with aliphatic amines in mixed solvents[140], or aniline in DMSO[98], and for spiro-complex formation in mixed and aqueous solutions[141,142,143]. Similar slow proton-transfers in DMSO solution have also been found between tetra-alkyl hydrazines and salicylic acid[148], and in the protonation/deprotonation reactions of tertiary amines[149] and piperidine[150]. However, proton exchange between NH_3 and NH_4^+ has been found[151] to proceed at similar rates in DMSO and in water. This suggests that there may be steric factors involved in the removal of a proton from a bulky molecule in DMSO.

Since the k_S term in the complex forming process is small, the $k_{SH^+}[SH^+]$ term in the expression for the reverse rate is also expected to be small, so k_{AH^+} can be calculated. k_{AH^+} has a similar value for each of the three primary amines.

For piperidine, a plot of k^2_f against amine concentration is linear over the whole range used. Thus, $k_{-1} >> k_A[A] + k_S$, and proton-transfer from 7.2 is rate-limiting throughout. Dabco is again a less efficient catalyst of proton removal than is the amine, although the difference between the two is less marked than for the primary amines. This is presumably a result of the greater crowding of the amino-nitrogen atom in piperidine compared with the primary amines. As before, proton removal by the solvent is a minor effect.

Reprotonation of 7.3 by the protonated amine (k_{AH^+}) is much slower than for the primary amines. This is again presumably a steric effect.

The pK_a values of the amines in water[145] are in the order PipNH > $^{i}PrNH_2$, $^{n}BuNH_2$ > $PhCH_2NH_2$. This order is unlikely to be changed in DMSO[146]. The values of K_1 (Table 7.23) are in the order PipNH > $^{n}BuNH_2$ > $^{i}PrNH_2$ > $PhCH_2NH_2$, reflecting the order of basicity of the amines. The value of K_1 for isopropylamine is a little lower than might be expected: this could be due to steric hindrance in the zwitterion, 7.2.

The measured rate constants for n-butylamine and piperidine may be compared with values obtained in 30% DMSO-water[140] and in 10% dioxan-water[139,140]. For both amines, k_1 is faster in pure DMSO, while k_{-1} is considerably slower. Thus K_1, for formation of the zwitterionic adduct, 7.2, is greater in pure DMSO than in the aqueous solutions. This is in line with observations on other substrate-nucleophile systems[8,105], that formation of the 1:1 adduct is enhanced in dipolar aprotic solvents, such as DMSO.

The results from the secondary amines (Table 7.24) are considerably less clear-cut, but some general remarks can be made. From steric considerations, nucleophilic attack by a secondary amine is likely to be slower than that by a primary amine. In agreement with this, measured k^2_f values for diethylamine and di-isopropylamine are smaller than those for the other amines studied here. Plots of k^2_f against amine concentration are linear, so k_{-1} is the dominant term in the denominator (it is expected to be large, because of steric crowding in the zwitterion, 7.2) and proton-transfer is rate-limiting throughout the range of amine concentrations used.

TABLE 7.24

A comparison of the data obtained for the bulky secondary amines with those for the other amines studied.

	λ_{max}	K_1k_S	K_1k_A	K_{eq}
	nm	$l\ mol^{-1}s^{-1}$	$l^2mol^{-2}s^{-1}$	$l\ mol^{-1}$
Et_2NH	448	0.3 ± 0.1	190 ± 40	22
	524			
$^iPr_2NH$	450	1.24	9.75	$2x10^{-3}$
	520			
PipNH	446	~100	$6x10^5$	$5x10^3$
	524			
$^iPrNH_2$	450	<1000	$3x10^6$	200
	528			
$^nBuNH_2$	450	<1000	$5x10^7$	1000
	534			
$PhCH_2NH_2$	450	<1000	$2x10^6$	100
	534			

k_B (for Dabco) is expected to be larger than k_A, as the nitrogen atom of Dabco is more readily available than is that of a bulky secondary amine, making the approach to the zwitterion by Dabco less sterically hindered. Although absolute values of k_A/k_B could not be obtained for diethylamine or di-isopropylamine, catalysis by Dabco does seem to be more effective than that by the amines (compare Tables 7.16 and 7.17(i) with 7.18, and 7.20 with 7.22). The very small increase in k^2_f with increasing di-isopropylamine concentration may be due to a medium effect rather than actual base catalysis by the amine[152,153]. Catalysis of proton removal from 7.2 by the solvent also appears to be more important for the secondary than for the primary amines (see below).

The situation with diethylamine is very unclear. In very dilute solutions (Table 7.17), a slow reaction with a small k^2_f was seen, while at higher amine concentrations, a fast reaction with much larger values of k^2_f was monitored by stopped-flow (Table 7.16). This fast process was followed by a much slower one, presumably corresponding to that (measured by conventional spectrophotometry) in Table 7.17.

The possibility that one of the reactions is attack by hydroxide ion (formed in equilibrium (7.32) from traces of water in the solvent) is ruled out on the grounds of the spectra of the species produced.

$$A + H_2O \rightleftharpoons AH^+ + HO^- \qquad (7.32)$$

That the two processes observed are the two stages of the reaction (Scheme 7.2) can also be ruled out. The first stage would have an observed rate constant given by

$$k_{obs} = k_1[A] + k_{-1} \qquad (7.33)$$

in which k_{-1} would be the dominant term (for steric reasons), with an expected value in the region of 10^4 s^{-1}. Virtually complete conversion to the adduct is achieved at 10^{-2} M amine, so K_1 would have to be of the order of 10^3 l mol^{-1}, very much larger than K_1 values obtained for the other amines. (In addition, this would give $k_1 \simeq 10^7$ l $mol^{-1}s^{-1}$, also very much larger than those for the other, less sterically hindered, amines).

The slow reaction seems unlikely to be the formation of the 'copper-pink' species, λ_{max} 515 nm (above), as this was only produced in the presence of diethylammonium perchlorate.

A further possibility is that the slower process is the reaction between trinitrobenzene and diethylamine, while the faster process is due to an impurity, presumably a more reactive amine. As little as 1% impurity would be sufficient to allow the detection of this reaction, owing to the high extinction coefficients of these adducts. This could explain the irreproducibility of results for the fast reaction using different samples of amine. In this case, the results in Table 7.17, obtained by conventional spectrophotometry, would apply to the reaction of diethylamine. As the equilibrium constant for complex formation, K_1, would be expected to differ for diethylamine and the impurity, this would also explain the widely different values of K_1k_S (which cover a range of about two orders of magnitude).

The rate constants for amine attack on the substrate, k_1, decrease in the order PipNH > $^nBuNH_2$ > $PhCH_2NH_2$ > $^iPrNH_2$ > $^iPr_2NH$ > Et_2NH, the values covering a range of four orders of magnitude.

The rate order is almost identical with that obtained[154] for the reaction of amines with 1-chloro-2,4-dinitrobenzene in ethanol at 25°C, the rate constants for which also span four orders of magnitude.

While the value of k_1 is higher for primary than for secondary amines, the reverse is expected for k_{-1}, the expulsion of the added amine, because of the greater crowding in the adduct formed from a secondary amine. Piperidine might be expected to behave more as a secondary than as a primary amine in this respect.

DMSO is a good hydrogen-bond acceptor[155], and so is expected to participate in the reaction in this capacity[156]. This interaction has also been proposed for the trinitrobenzene-anilide adduct in DMSO[134]. Intramolecular hydrogen-bonding with an ortho nitro-group is also possible, but may be more important in non-polar solvents[13]. As well as aiding the formation of the zwitterionic intermediate, 7.2, hydrogen-bonding will also affect the rates of deprotonation. Removal of the proton requires the hydrogen-bond to be broken, which raises the activation energy and so reduces the rate of proton removal by another species[157] (e.g. amine, Dabco). This effect will be less important in the primary amines, in which only one proton is expected to be involved in hydrogen-bonding, leaving the second proton open to attack by the amine or Dabco, subject to steric difficulties.

Hydrogen-bonding with DMSO may also help to explain the greater relative importance of the k_S term in proton removal from the adducts of secondary amines. The molecule of DMSO hydrogen-bonded to the (already crowded) zwitterionic complex may hinder the approach of other bases and so favour proton abstraction by DMSO.

APPENDIX

The Board of Studies in Chemistry requires that each postgraduate research thesis contain an appendix listing (a) all research colloquia, research seminars and lectures (by external speakers) arranged by the Department of Chemistry since 1 October 1977 (*signifies those attended);
(b) all research conferences attended and papers read out by the writer of the thesis, during the period when the research for the thesis was carried out;
(c) details of the first-year induction course.

(a) Research Colloquia, Seminars and Lectures

1977-78

October 19: Dr. B. Heyn (University of Jena, D.D.R.). 'σ-Organo-molybdenum complexes as alkene polymerisation catalysts'.

November 2: Dr. N. Boden (University of Leeds). 'N.m.r. spin-echo experiments for studying structure and dynamical properties of materials containing interacting spin-$\frac{1}{2}$ pairs'.

* November 9: Dr. A.R. Butler (University of St. Andrews). 'Why I lost faith in linear free energy relationships'.

December 7: Dr. P.A. Madden (University of Cambridge). 'Raman studies of molecular motions in liquids'.

December 14: Dr. R.O. Gould (University of Edinburgh). 'Crystallography to the rescue in ruthenium chemistry'.

January 25: Dr. G. Richards (University of Oxford). 'Quantum pharmacology'.

January 26: Prof. R.A. Filler (Illinois Institute of Technology, U.S.A.).
'Reactions of organic compounds with xenon fluorides'.

*February 1: Prof. K.J. Irvin (Queen's University, Belfast).
'The olefin metathesis reaction: mechanism of ring-opening polymerisation of cycloalkenes'.

February 3: Dr. A. Hartog (Free University, Amsterdam).
'Some surprising recent developments in organo-magnesium chemistry'.

*February 22: Prof. J.D. Birchall (Mond Division, I.C.I. Ltd.).
'Silicon in the biosphere'.

*March 1: Dr. A. Williams (University of Kent).
'Acyl group transfer reactions'.

March 3: Dr. G. van Koten (University of Amsterdam).
'Structure and reactivity of arylcopper cluster compounds'.

*March 15: Prof. G. Scott (University of Aston).
'Fashioning plastics to match the environment'.

March 22: Prof. H. Vahrenkamp (University of Freiburg).
'Metal-metal bonds in organometallic complexes'.

April 19: Dr. M. Barber (U.M.I.S.T.).
'Secondary ion mass spectra of surface adsorbed species'.

May 15: Dr. M.I. Bruce (University of Adelaide).
'New reactions of ruthenium compounds with alkynes'.

May 16: Dr. P. Ferguson (C.N.R.S., Grenoble).
'Surface plasma waves and adsorbed species on metals'.

May 18: Prof. M. Gordon (University of Essex).
'Three critical points in polymer science'.

May 22: Prof. Tuck (University of Windsor, Ontario).
'Electrochemical synthesis of inorganic and organometallic compounds'.

*May 24-25: Prof. P. von R. Schleyer (University of Erlangen, Nurnberg).

(i) 'Planar tetra-coordinate methanes, perpendicular ethylenes and planar allenes'.

(ii) 'Aromaticity in three dimensions'.

(iii) 'Non-classical carbocations'.

June 21: Dr. S.K. Tyrlik (Academy of Sciences, Warsaw).
'Dimethylglyoxime-cobalt complexes - catalytic black boxes'.

June 23: Prof. W.B. Person (University of Florida).
'Diode laser spectroscopy at 16μm'.

June 27: Prof. R.B. King (University of Georgia, U.S.A.).
'The use of carbonyl anions in the synthesis of organometallic compounds'.

*June 30: Prof. G. Mateescu (Case Western Reserve University).
'A concerted spectroscopy approach to the characterisation of ions and ion-pairs: facts, plans and dreams'.

1978-79

September 15: Prof. W. Siebert (University of Marburg, West Germany).
'Boron heterocycles as ligands in transition metal chemistry'.

September 22: Prof. T. Fehlner (University of Notre-Dame, U.S.A.)
'Ferroboranes: synthesis and photochemistry'.

*December 12: Prof. C.J.M. Stirling (University College of North Wales, Bangor).
'Parting is such sweet sorrow - the leaving group in organic reactions'.

February 14: Prof. B. Dunnell (University of British Columbia).
'The application of n.m.r. to the study of motions in molecules'.

February 16: Dr. J. Tomkinson (Institute Laue-Langevin, Grenoble).
'Studies of adsorbed species'.

March 14: Dr. J.C. Walton (University of St. Andrews).
'Pentadienyl radicals'.

March 28: Dr. A. Reiser (Kodak Ltd.).
'Polymer photography and the mechanism of cross-link formation in solid polymer matrices'.

April 5: Dr. S. Larsson (University of Uppsala).
'Some aspects of photoionisation phenomena in inorganic systems'.

*April 25: Dr. C.R. Patrick (University of Birmingham).
'Chlorofluorocarbons and stratospheric ozone: an appraisal of the environmental problem'.

May 1: Dr. G. Wyman (European Research Office, U.S. Army).
'Excited state chemistry in indigoid dyes'.

May 2: Dr. J.D. Hobson (University of Birmingham).
'Nitrogen-centred reactive intermediates'.

May 8: Prof. A. Schmidpeter (Institute of Inorganic Chemistry, University of Munich).
'Five-membered phosphorus heterocycles containing dicoordinate phosphorus'.

*May 9: Dr. A.J. Kirby (University of Cambridge).
'Structure and reactivity in intramolecular and enzymic catalysis'.

May 9: Prof. G. Maier (Lahn - Giessen).
'Tetra-tert-butyltetrahedrane'.

*May 10: Prof. G. Allen, F.R.S. (S.R.C.).
'Neutron scattering studies of polymers'.

May 16: Dr. J.F. Nixon (University of Sussex).
'Spectroscopic studies on phosphines and their coordination complexes'.

May 23: Dr. B. Wakefield (University of Salford).
'Electron transfer in reactions of metals and organometallic compounds with polychloro-pyridine derivatives'.

June 13: Dr. G. Heath (University of Edinburgh).
'Putting electrochemistry into mothballs (redox processes of metal porphyrins and phthalocyanines)'.

*June 14: Prof. I. Ugi (University of Munich).
'Synthetic uses of super nucleophiles'.

June 20: Prof. J.D. Corbett (Iowa State University, U.S.A.).
'Zintl ions: synthesis and structure of homopolyatomic anions of the post-transition elements'.

June 27: Dr. H. Fuess (University of Frankfurt).
'Study of electron distribution in crystalline solids by X-ray and neutron diffraction'.

1979-80

November 21: Dr. J. Muller (University of Bergen).
'Photochemical reactions of NH_3'.

November 28: Prof. B. Cox (University of Stirling).
'Macrobicyclic cryptate complexes: dynamics and selectivity'.

December 5: Dr. G.C. Eastmand (University of Liverpool).
'Synthesis and properties of some multi-component polymers'.

December 12: Dr. C.I. Ratcliffe.
'Rotor motions in solids'.

December 18: Dr. K.E. Newman (University of Lausanne).
'High pressure multinuclear n.m.r. in the elucidation of the mechanisms of fast, simple inorganic reactions'.

January 30: Dr. M.J. Barrow (University of Edinburgh).
'The structures of some simple inorganic compounds of silicon and germanium - pointers to structural trends in Group IV'.

May 14: Dr. R. Hutton (Waters Associates).
'Recent developments in multi-milligram and multi-gram scale preparative high performance liquid chromatography'.

May 21: Dr. T.W. Bently (University College of Wales, Swansea).
'Medium and structural effects on solvolytic reactions'.

July 10: Prof. P. des Marteau (University of Heidelburg).
'New developments in organonitrogen fluorine chemistry'.

(b) Conferences Attended

September 10-20, 1978 (University College of Wales, Aberystwyth).
N.A.T.O. Advanced Study Institute: "New Applications of Chemical Relaxation Spectrometry and Other Fast Reaction Techniques in Solution".

September 14-15, 1978 (University College of Wales, Aberystwyth).
1978 Meeting of the 'Fast Reactions in Solution' group.

April 9-11, 1980 (University of Durham).
The Chemical Society and Royal Institute of Chemistry, Annual Chemical Congress.

(c) First-Year Induction Course (1977)
A series of one-hour presentations on the services available in the department:
October 3: Departmental organisation.
October 5: Safety matters.

October 7: Electrical appliances.

October 10,12: Chromatography and microanalysis.

October 14: Library facilities.

October 17: Atomic absorptiometry and inorganic analysis.

October 19,21: Mass Spectrometry.

October 24,26: Nuclear magnetic resonance spectroscopy.

October 31 - November 4: Glassblowing technique.

REFERENCES

1. J. March, 'Advanced Organic Chemistry: Reactions, Mechanisms and Structure'. London: McGraw-Hill, 1968.

2. J.F. Bunnett, Quart.Rev., 1958, 12, 1.

3. J. Miller, 'Aromatic Nucleophilic Substitution'. Amsterdam: Elsevier, 1968.

4. J.F. Bunnett, Accounts Chem.Res., 1978, 11, 413.

5. J. Hirst and S.J. Una, J.Chem.Soc.(B), 1971, 2221.

6. J. Miller and K. -Y. Wan, J.C.S. Perkin 2, 1976, 1320.

7. E. Buncel, A.R. Norris, and K.E. Russell, Quart.Rev., 1968, 22, 123.

8. M.R. Crampton, Adv.Phys.Org.Chem., 1969, 7, 211.

9. S.D. Ross, in C. H. Bamford and C.F.H. Tipper, Eds., 'Comprehensive Chemical Kinetics', Vol.13. Amsterdam: Elsevier, 1972.

10. C.A. Fyfe, M. Cocivera, and S.W.H. Damji, Accounts Chem.Res., 1978, 11, 277.

11. C.A. Fyfe, A. Koll, S.W.H. Damji, C.D. Malkiewich, and P.A. Forte, J.C.S.Chem.Comm., 1977, 335.

12. C.A. Fyfe, S.W.H. Damji, and A. Koll, J.Amer.Chem.Soc., 1979, 101, 956.

13. C.F. Bernasconi, in M.T.P. Internat.Rev.Sci.: Org.Chem., Ser.One, 1973, 3, 33.

14. F. Pietra and D. Vitali, J.C.S.Perkin 2, 1972, 385.

15. P. Hepp, Annalen, 1882, 215, 344.

16. C.L. Jackson and F.H. Gazzolo, Amer.Chem.J., 1900, 23, 376.

17. J. Meisenheimer, Annalen, 1902, 323, 205.

18. H. Wennerström and O. Wennerström, Acta Chem.Scand., 1972, 26, 2883.

19. R. Destro, C.M. Gramaccioli, and M. Simonetta, Acta Cryst., 1968, B24, 1369.

20. H.A. Benesi and J.H. Hildebrand, J.Amer.Chem.Soc., 1949, 71, 2703.

21. R. Foster and R.K. Mackie, J.Chem.Soc., 1963, 3796.

22. L.K. Dyall, J.Chem.Soc., 1960, 5160.

23. M.R. Crampton and V. Gold, Proc.Chem.Soc., 1964, 298.

24. M.R. Crampton and V. Gold, J.Chem.Soc., 1964, 4293.

25. G.A. Olah and H. Mayr, J.Org.Chem., 1976, 41, 3448.

26. C.F. Bernasconi, J.Amer.Chem.Soc., 1971, 93, 6975.

27. G. Bartoli and P.E. Todesco, Accounts Chem.Res., 1977, 10, 125.

28. V. Gold and C.H. Rochester, J.Chem.Soc., 1964, 1692.

29. R. Destro, C.M. Gramaccioli, and M. Simonetta, Nature, 1967, 215, 389.

30. C.F. Bernasconi, J.Amer.Chem.Soc., 1970, 92, 4682.

31. C.A. Fyfe, S.W.H. Damji, and A. Koll, J.Amer.Chem.Soc., 1979, 101, 951.

32. K.L. Servis, J.Amer.Chem.Soc., 1965, 87, 5495.

33. K.L. Servis, J.Amer.Chem.Soc., 1967, 89, 1508.

34. B. Gibson and M.R. Crampton, J.C.S. Perkin 2, 1979, 648.

35. C.A. Fyfe, M.I. Foreman, and R. Foster, Tetrahedron Letters, 1969, 1521.

36. M.R. Crampton, J.C.S. Perkin 2, 1978, 343.

37. R.H. de Rossi, O.D. Madoery, and E.B. de Vargas, J.Org.Chem., 1980, 45, 649.

38. C.F. Bernasconi and R.G. Bergstrom, J.Amer.Chem.Soc., 1974, 96, 2397.

39. M.R. Crampton and M. El-Ghariani, J.Chem.Soc.(B), 1969, 330.

40. M.R. Crampton and V. Gold, Chem.Comm., 1965, 256.

41. M.R. Crampton and V. Gold, J.Chem.Soc.(B), 1966, 893.

42. M.R. Crampton and H.A. Khan, J.C.S. Perkin 2, 1972, 733.

43. M.R. Crampton and H.A. Khan, J.C.S. Perkin 2, 1973, 710.

44. C.A. Fyfe, M. Cocivera, and S.W.H. Damji, J.Amer.Chem.Soc., 1975, 97, 5707.

45. M.R. Crampton, J.C.S. Perkin 2, 1977, 1442.

46. A.D.A. Al Aruri and M.R. Crampton, J.Chem.Res.(S), 1980, 140.

47. M.R. Crampton, B. Gibson, and F.W. Gilmore, J.C.S.Perkin 2, 1979, 91.

48. V. Gold and C.H. Rochester, J.Chem.Soc., 1964, 1697.

49. M.R. Crampton and B. Gibson, J.C.S.Perkin 2, 1980, 752.

50. M.R. Crampton, M.A. El Ghariani, and H.A. Khan, Tetrahedron, 1972, 28, 3299.

51. L.H. Gan, Aust.J.Chem., 1975, 28, 2403.

52. C.F. Bernasconi, Accounts Chem.Res., 1978, 11, 147.

53. J.A. Chudek and R. Foster, J.C.S. Perkin 2, 1979, 628.

54. M.R. Crampton, J.Chem.Soc.(B), 1968, 1208.

55. M.R. Crampton and M.A. El Ghariani, J.Chem.Soc.(B), 1971, 104

56. G. Biggi and F. Pietra, J.C.S.Perkin 1, 1973, 1980.

57. G. Biggi and F. Pietra, J.C.S.Chem.Comm., 1973, 229.

58. M.R. Crampton, J.Chem.Soc.(B), 1967, 1341.

59. N. Marendic and A.R. Norris, Canad,J.Chem., 1973, 51, 3927.

60. E. Buncel, A.R. Norris, K.E. Russell, and P.J. Sheridan, Canad.J.Chem., 1974, 52, 25.

61. M.R. Crampton and M.J. Willison, J.C.S.Chem.Comm., 1973, 215.

62. M.J. Strauss and S.P.B. Taylor, J.Amer.Chem.Soc., 1973, 95, 3813.

63. C.F. Bernasconi and R.G. Bergstrom, J.Amer.Chem.Soc., 1973, 95, 3603.

64. E. Buncel, A.R. Norris, W. Proudlock, and K.E. Russell, Canad.J.Chem., 1969, 47, 4129.

65. L.H. Gan and A.R. Norris, Canad.J.Chem., 1974, 52, 1.

66. L.H. Gan and A.R. Norris, Canad.J.Chem., 1974, 52, 8.

67. C.A. Fyfe and R. Foster, Chem.Comm., 1967, 1219.

68. M.J. Strauss, Accounts Chem.Res., 1974, 7, 181.

69. R.R. Bard and M.J. Strauss, J.Org.Chem., 1977, 42, 435.

70. S. Sekiguchi and K. Okada, J.Org.Chem., 1975, 40, 2782.

71. K. Okada and S. Sekiguchi, J.Org.Chem., 1978, 43, 441.

72. R.P. Taylor, J.Org.Chem., 1970, 35, 3578.

73. R.P. Taylor, Chem.Comm., 1970, 1463.

74. F. Terrier, G. Ah-Khow, M. -J. Pouet, and M.P. Simonnin, Tetrahedron Letters, 1976, 227.

75. G. Illuminati, Adv.Heterocyclic Chem., 1964, 3, 285.

76. F. Terrier, F. Millot, and W.P. Norris, J.Amer.Chem.Soc., 1976, 98, 5883.

77. D. Spinelli, G. Consiglio, and R. Noto, J.Chem.Res.(M), 1978, 2984.

78. F. Terrier, A. -P. Chatrousse, and C. Paulmier, J.Org.Chem., 1979, 44, 1634.

79. D. Spinelli, G. Consiglio, and R. Noto, J.Org.Chem., 1978, 43, 4038.

80. C.M. Lok, M.E. den Boer, and J. Cornelisse, Rec.Trav.Chim., 1973, 92, 340.

81. T. Abe and T. Asao, Tetrahedron Letters, 1973, 1327.

82. C.H. Rochester, 'Acidity Functions'. London: Academic Press, 1970.

83. C.H. Rochester, Quart.Rev., 1966, 20, 511.

84. K. Bowden, Chem.Rev., 1966, 66, 119.

85. P. Buck, Angew.Chem.Int.Ed.Engl., 1969, 8, 120.

86. J.H. Fendler, E.J. Fendler, and C.E. Griffin, J.Org.Chem., 1969, 34, 689.

87. E.J. Fendler, J.H. Fendler, C.E. Griffin, and J.W.Larsen, J.Org.Chem., 1970, 35, 287.

88. C.M. Gramaccioli, R. Destro, and M. Simonetta, Chem.Comm., 1967, 331.

89. A.J. Parker, Proc.Chem.Soc., 1961, 371.

90. M.R. Crampton and H.A. Khan, J.C.S.Perkin 2, 1972, 2286.

91. M.R. Crampton and H.A. Khan, J.C.S.Perkin 2, 1973, 1103.

92. M.R. Crampton, J.C.S.Perkin 2, 1975, 825.

93. J.J.K. Boulton, P.J. Jewess, and N.R. McFarlane, J.Chem.Soc.(B), 1971, 928.

94. 'Dictionary of Organic Compounds', 4th Edn.,London: Eyre and Spottiswoode, 1965.

95. A.F. Holleman, Rec.Trav.Chim., 1930, 49, 112.

96. M.R. Crampton and M. El Ghariani, J.Chem.Soc.(B), 1970, 391.

97. J. von Jouanne and J. Heidberg, J.Amer.Chem.Soc., 1973, 95, 487.

98. E. Buncel and W. Eggimann, J.Amer.Chem.Soc., 1977, 99, 5958.

99. E. Buncel and W. Eggimann, J.C.S.Perkin 2, 1978, 673.

100. M.C. Haulait and P.L. Huyskens, J.Phys.Chem., 1975, 79, 1812.

101. R.A. Robinson and R.H. Stokes, 'Electrolyte Solutions', 2nd Edn.London: Butterworths, 1970.

102. E.A. Guggenheim, Phil.Mag., 1926, 2, 538.

103. L.H. Gan and A.R. Norris, Canad.J.Chem., 1971, 49, 2490.

104. J. Barthel, R. Wachter, and M. Knerr, Electrochim.Acta, 1971, 16, 723.

105. M.J. Strauss, Chem.Rev., 1970, 70, 667.

106. V. Gold and C.H. Rochester, J.Chem.Soc., 1964, 1687.

107. C.M. Gramaccioli, R. Destro, and M. Simonetta, Acta Cryst., 1968, B 24, 129.

108. V. Gold and C.H. Rochester, J.Chem.Soc., 1964, 1710.

109. V. Gold and C.H. Rochester, J.Chem.Soc., 1964, 1722.

110. V. Gold and C.H. Rochester, J.Chem.Soc., 1964, 1727.

111. R. Gaboriaud, R. Schaal, and P. Letellier, Bull.Soc. Chim.France, 1969, 2683.

112. L.H. Gan and A.R. Norris, Canad.J.Chem., 1974, 52, 18.

113. C.F. Bernasconi and R.G. Bergstrom, J.Org.Chem., 1971, 36, 1325.

114. E. G. Kaminskaya, S.S. Gitis, A. Ya. Kaminskii, and Yu.D. Grudtsyn, Zh.Org.Khim., 1976, 12, 917.

115. C.A. Bunton and L. Robinson, J.Amer.Chem.Soc., 1968, 90, 5965.

116. J.H. Fendler, E.J. Fendler, and M.V.Merritt, J.Org.Chem., 1971, 36, 2172.

117. A.A. Frost and R.G. Pearson, 'Kinetics and Mechanism', 2nd.Edn. London: Wiley, 1961.

118. D.J.G. Ives and P.G.N. Moseley, J.Chem.Soc.(B), 1966, 757.

119. Yu.D. Grudtsyn and S.S. Gitis, Zh.Org.Khim., 1975, 11,2544.

120. E. Bergman, N.R. McFarlane and J.J.K. Boulton, Chem.Comm., 1970, 511.

121. L.B. Clapp, H. Lacey, G.G. Beckwith, R.M. Srivastava, and N. Muhammad, J.Org.Chem., 1968, 33, 4262.

122. M. Eigen, N. Kruse, G. Maass, and L. De Maeyer, Prog. React.Kinet., 1964, 2, 285.

123. M.R. Crampton and H.A. Khan, J.C.S.Perkin 2, 1972, 1173.

124. M.R. Crampton, M.A. El Ghariani, and H.A. Khan, J.C.S.Perkin 2, 1972, 1178.

125. R. Foster, C.A. Fyfe, P.H. Emslie, and M.I. Foreman, Tetrahedron, 1967, 23, 227.

126. C.A. Fyfe, C.D. Malkiewich, S.W.H. Damji, and A.R. Norris, J.Amer.Chem.Soc., 1976, 98, 6983.

127. J. Heidberg, J.A. Weil, G.A. Janusonis, and J.K. Anderson, J.Chem.Phys., 1964, 41, 1033.

128. C.H. Rochester, J.Chem.Soc., 1965, 2404.

129. M.R. Crampton and M.J. Willison, J.C.S.Perkin 2, 1974, 1681.

130. W.L. Hinze, L.-J. Liu, and J.H. Fendler, J.C.S.Perkin 2, 1975, 1751.

131. J. Murto, Acta Chem.Scand., 1964, 18, 1029.

132. J. Murto, Acta Chem.Scand., 1964, 18, 1043.

133. M.R. Crampton and V. Gold, J.Chem.Soc.(B), 1967, 23.

134. E. Buncel and J.G.K. Webb, Canad.J.Chem., 1974, 52, 630.

135. E. Buncel and H.W. Leung, J.C.S.Chem.Comm., 1975, 19.

136. M.R. Crampton, B. Gibson, and R.S. Matthews, Org.Mag. Resonance, in the press.

137. J.F. Bunnett and R.E. Zahler, Chem.Rev., 1951, 49, 273.

138. M.R. Crampton and V. Gold, Chem.Comm., 1965, 549.

139. C.F. Bernasconi, J.Amer.Chem.Soc., 1970, 92, 129.

140. C.F. Bernasconi, M.C. Muller, and P. Schmid, J.Org.Chem., 1979, 44, 3189.

141. C.F. Bernasconi and C.L. Gehriger, J.Amer.Chem.Soc., 1974, 96, 1092.

142. C.F. Bernasconi and F. Terrier, J.Amer.Chem.Soc., 1975, 97, 7458.

143. C.F. Bernasconi, C.L. Gehriger, and R.H. de Rossi, J.Amer.Chem.Soc., 1976, 98, 8451.

144. J.A. Orvik and J.F. Bunnett, J.Amer.Chem.Soc., 1970,92,2417.

145. N.F. Hall and M.R. Sprinkle, J.Amer.Chem.Soc., 1932,54,3469.

146. A. Mucci, R. Domain, and R.L. Benoit, Canad.J.Chem., 1980, 58, 953.

147. M. Eigen, Angew.Chem.Int.Ed.Engl., 1964, 3, 1.

148. S.F. Nelson, P.J. Kinlen, and D.H. Evans, J.Amer.Chem.Soc., 1979, 101, 1875.

149. M.M. Kreevoy and Y. Wang, J.Phys.Chem., 1977, 81, 1924.

150. J. -J. Delpuech and B. Bianchin, J.Amer.Chem.Soc., 1979, 101, 383.

151. B. Bianchin and J. -J. Delpuech, Bull.Soc.Chim.France, 1973, 34.

152. J.F. Bunnett and R.H. Garst, J.Amer.Chem.Soc., 1965, 87, 3875.

153. C.F. Bernasconi, R.H. de Rossi, and P. Schmid, J.Amer.Chem.Soc., 1977, 99, 4090.

154. H.K. Hall, J.Org.Chem., 1964, 29, 3539.

155. A.J. Parker, Quart.Rev., 1962, 16, 163.

156. A.J. Parker, Chem.Rev., 1969, 69, 1.

157. C.F. Bernasconi and R.H. de Rossi, J.Org.Chem., 1976, 41, 44.